TEXTILE RESEARCH JOURNAL

Publication of

TEXTILE RESEARCH INSTITUTE

VOLUME XXIX JULY 1959 NUMBER 7

FIBER SCIENTIST wanted for leading cosmetic company with extensive research facilities, for physical testing laboratory. Duties include measurement of mechanical properties of fibers on conventional and special equipment; research on new techniques for assessing physical changes resulting from chemical treatments; interpretation and reporting of physical data to other research groups. Minimum requirements are B.S. in chemistry or physics with two years practical experience in fiber laboratory preferably including protein fibers. Special training in fiber physics or advanced degree desirable but not required. Write in confidence to **Jack Hamilton, The Toni Company, 456 Merchandise Mart, Chicago 54, Illinois.**

TEXTILE RESEARCH JOURNAL

VOL. XXIX *July 1959* NUMBER 7

Editor: **Richard K. Toner**

Production Editor: **Candida Frenking**

Advisory Board

Herbert J. Ball
Earl E. Berkley
John Boulton
C. H. Fisher
Walter J. Hamburger
Milton Harris
R. M. Hoffman
Harold P. Lundgren
Herman Mark
Edward R. Schwarz
George Switlyk
Helmut Zahn

TEXTILE RESEARCH JOURNAL, published monthly at Prince and Lemon Streets, Lancaster, Pa., is devoted to the interest of research in textile and allied industries. It is published by Textile Research Institute.

Manuscripts and communications should be sent to the Publications Department, P.O. Box 625, Princeton, N. J.

Second-class postage paid at Lancaster, Pa.

Subscription rates: $25.00 per year; additional for postage, 50 cents to Canada, $1.00 to all other countries. Single copies, $2.50 each.

Contents copyrighted © 1959 by Textile Research Institute Advertising rates supplied on request.

IN THIS ISSUE

Structure-Property Relationships in Synthetic Fibers. Part I: Structure as Revealed by Sonic Observations. *W. H. Charch and W. W. Moseley, Jr.* 525

Part II: Elastomeric Condensation Block Copolymers. *W. H. Charch and Joseph C. Shivers* 536

A Kinetic Study of the Supercontraction of Wool Fibers in Solutions of Salts, Acids, and Alkalies. *W. G. Crewther and L. M. Dowling* 541

Photoelectric Twist Irregularity Tester. *M. Uno, H. Saito, A. Shiomi, and T. Hiramatu* 550

Phenolic-Formaldehyde Resins as Finishing Agents for Cotton Fabrics. *Leon H. Chance, Fred S. Perkerson, and Oscar J. McMillan, Jr.* 558

Some Mechanical Properties of Single Wool Fibers in D_2O. *M. Feughelman, A. R. Haly, and T. W. Mitchell* 564

Properties of Fabrics Produced from Three Extra Long Staple Cottons. *George Ruppenicker, Jr. and John J. Brown* 567

Isolation and Identification of Urocanic Acid Found in Extracts of Raw Wool. *Charles H. Binkley and Francis T. Jones* 574

The Mechanism of Pilling. *Daniel Gintis and Edward J. Mead* 578

Moisture Regain of Specialty Hair and Fur Fibers. *Werner von Bergen* 586

LETTERS TO THE EDITOR

The Relationship Between Breaking Time and Breaking Load for a Worsted Fabric Tested on CRE and CRT Machines. *Audrey S. Tweedie and Margaret T. Mitton* 589

Space Density of Fibers in Idealized Singles Yarn. *Milton M. Platt, William G. Klein, and Walter J. Hamburger* 592

Acrylonitrile-Stabilized Wool Keratin Derivatives. *Yoshio Tomimatsu, John J. Bartulovich, and Wilfred H. Ward* . 593

REPRINT REQUESTS SHOULD BE DIRECTED TO THE AUTHORS
SEE ARTICLES FOR ADDRESSES

JULY 1959
VOL. XXIX NO. 7

TEXTILE RESEARCH JOURNAL

Structure-Property Relationships in Synthetic Fibers[1]

Part I: Structure as Revealed by Sonic Observations

W. H. Charch[2] and W. W. Moseley, Jr.

Pioneering Research Division, Textile Fibers Department, E. I. du Pont de Nemours & Company, Inc., Wilmington, Del.

THE study of structure–property relationships in synthetic fibers employs various tools with which to delineate their properties and behavior. This paper deals with sound velocity data as one of these tools, and includes certain interpretations which we believe to be related to both the physical and chemical structure of synthetic fibers over a broad spectrum.

Fiber stiffness can cover a scale from rubberlike limpness to glasslike stiffness. Whether from a practical or theoretical standpoint, stiffness is one of the most fundamental properties of a fiber. Following through to a molecular scale, the chemical composition of the polymer chain of which the fiber is composed is of fundamental importance in determining the position of a given fiber on the stiffness scale of the fiber itself when in use or under the various tests performed on it. If the polymer is composed largely of flexible, rotatable bonds, and its second order transition point is well below room temperature, we usually encounter lower melting, rubber-like, plastic, or even puttylike fibers. At the other end of the spectrum, if the polymer chain includes a substantial content of rigid chemical bonds, hydrogen bonds, and/or rings, either alone or in combination, and its second-order transition temperature is well above room temperature, we usually deal with progressively harder and stiffer fibers.

Classical physics describes this scale in terms of Young's modulus of elasticity, with the qualification that it applies only to perfectly elastic materials or only to the very limited initial portion of a stress–strain curve where a material exhibits essentially elastic behavior, as opposed to plastic flow and permanent deformation.

In testing fibers on ordinary mechanical equipment currently in use, it is customary to measure the initial slope of the stress–strain curve over the first percent or two of extension and to then call this slope, measured in grams per denier, the modulus of elasticity of the fiber. For many practical purposes, this figure is very useful. However, for the study of fundamental structure, it has its limitations.

[1] Presented by W. H. Charch September 12, 1957, at Columbia University, as part of the Charles Francis Chandler Lecture.

[2] Former Research Director, Pioneering Research Division, Textile Fibers Department, E. I. du Pont de Nemours & Company, Inc. Deceased July 25, 1958.

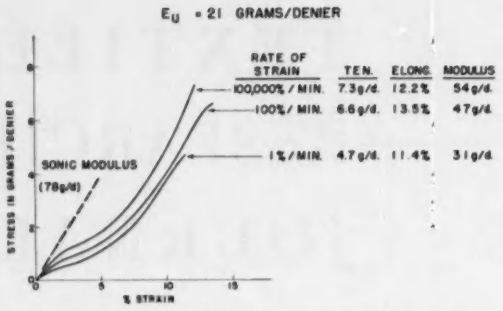

Fig. 1. Stress-strain curves for oriented 6-6 nylon at three different rates of strain.

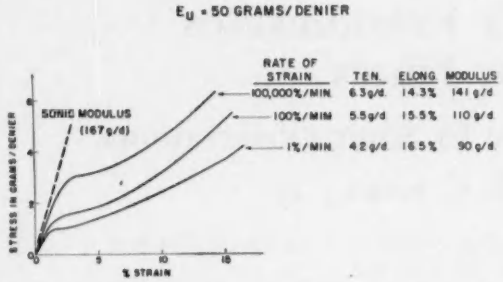

Fig. 2. Stress-strain curves for Orlon acrylic yarn (oriented) at three different rates of strain.

In Figure 1, the solid lines represent a set of stress–strain curves for 6-6 nylon, all on the same fiber sample but taken at different rates of application of strain, ranging from 1% to 100% and finally to 100,000%/min. If we wish to use such data to determine a fundamental elastic modulus for this fiber (or for the elements of structure in the fiber that are elastic), we have the choice of any figure from 31 to 54 g./den. One also observes, incidentally, that the breaking strength of this particular fiber sample is very different at these testing rates, varying from 4.7 g./den. at low rates to 7.3 g./den. at the higher rates.

Orlon[3] acrylic fiber, in Figure 2, shows a similar pattern. Its modulus varies from 90 to 141 g./den. depending on rate of application of strain.

A sample of a linear polyethylene fiber is even more sensitive to testing conditions. Its modulus varies over 100%, and its strength much more, as shown in Figure 3.

That the elastic modulus and other fiber properties measured in this manner are highly time dependent is commonly recognized. Thus, if we are interested in a modulus that bears some more fundamental relationship to the chemical and physical constitution of the polymer, and its intrinsic chain stiffness, we would do well to examine any other measurements that may be available for such study.

[3] Du Pont trademark.

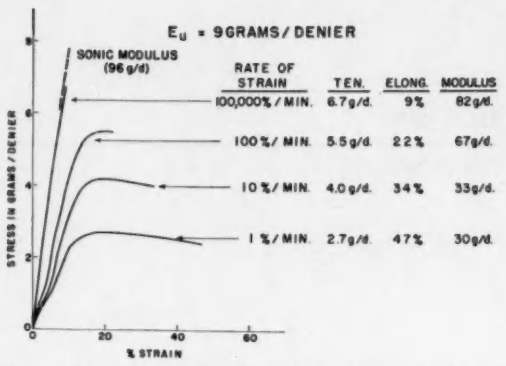

Fig. 3. Stress-strain curves for oriented linear polyethylene yarn at four different rates of strain.

In this connection, classical physics states that the velocity of sound in a material in rodlike form is related to its elastic modulus through the following equation:

$$C = \sqrt{\frac{E}{\text{Density}}} \tag{1}$$

where C is the velocity of sound and E is Young's modulus of elasticity. Since we expect to apply this equation to unoriented synthetic polymers, the subscript u is added to both E and C, to give:

$$C_u = \sqrt{\frac{E_u}{\text{Density}}} \tag{2}$$

When so used, these quantities then relate to polymer masses wherein the molecular chains lie in wholly random positions. When the polymer exists as a fiber, we say it is "unoriented."

Equation 2 can be simply converted to read in the gram per denier units of the textile technologist, whence one has:

$$E_u(\text{g./den.}) = 11.3\, C_u^2 \tag{3}$$

where C_u is in km./sec., and it is now not necessary to correct for density. When one deals with molecularly *oriented* fibers, the subscript u will be omitted. The sound waves used in the experiments described in the following pages had a frequency of 10,000 cycles/sec. One would expect the elastic

modulus associated with sound waves at this frequency to be relatively high, relatively insensitive to a decrease in experimental time scale (increase in frequency), and representative of more nearly perfect elastic behavior.

Methods of measuring sound velocity in fibers are given in the literature [1, 2]. Since little appears in current literature relating sonic measurements to fiber structure and properties, these aspects will receive attention below.

Figures 1, 2, and 3 also include the modulus of elasticity in grams per denier determined sonically, shown by the dotted lines. In every case, the sonic moduli are substantially greater for each fiber than the mechanical moduli, even for the highest rate of strain used to obtain the latter. With nylon, for instance, the sonic modulus is about 2½ times as great as that obtained from the lowest rate of mechanical strain. Orlon acrylic fiber shows a similar behavior. The case of linear polyethylene is interesting in that its mechanically determined modulus at the highest rate of strain closely approaches its sonic modulus. In other words, polyethylene fibers at very high rates of testing approach ideal elastic behavior, whereas at lower rates of testing, a highly plastic behavior is clearly illustrated.

With all polymers we have studied, the sonic modulus invariably yields the highest values for elastic modulus, being the figure to which all mechanically measured moduli approach as higher and higher rates of loading are employed.

The fundamental importance of the sonic modulus, in our view, derives from the fact that synthetic fibers are aggregations of many different microstructural elements, some of which behave as elastic components of the structure (recoverable) and others as plastic components (nonrecoverable), as illustrated so typically by the family of curves shown by the polyethylene fiber in Figure 3. The behavior of these structural elements on a time scale is spread over a spectrum of relaxation times of several decades. Mechanical methods of testing always involve a significant time element such that when a fiber is stretched, a certain amount of plastic or nonrecoverable deformation takes place during the time of the test itself. Those structural elements in the fiber responsible for this behavior do not all return to their original positions when the stress on the fiber is released, or, when they sometimes partially do, it is only after very long time intervals. This behavior is qualitatively illustrated by the creep and recovery curves in Figure 4 taken on a nylon and a cellulose acetate fiber.

In this typical test, both fibers were put under a dead load for 24 hr. (2 g./den. on the nylon and 0.5 g./den. on the acetate), these stresses being about ¼ of the breaking load of each fiber. Growth took place during this period with each fiber. After the load was removed, some immediate recovery takes place on each, but further recovery is very slow. Nylon is outstanding for the extent of its immediate recovery, whereas cellulose acetate is notable for its relatively large nonrecoverable or permanent deformation. These curves are merely illustrative. Every different fiber should exhibit its own characteristic creep and recovery behavior, depending upon the nature and distribution of the elastic and plastic elements in its structure. It is doubtful whether any two fibers, differing however little in chemical constitution, are wholly identical in their total creep and recovery patterns when all time, temperature, humidity, stress, and other factors are taken into account.

As opposed to these mechanical behaviors which involve large strains and a long time scale, let us now consider the effects of sonic vibrations as applied to the fiber structure. The forces of stress and relaxation imposed by this means act, in our studies, over infinitesimal strains during a time interval of only 0.001 sec. They affect only a very few elements of structure (those with very short relaxation times) and for our own purposes nicely ignore other structural elements in the fiber, that is, those with long relaxation times associated with plastic deformation. In this way sonic data offer a selective tool with which to study those structural elements associated with what we may call true polymer or fiber elasticity.

Table I is a list of unoriented synthetic polymers

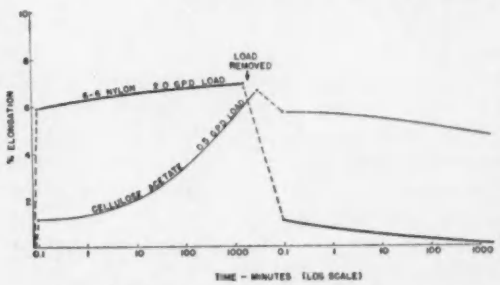

Fig. 4. Creep and recovery behavior for 6-6 nylon and cellulose acetate.

TABLE I. Sound Velocity and Related Characteristics for Various Polymers

Polymers	Sound velocity, km./sec.	Sonic modulus of unoriented polymers, g./den.	% Flexible bonds	T_g, °C.
Rubbers	Ca. 0.3	Ca. 1	75–100	Below −50
Polyethylene	0.9	9	100	−24
PIP-10	1.2	15	85	—
6 Nylon	1.3	18	100	40
6-6 Nylon	1.4	21	100	50
Pip-2 U	1.4	23	78	60
"Dacron"*	1.5	24	78	68
DMe Pip-T	1.5	27	50	292
7-T	1.6	30	86	123
3-T	2.0	46	80	180
"Orlon"**	2.1	50	100	73
3 Rings (1 meta)	2.3	58	54	253
3 Rings (all para)	2.5	72	54	250
3 Rings (all para)	2.7	80	54	205

* Trademark DuPont polyester fiber.
** Trademark DuPont acrylic fiber.

(typical of more extensive data) arranged in ascending order of sonic modulus E_u. The velocity of sound in these fibers varies over a ninefold range. From this measurement the sonic modulus of elasticity is calculated by Equation 3 and is given in the next column. It is seen to vary over an eightyfold range. Figures in the column headed "Percent Flexible Bonds" are derived by simply writing down the organic structural formula for the polymer, counting up the number of rotatable bonds in the monomer repeat unit, and then expressing this number as a percentage of the total number of bonds. This gives an elementary measure of chain flexibility of a single isolated polymer molecule as the organic chemist thinks of it. The column "T_g" gives the second-order or glass transition temperature of these polymers, the significance of which will be referred to later.

It is seen that the sonic modulus only very roughly follows the elementary chain stiffness values as read from the organic structural formulas. The lack of better correlation here is not as disturbing as it appears, since the crude method of estimating chain stiffness from a structural formula only takes no account of hydrogen bonding between chains. Actually, the polyamides (6, 6-6, 7-T, and 3-T) which appear out of line in the table all exhibit hydrogen bonding between chains. This has the practical effect of causing these chains in an actual polymer mass to seem much stiffer than would be

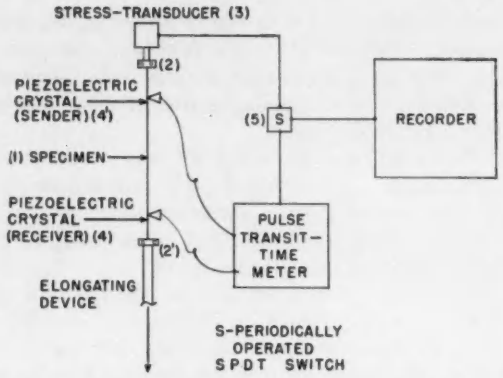

Fig. 5. Schematic of device for measuring sound velocity and stress-strain behavior simultaneously.

indicated by their structural formulas, so that the discrepancy between sonic moduli rating and percent flexible bonds as estimated from chemical formulas actually reflects on the crudity of the latter method in predicting the stiffness of an actual fiber from this polymer.

Similarly, in the case of "Orlon," a simple reading of its structural formula would indicate 100% chain flexibility. However, the large nitrile groups of this polymer give rise to steric hindrance effects which prevent wholly free rotation of all carbon to carbon bonds, so that, again, a naive reading of chain stiffness from structural formulas can be misleading unless this point is considered. Taking such secondary factors into mental account, there is a more rational correspondence between sonic moduli and actual chain stiffness of the polymer as exhibited in a physical mass than would appear at first sight.

Beyond chemical structure, fiber properties are commonly known to be dependent to a large degree on the extent of crystallinity in the material. Table II compares the sonic modulus of a series of polymers again ranging downward from those having stiff to those having flexible chains, measured first on the amorphous or lowly crystalline polymer and then on the medium to highly crystalline polymer of identical chemical composition and molecular weight.

The first column gives the second-order or glass transition temperature, T_g, of the polymer. One notes that with polymers above the line, whose second-order transition points are clearly above room temperature, there is no significant effect of crystallinity on the sonic modulus, seen by com-

TABLE II. Effect of Crystallinity on the Sonic Modulus of Various Unoriented Polymers; *Eu* in g./den.

Polymer	T_g, ° C.	Amorphous or low crystallinity	Medium to high crystallinity
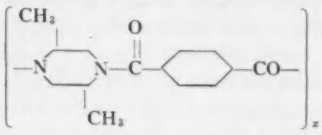	~350	28 ± 2	31 ± 2
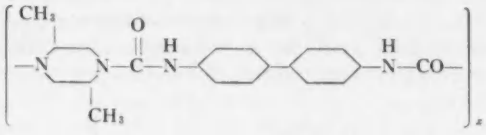	250	72 ± 2	72 ± 2
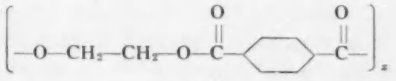	80	23 ± 1	23 ± 1
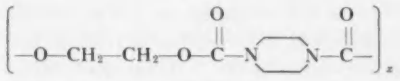	60	28 ± 1	28 ± 1
6–10 Nylon	30	10.1 (7% Crystallinity)	19.7 (37% Crystallinity)
"Teflon"*	Below 30	1.38 (47% Crystallinity)	6.35 (90% Crystallinity)
Polyethylene	−24	9 ± 1	19 ± 1

* Trademark DuPont tetrafluoroethylene fiber.

paring the figures in the two columns to the right. However, with polymers below the line, which possess second-order transition points near or below room temperature, there is a marked difference in the sonic modulus depending on the degree of crystallinity. This and more extensive data not included here support the generalization that sonic modulus is independent of crystallinity considerations up to quite high crystalline–amorphous ratios just so long as observations are carried out at temperatures significantly below the second-order transition point of the polymer.

For purposes of study this is a most fortunate situation, since it tends to simplify the structural meaning of sonic moduli in these cases (polymers with T_g significantly above room temperature) and makes the sonic modulus closer to the intrinsic stiffness of the polymer chains, since crystallinity does not have to be considered in the picture.

Following a knowledge of the chemical constitution and crystallinity, the fiber technologist is next concerned with the relative position, or orientation, of polymer chains in his fibers. If the sonic modulus is measured at room temperature on an oriented strip of film made from a polymer with a transition point well above room temperature, one will observe that it is substantially greater in the direction of orientation than it is when measured on a randomly oriented strip. The following expression[4] defines the relationship between these two moduli in a quantitative way:

$$E \doteq \frac{2E_u}{3\,(1 - \overline{\cos^2\theta})}$$

where E = sonic modulus (oriented fiber), E_u = sonic modulus (unoriented polymer or fiber), θ = angle of molecular chain to fiber axis, and $\overline{\cos^2\theta}$ = mean square projection of chains on fiber axis.

$\overline{\cos^2\theta}$ is a sort of average molecular orientation in the oriented sample having a modulus E. This approximate expression clearly does not hold for extremely high orientations, but these are very rarely reached in real fibers. For all practical purposes, this expression quantitatively connects sonic modulus and average molecular orientation, so that one may calculate the latter quantity in a

[4] The derivation of this expression will be published in a future paper.

fiber directly from sonic data for the cases where transition temperatures of the polymer permit, provided E_u is available through a separate measurement on an unoriented specimen of the same polymer.

The method has the great practical advantage of being capable of reduction to an electronic instrument where one can simultaneously follow the orientation changes taking place in a fiber specimen for all points on its mechanical stress–strain curve at the time that the latter is being run. Figure 5 illustrates such a device.

For simplicity, details of the electronic circuits are omitted. A specimen fiber (1) is mounted between the jaws (2 and 2′) of a conventional stress–strain tester. The lower jaw moves downward, elongating the specimen, while the upper stationary jaw (2) is connected to a stress transducer (3). The specimen is probed by a piezoelectric crystal receiver (4) and sender (4′) connected to a pulse transit time meter[5] which instantaneously measures the velocity of a sound pulse in the sample. The stress–strain data from the stress transducer and the sound velocity data from the transit time meter are both fed continuously into the same switch (5), which oscillates and sends the data to a moving recorder chart, recording at one instant a stress–strain point and at the next instant a point corresponding to sound velocity in the sample. The chart thus records simultaneously both the mechanical stress–strain curve and a sonic velocity–strain curve for the same sample. Figure 6 is an illustration. An undrawn fiber of 6-6 nylon is placed in the tester and elongated at the rate of 10% /min. up to its breaking point. The abscissa is calibrated both in grams per denier of stress and in an orientation parameter called fractional molecular orientation α related to $\overline{\cos^2\theta}$ as follows:

$$\alpha = \tfrac{1}{2}\,(3\,\overline{\cos^2\theta} - 1) = \left[1 - \frac{E_u}{E}\right]$$

Thus α goes from 0 to 1 as orientation goes from random to complete axial alignment.

The solid line is the stress–strain curve for the sample. Stress at first increases rapidly to initiate cold drawing (and orientation). Thereafter, stress levels off for a time, during which cold drawing and orientation take place, following which stress again climbs until the fiber breaks at about 0.85 g./den. The dotted line represents the progress of molecular orientation (measured sonically) in the fiber during the test. Orientation is building up most rapidly during the time when stress is increasing the least (between about 15% and 150% extension of the fiber). However, only small increases in orienta-

[5] Pulse Propagation Meter made by Janszen Laboratory, Inc., of Cambridge, Mass.

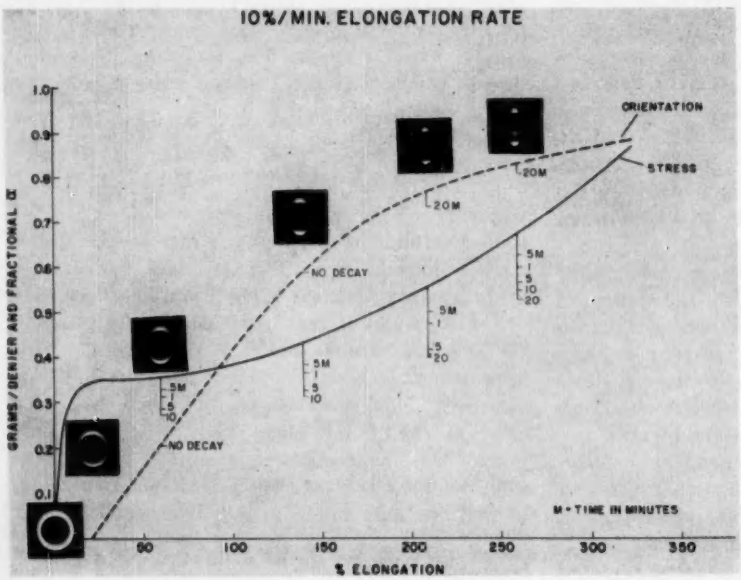

Fig. 6. Stress-strain and orientation-strain curves for undrawn 6–6 nylon.

tion occur at the higher end of the stress–strain curves. X-ray diffraction photographs have been added at the proper positions on this curve for correlation with the degree of orientation measured sonically and the points of the stress–strain curve itself.

Very interesting data can be obtained during the course of such a test if the tester is stopped at any point and the specimen held at constant length for various periods of time. The four scales attached downward to the stress–strain curve are calibrated in minutes. The stress decay which they represent is read off the scale on the abscissa. Corresponding points are noted on the orientation scale (dotted line). Whereas stress decays substantially at extensions of 50% and 150%, there is no decay or change in the orientation taking place at these strains. Only at stresses in the fiber of 0.7–0.8 g./den. and at higher extensions, where mechanical stress decay is quite pronounced, is there a decay or relaxation in the actual orientation of the molecules in the fiber.

The equipment described can be used in many different ways to furnish data simultaneously correlating orientation changes with stress, stress decay, cyclical changes, and other fiber behavior, according to the interests of the research problem at hand. The method is a research tool which, when broadly applied, should aid one or another structure–property study to produce useful information.

Another application of similar sonic measurements is to describe the variations in molecular orientation continuously along the length of a fiber. These variations are of considerable importance to the fiber technologist, since they are intimately associated with variations in strength, dyeing, fatigue, toughness, brittleness, and many other useful properties of the fiber.

If we modify the instrument just described above so as to continuously move a length of yarn past the two sonic probes, as shown in Figure 7, a record is obtained from which one can describe the variations in molecular orientation along the length of the test fiber.

Figure 8 illustrates such a record for a polyacrylonitrile yarn, where the very same length of yarn was run through the instrument twice to illustrate the reproducibility of the measurement. Comparison of the top and bottom curves shows excellent agreement. The small vertical lines on these curves represent acoustic or electronic noise and should be ignored.

Figure 9A is a trace for an acrylonitrile fiber drawn in hot water to twice its length. Great

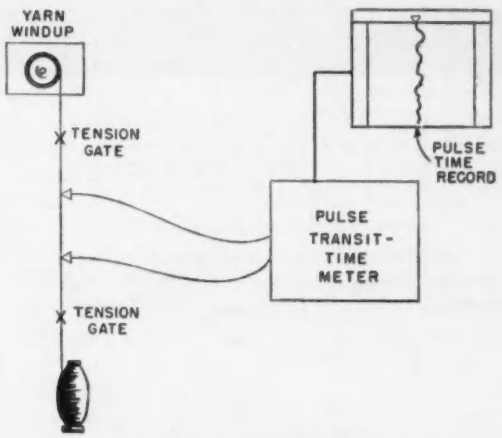

Fig. 7. Method of measuring variation in molecular orientation along a yarn.

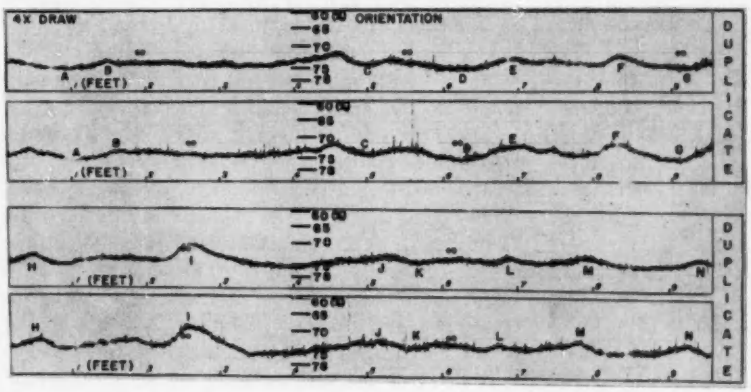

Fig. 8. Orientation uniformity in polyacrylonitrile yarn drawn 4×, showing reproducibility.

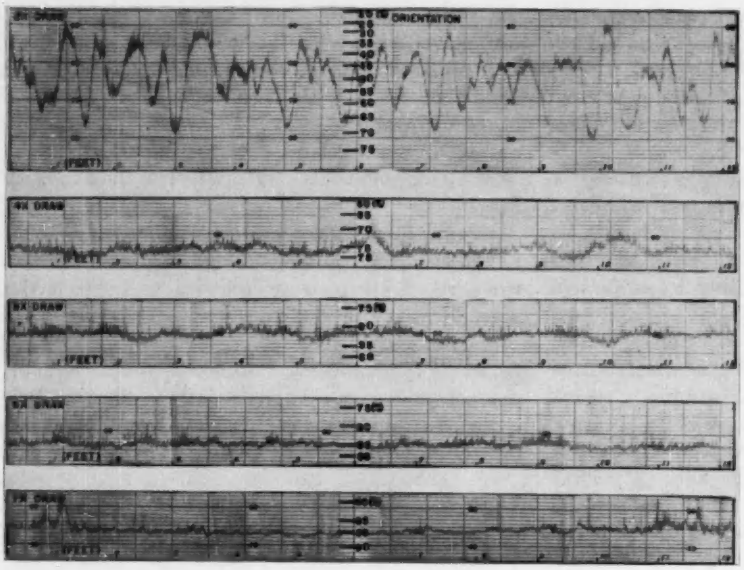

Fig. 9. Orientation uniformity in polyacrylonitrile yarn at various draw ratios.

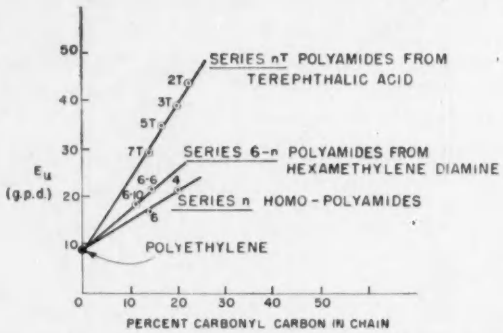

Fig. 10. Sonic modulus vs. carbonyl content in unoriented polyamides.

variations in molecular orientation along the fiber are seen to result from this processing step. The trace in Figure 9B was obtained when the fiber was drawn 4×, when it is seen that orientation has leveled out very considerably. By extension of the drawing of the fiber to 5× and 6×, the traces (Figures 9C and 9D) show some further increases in uniformity, but at 7× it would seem (Figure 9E) that no further uniformity is achieved. This chart also illustrates how the average orientation increases with increasing draw ratio. At 2× it averages about 50% ($\alpha = 0.5$); at 4× about 75%; 5×, 82%; 6×, 85%; and 7×, 88%.

Let us now turn to correlations between sonic data and chemical structure. Table III presents some limited sonic modulus data for a group of typical polyamides. The code given in the first column refers to the intermediates used in the preparation of the polymer. In the first group of four polymers, the numbers stand for the number of methylene groups in the diamine and *T* stands for terephthalic acid. In the second group of two polymers, the first number also stands for the methylene groups, as above, and the second number for the number of chain carbon atoms in the acid intermediate. In the third group of two polymers, the number stands for the number of chain carbon atoms in the amino acid intermediate. The reader should recall that hydrogen bonds contribute substantially to the high melting points of these polymers and tend to increase the over-all polymer stiffness in the mass beyond that of an imaginary single isolated molecule all by itself in space.

The first group shows a series of polyamides based on terephthalic acid with diamines from 2 to 7 carbons long, the benzene ring of terephthalic acid representing a very stiff element in the polymer chain. The percent carbonyl or H-bonds in the chain is given in Column 3. The sonic modulus in the second column is seen to increase with the increase in percent carbonyl content, which is to say with the hydrogen bonding capacity of the polymer. It is also true that in this series we have a decrease

TABLE III. Relation of Structure to Stiffness (E_u) in Polyamides

Polymer	E_u, g./den.	% Carbonyl	n	General formula
2 T	45.3 ± 0.5	22.2	2	
3 T	38.8	20.0	3	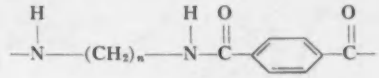
5 T	35.0	16.7	5	
7 T	29.2	14.3	7	
6–6	21.5	14.3	6	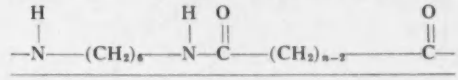
6–10	18.4	11.1	10	
4	21.0	20.0	4	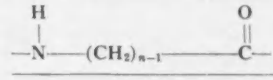
6	16.2	14.3	6	
$(CH_2)_n$	9	0		

in the total number of rotatable bonds at the same time, which would tend to exert an additional effect on the sonic modulus in the same direction. However, from other data we know that this alone would not account for a modulus increase of the magnitude seen here.

This is illustrated in Table III (the next pair of 6-6 and 6-10), where all bonds are rotatable and no stiff elements such as the benzene ring are present. We again see that 6-6, with the higher content of H-bonds, shows the higher modulus. The relationship is also visible in the last pair of 6 and 4 nylons. For the sake of comparison, the sonic modulus of amorphous unoriented polyethylene (an uninterrupted carbon chain) is given as 9. The effect of H-bonding on modulus or effective chain stiffness is, in effect, the difference between that of a pure CH_2 chain and one which is stiffened in the polymer mass by hydrogen bonds distributed along the polymer chain.

Figure 10 perhaps represents this data to better advantage. The stiffening effect of the benzene rings of terephthalic acid is illustrated by the fact that the sonic moduli of the *T* series all lie above those for the aliphatic, more flexible chain polymers. Yet, in all three cases, a progression to higher moduli results with a decrease in the number of rotatable bonds and with increases in hydrogen bond content.

It should be noted that all three curves extrapolate to a modulus of 9 g./den., which is the sonic modulus of amorphous polyethylene. We see this as support for our broader interpretations relating chain stiffness and sonic moduli data.

The effects of other environments on polymer stiffness can also be viewed through sonic modulus. Almost all fiber properties vary with temperature. At the same time, one should recall that there is a wide distribution of molecular weights in any polymer, as well as variations in amorphous and crystalline regions both as to average size and shape. Superimposed on all these are orientation variables in both crystalline and amorphous areas. Only the most elementary physical picture of this complex structure is possible at this time, but we do know that these features result in a broad distribution of what we call structural elements. This distribution of structural elements in the fiber as a whole will have one or more characteristic response or relaxation time peaks due to different predominating mechanisms, such as main chain rotation, end group motion, side chain vibration, etc. The peaks are called the more probable relaxation times. If the temperature at which the fiber is tested is raised, these peaks will shift to shorter times. If the position of a peak approaches 1/10,000 sec. the sonic modulus will drop, because during one cycle of vibration, a certain mechanism associated with this peak will relax at the higher temperature and the stress will decay appreciably in this period. One temperature where this phenomenon takes place turns out to be a glass transition temperature, T_g, of the polymer. Above this temperatue the polymer passes from a glassy to a more rubbery state at the time scale in question.

This kind of temperature effect on sonic velocity is shown in Figure 11 for polyethylene terephthalate (2GT), but with the same fiber in three different physical states. The sonic velocity scale is logarithmic.

The top curve is a plot of sonic velocity for a

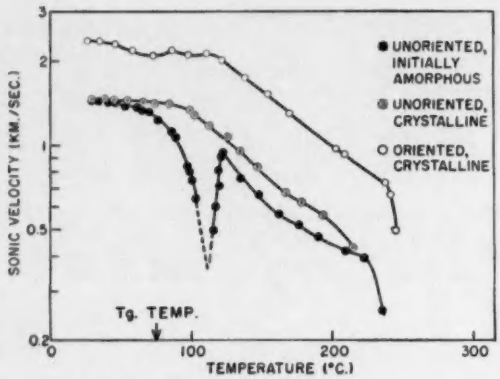

Fig. 11. Sonic velocity vs. temperature for polyethylene terephthalate fibers.

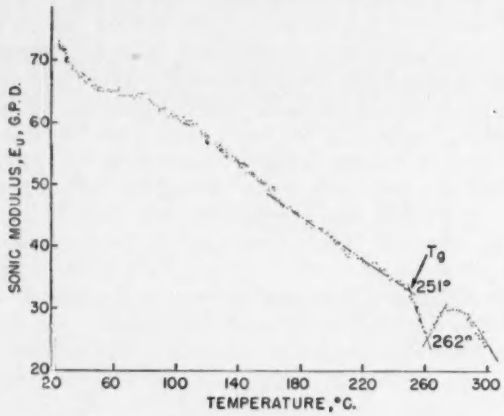

Fig. 12. Sonic modulus vs. temperature for an unoriented very stiff chain polymer.

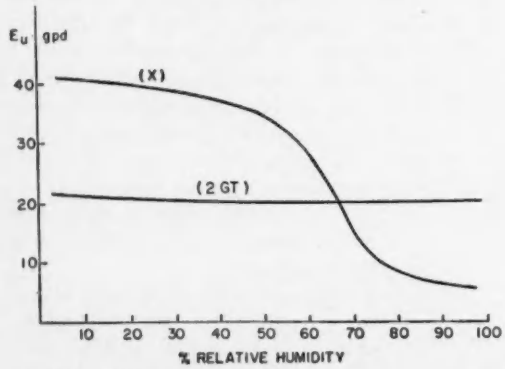

Fig. 13. Sonic modulus vs. relative humidity for an unoriented polyethylene terephthalate fiber (2GT) and a fiber showing much more moisture sensitivity (x).

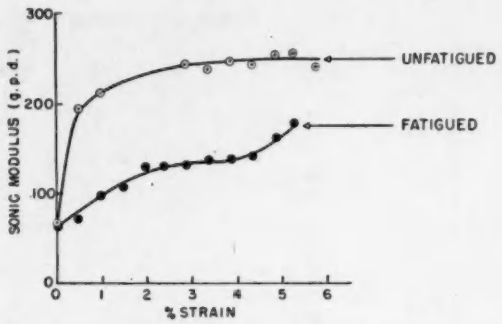

Fig. 14. Effect of fatigue on sonic modulus vs. strain curves in viscose rayon.

highly oriented crystalline fiber as its temperature is gradually raised to just below its melting point of 260° C. The middle curve represents a similar plot, starting with an unoriented but crystalline sample. The curves are notably similar in shape, but their difference in position is attributable to the fact that the first one relates to an oriented crystalline fiber while the second represents an unoriented but still crystalline fiber.

The bottom curve represents an initially unoriented amorphous fiber. It starts out at room temperature along with the unoriented crystalline sample, but as the glass transition temperature of about 80° C. is approached, relaxation peaks in the amorphous sample shift and sonic velocity drops sharply as more sound energy is abosrbed or converted into heat. However, as the temperature of the experiment comes into and above the transition temperature range for this polymer, crystallization sets in and sonic velocity rises sharply until crystallization is completed. The curve then shows essentially the same trend with temperature as though one had started initially with an unoriented crystallized sample.

Sonic modulus is independent of crystallinity only appreciably below the transition temperature. However, in the region of the transition temperature where this does not apply, we see how sonic data can be used to follow both the rate and the extent of crystallinity from instant to instant.

Another illustration of this effect is shown in Figure 12 for an extremely stiff, very high melting point polymer, where a temperature of 262° C. is required to induce crystallization of its very inflexible chains.

It is well known that many fiber properties are

dependent upon relative humidity, which, in turn, affects the moisture content of the fiber.

In Figure 13, the sonic modulus of the hydrophobic "Dacron"[6] polyester fiber fully reflects the insensitivity of this fiber to relative humidity. However, the other curve is an extreme example of a fiber whose properties change profoundly with relative humidity and moisture content. This is a normal hard fiber when dry, but when wet with water, it takes on the character of a very limp material, such as wet viscose rayon. This change from one state to the other is fully reflected in the sonic modulus–humidity curves for this fiber.

Sonic measurements can also be used to study certain changes taking place when a fiber is fatigued, as it is in use in tire cords where it is subject to repeated strain and relaxation. Most fibers which have been fatigued at room temperature usually fail to show any change in orientation or x-ray diffraction patterns much short of the breaking point. Indeed, the progress of fiber fatigue is a very elusive property to follow by any physical measurement short of the time when the fiber itself breaks.

The curves in Figure 14, however, disclose a most important difference between a fresh and a partially-fatigued viscose fiber. The upper curve is the sonic modulus measured on a fresh fiber during a mechanical stress–strain test, as described earlier. The lower curve is from the same fiber after a limited number of fatigue cycles short of the break. Recalling that sonic observations go hand in hand with molecular orientation, it will be noted that while the two curves start out at the same point, indicating equivalent orientation in the unstressed fibers, the orientation efficiency—or if one prefers, the orientation response—of the fiber to strain during a stress–strain test is much less for the fatigued sample than for the fresh one. In an almost real sense, the structure of the fatigued fiber has become tired. Its molecular structure just can't respond to new stress as it once did before it was put through a fatigue cycle.

Other sonic studies have related polymer constitution to orientation efficiency, and to ultimate strength, fiber liveliness, fiber resilience, creep, and growth properties, but space here does not permit discussion of all these detailed applications. If what has been reviewed demonstrates the usefulness of sonic phenomena as a research tool related to both physical and chemical constitution of synthetic fibers, this presentation will have accomplished its purpose. The method is not too complex; in many instances its data are unique. Best of all, the tool is far from having reached its full state of development and application.

[6] Du Pont trademark.

Literature Cited

1. Ballou, J. W. and Smith, J. C., *J. Appl. Phys.* **20**, 493–502 (1949).
2. Hamburger, W. J., TEXTILE RESEARCH JOURNAL **18**, 705–743 (1948).

Part II: Elastomeric Condensation Block Copolymers[1]

W. Hale Charch[2] and Joseph C. Shivers

Pioneering Research Division, Textile Fibers Department, E. I. du Pont de Nemours and Company, Inc., Wilmington, Del.

FROM physics and hard fibers, we would like to return to chemistry and the other end of the spectrum to examine a family of rubbery polymers to see the effects of chemical structure on long-range elastic properties. We shall not discuss the usual diene elastomers, which have been so extensively studied, but rather look at the less familiar class of elastomeric materials based on condensation block copolymers.

It has been shown by Wittbecker and coworkers [5] that a crystalline high-melting polyamide such as 6-10 can be converted to an elastomeric polymer by substituting part of the amide hydrogens with alkyl groups. Table I illustrates how profoundly physical properties of a 6-10 polyamide fiber change when half of the amide hydrogens in the polymer are substituted with isobutyl groups. Breaking elongation changes from 25% to 400%, or 16-fold. Furthermore, much of this elongation is reversible. The drop in melting point demonstrates how importantly hydrogen bonds function in tying adjacent chains together in a hard polyamide fiber. Strength and modulus of the fiber drop by the substitution, but this must always occur when elastomeric properties appear. Comparable data for vulcanized rubber are cited in the last column.

Figure 1 illustrates the changes which occur by progressive substitution of the amide hydrogens from 0 to 100%. It is typical of a large number of polyamide systems. Here, sebacic acid is polymerized with different ratios of three diamines—hexamethylenediamine, N-isobutylhexamethylenediamine, and N,N′-diisobutylhexamethylenediamine. As the ratio of the N-substituted ingredient increases, melting points drop. When about half the hydrogen bonds are destroyed in the middle zone, long-range elastomeric properties appear. Further substitution gives extremely soft, sluggish, or even puttylike materials in the zone on the right. The notable point is that, for recoverable elasticity, there is an optimum degree of N-substitution. Unless some part of the polar hydrogen bonds be retained in the polymer to prevent undue chain slippage when the fibers are stretched, one will fail to realize significant elastic recovery. Hydrogen bonds in this type of elastomer are regarded as the structural counterparts of the chemical cross-links introduced into natural and synthetic rubbers by vulcanization.

Elastomeric condensation polymers are by no means limited to polyamides. Polyethylene terephthalate is a high melting crystalline polyester of medium-high chain stiffness. Even so, Snyder [4] demonstrated that progressive substitution of the stiff terephthalic acid elements by the 10-carbon flexible chain sebacic acid gave the composition property map in Figure 2. Both polymer melting points and transition temperatures drop with increasing content of sebacic acid. However, in contrast with the polyamide case, the polyester has no hydrogen bonds to be destroyed, rather only its crystallinity to lose as increasing amounts of terephthalic acid are replaced with sebacic acid in the copolymer. Nevertheless, recoverable elastic properties again appear in the middle zone and disappear as we move into the zone to the right, where the properties of ethylene sebacate as a low melting crystalline homopolymer appear. In the middle elastic zone, it is the residual crystallinity of the polyethylene terephthalate units which furnish tie

TABLE I

	6-10 Polyamide	6-10 Polyamide with 50% N-substitution	
	Crystalline oriented hard fiber	Amorphous elastomeric	Natural rubber Vulcanized
Strength, g./den.	4.5	1.25	0.20
Elongation, %	25	400	600–1000
Modulus from stress-strain curves	20	0.3–0.5	0.01–0.02
Elastic recovery, %	—	95–98	100
Polymer melting point, ° C.	230	146	

[1] Presented by W. H. Charch, September 12, 1957 at Columbia University, as part of the Charles Francis Chandler Lecture.

[2] Former Research Director, Pioneering Research Division, Textile Fibers Department, E. I. du Pont de Nemours & Company, Inc. Deceased July 25, 1958.

points preventing undue chain slippage under stress and causing a very high degree of recovery from strain.

For the synthetic fiber technologist it is significant that many elastic polymer structures possess no chemical cross links; hence they can be melted or dissolved and spun into fine fibers by conventional methods. Unfortunately, however, the melting points of typical fibers from the classes of polymers mentioned above are too low to permit them to be ironed when used along with other fibers in a fabric. Hence, if one would have an elastic textile fiber, one confronts the awkward problem of combining good elastic properties, which call for a low polymer melting point and low transition temperature, with a high ironing temperature, which calls for a high melting point, in one and the same polymer.

In the copolyester system just discussed, the polymer chain is composed of units of ethylene terephthalate "hard" segments and ethylene sebacate "soft" segments. Each segment tends to have a destructive effect on the crystallinity of the other. A roundabout way to prepare such a copolymer is to start with the two homopolymers in some chosen ratio and melt-blend these together at a temperature where ester interchange occurs. The interchange will take place first in very large segments, a part of one polymer chain joining with a large segment of the other species. As reaction proceeds, these large segments continue to interchange and split into smaller and smaller segments, until final equilibrium yields the same final distribution of the two components in the chain approaching a more or less regular distribution of the two elements just as though one had conducted a conventional polymerization starting with monomeric intermediates.

This type of melt blending of polymers was carried out by Snyder [3]; Figure 3 illustrates schematically the course of this typical interchange reaction, the polymer melting temperatures progressively dropping as interchange proceeds. The dashes represent units of ethylene sebacate and the X's units of ethylene terephthalate; that is, flexible and stiff elements, respectively. Early stages of the reaction result in interchange in large blocks, which break into smaller blocks at intermediate stages and into a random copolymer at the final stage. Through all stages, the chemical composition of the copolymer remains at a constant 60–40 mole ratio. It is merely the distribution and size of elements as

TABLE II. Elastic Copolyesters

	Ten., g./den.	Elong., %	Modulus at 100% elong., g./den.	Recovery, %	Polymer melt temp., °C.
Random copolymer	0.7	300	0.40	95	120
Block copolymer	0.7–0.6	200	0.55	96	165

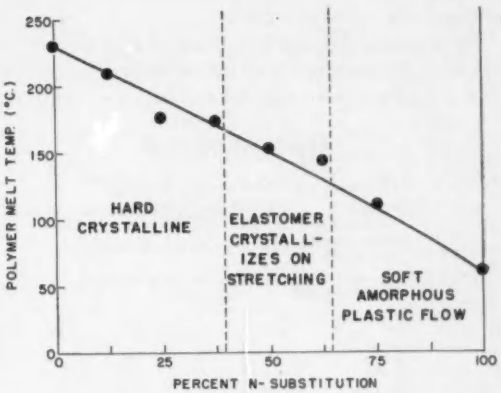

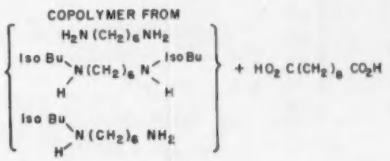

Fig. 1

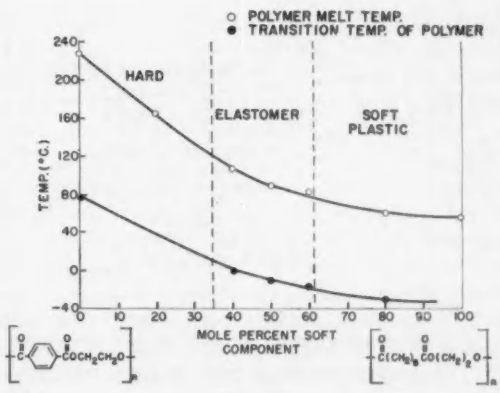

Fig. 2.

blocks up and down the chain that changes. The process can be interrupted at any point on the time scale.

Table II presents typical data where interchange was interrupted about halfway through. The block copolymer existing at this stage possesses a 40° higher melting point than the random copolymer. Strength, modulus, and elastic recoveries are very similar, although the block polymer shows somewhat less total elongation. Detailed study of such cases teach that it is qualitatively possible to a marked degree to combine significantly high melting points with significant elastic properties in one and the same polymer.

As a practical operation, interchanges of this sort are very difficult to carry out with precise control. One would prefer to directly introduce an appropriate low-melting elastic segment into the polymer which could not undergo interchange or other reaction during a conventional polymerization cycle.

Edgar and Hill [1] in England, in 1952, described certain polyethylene terephthalates modified by large blocks of polyethylene glycol. They showed that relatively large weight percentages of a 4000 molecular weight polyethylene glycol introduced into the polymer exerted only minimal effects on melting point. On the other hand, the same weight percents of diethylene glycol caused very substantial depressions in melting points, as shown in Figure 4.

While the weight percent of the polyglycol here is 17, its molar percent is only 1. Flory's early work [2] also showed that melting point depression in copolymers depends on the mole percent of the modifier, rather than its actual weight.

The English workers disclosed only hard polymers with up to 30 weight percent modification. Meanwhile, our laboratories were investigating the entire spectrum of polyglycol modification of polyethylene terephthalate, particularly the higher weight percents which produce elastomeric properties. Figure 5 is the property map for this copolymer system.

Again, elastic compositions emerge in the zone between hard-crystalline and soft low-melting polymers. It is to be noted here that melting points or stick temperatures of this block copolymer drop off only moderately in the elastic region and much less so than in the systems presented earlier. This is particularly notable in view of the fact that the x-ray crystalline melting points of the polymer drop quite fast in the elastic range, the curves crossing at 65% modification.

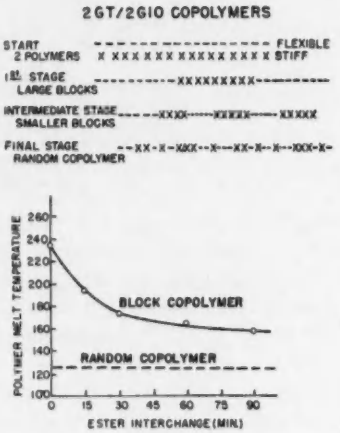

Fig. 3

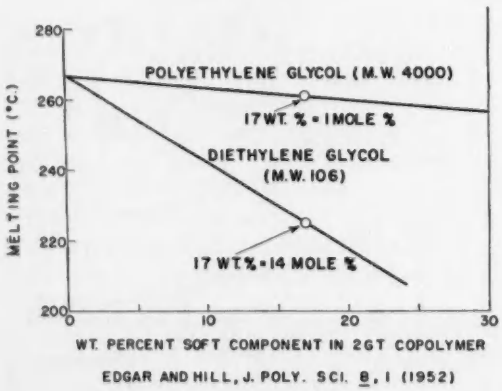
MELTING POINT (°C.)
POLYETHYLENE GLYCOL (M.W. 4000)
17 WT. % = 1 MOLE %
DIETHYLENE GLYCOL (M.W. 106)
17 WT.% = 14 MOLE %
WT. PERCENT SOFT COMPONENT IN 2GT COPOLYMER
EDGAR AND HILL, J. POLY. SCI. 8, 1 (1952)

Fig. 4

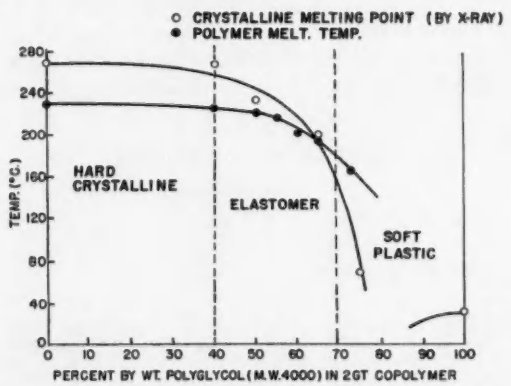

Fig. 5

TABLE III

	Polymer melting point, ° C.	Elongation, %	Short term stress decay, %
Copolyamide 6–10 (50% N-substitution)	140	280	20
Copolyester (random) 2 GT/2G10	120	300	20
Copolyester (block) 2 GT/2G10 by ester interchange	170	200	
Copolyester polyglycol modified	200	350	8

Table III now presents the melting point summary for the four classes of elastomers just discussed (N-substituted polyamides, random copolyesters, block polyester interchange, and block polyesters with fixed blocks). The polyglycol block copolymer at the bottom of the chart exhibits at one and the same time the highest melting point, highest elongation, and, most significantly, the lowest stress decay. It also illustrates how, by employing large blocks, properties of two different polymers can often be combined to a large degree rather than averaged out, as when we have random distribution of monomeric units in a polymer chain.

Since the large polymeric block seems to be responsible for this combination of properties, we may now examine how the molecular weight of this block affects melting point.

In Figure 6 the molecular weight of the polyglycol is varied over an eightfold range from 750 to 6000 while keeping its total weight percent in the polymer constant at 60%. The effect is profound and, for a high melting point, the choice lies clearly with the use of the higher molecular weight soft segments.

With this point established, one next inquires as to the effect of the molecular weight of this same block on elastic properties.

In Figure 7 the molecular weight of the soft segments is carried through the same eightfold range of molecular weights for a 50% by weight polyglycol content. An ideal elastic fiber will possess the lowest stress decay, measured by the scale on the left, and the highest tensile recovery, measured by the scale on the right. It is seen that the optimum for both these properties occurs with a polyglycol of 4000 molecular weight; from Figure 6 it is known

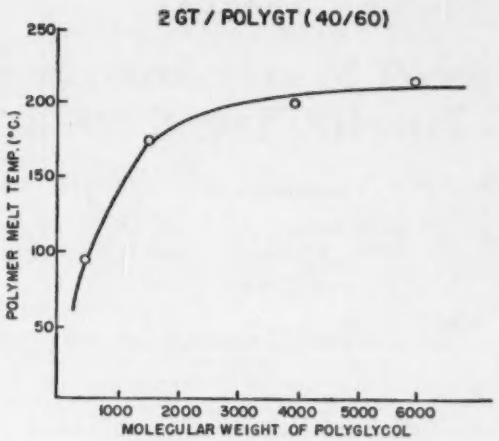

Fig. 6

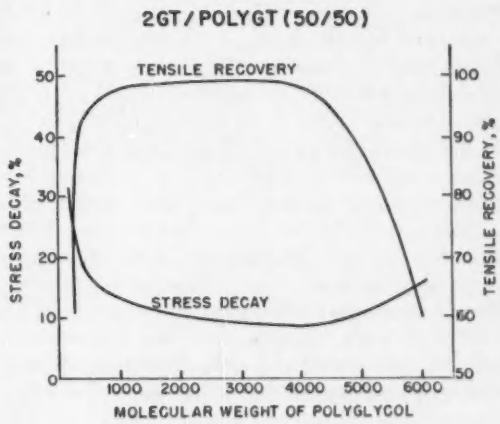

Fig. 7

that the polymer will still be relatively high melting. With all the data now favoring a 4000 molecular weight block, one now makes a final check of tensile recovery and stress decay as related to the optimum weight percent of this segment in the polymer.

Figure 8 shows that the optimum content of the preferred soft segment in the polymer for both stress decay and tensile recovery differs slightly, but at this point there is nothing further we can do about bringing them together. However, 60 weight percent of the soft segment represents a good compromise, so we can settle for this composition without sacrifice of a high melting point such as we wish to retain in the fibers spun from this polymer.

The copolymer systems here discussed are pre-

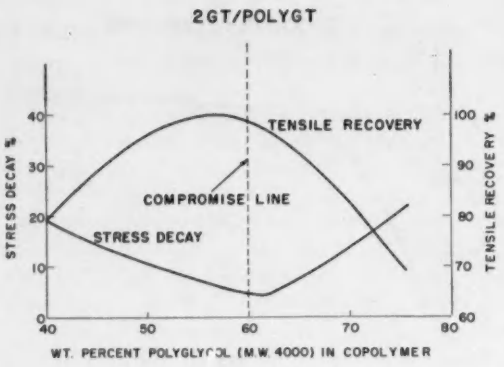

Fig. 8

sented only as prototypes of a very large family of condensation elastomers which combine both hard and soft blocks, that is, flexible and stiff segments in the same polymer chain. The polyether blocks must be randomly coiled in the relaxed fiber, but, being largely free from interchain bonding or crystallization with themselves, they can uncoil when the fiber is stretched and retract when stress on the fiber is released. At the same time, a substantial content of high melting crystalline segments remain in the polymer. Since these tend to crystallize even further when the fiber is stretched, they then act as tie points between polymer chains when the fiber is extended; they prevent any significant permanent plastic flow.

Without one's departing from the above principles, there is a wide choice of structures for both hard and soft segments. However, a given soft segment will produce somewhat different fiber properties as it is combined with one or another hard segment.

The low melting macrosegments usually have between 125 and 250 atoms in the chain. If they are too long they themselves may tend to crystallize and so adversely affect elastic recovery. Other soft segments known to convey elastic properties are the polyglycols, oxides, and sulfides of polypropylene and polybutylene.

For hard segments, almost any high melting well-crystallizable polymer melting over 200° C. will do; polyamides, polyurethanes, polyesters, polyureas, etc. Some of the highest melting of these are the most suitable to combine with the lowest melting of soft segments. The weight percent of the hard segment for use with a given soft segment will usually vary inversely with the melting point of the hard segment. In some cases, as little as 10% hard segment will suffice. In others, as much as 50% will be needed.

Generally speaking, each polymer system is a separate structure-property study if one would go into its finer detail. We have presented the analysis above only as a typical case which it is hoped will illustrate certain principles that may be employed in the formulation of polymer composition to yield certain prescribed fiber properties.

Acknowledgment

The authors wish to acknowledge the use of experimental data taken from work carried out by R. E. Albert, J. D. Grandine, and F. B. Moody in the Pioneering Research Laboratory.

Literature Cited

1. Edgar, O. B. and Hill, R., *J. Polymer Sci.* **8**, 1 (1952).
2. Flory, P. J., *J. Chem. Phys.* **17**, 223 (1949).
3. Snyder, M. D., U. S. Patent 2,623,031.
4. Snyder, M. D., U. S. Patent 2,623,033.
5. Wittbecker, E. L., Houtz, R. C., and Watkins, W. W., *Ind. Eng. Chem.* **40**, 875 (1948).

Manuscript received February 9, 1959.

A Kinetic Study of the Supercontraction of Wool Fibers in Solutions of Salts, Acids, and Alkalies

W. G. Crewther and L. M. Dowling

Division of Protein Chemistry (formerly Biochemistry Unit), Wool Research Laboratories, C.S.I.R.O., Parkville, N.2. (Melbourne), Victoria, Australia

Abstract

Wool fibers contract in hot solutions of acids or alkalies, the initial rate of contraction increasing with increasing concentration of the acid or alkali. At the higher concentrations contraction is followed by elongation of the fibers to lengths which may exceed the original length. The maximum contraction obtained decreases with increasing concentration of acid or alkali used. Comparison of the rates of contraction of wool fibers in solutions of different salts in 1 or 4 *N* HCl shows that cations and anions fall in the following order of decreasing contraction rate: $Li^+ > Na^+ > K^+$ and $I^- > Br^- > Cl^-$.

Kinetic curves for the contraction of wool fibers in 1 *N* HCl containing salts show well-defined two-stage contraction. With 4 *M* LiBr or NaI this appears as a shelf in the curve at 25–30% contraction, and with many fibers the final level of contraction exceeds 70%. With 5 or 6 *M* LiI or 6 *M* NaI the fibers contract by about 25%, elongate to a length which may approach the original, and then again contract; in such solutions a considerable proportion of the wool protein is dissolved, leaving a sulfur-rich residue. Two-stage contraction kinetics have been observed only when using solutions with pH values in the lower range. As the pH is increased the rate of contraction also increases, particularly at pH values greater than about 8.

The two-stage contraction kinetics have been interpreted in terms of the contraction at different rates of two structures in the wool fiber.

Introduction

The important effect of pH on the rate of supercontraction of horsehair, silk, and polyamide fibers has been demonstrated by Elod and Zahn [21] using phenol as the supercontracting agent. With horsehair the rate increases with increasing pH, particularly at values above about 5, whereas polyamide and silk fibers contract readily at pH values near neutrality but relatively slowly in acidic or alkaline solutions of phenol. Wool, like horsehair, shows a marked increase in rate of contraction in phenol as the pH is increased above 5, an effect which is partly due to ionization of the phenol [3]. Because of this ionization, with its concomitant changes in concentration of reactants and in ionic strength, only limited conclusions can be drawn from this work regarding the effect of pH on the thermal stability of the wool proteins, particularly in alkaline solutions. From this point of view supercontraction studies using salt solutions at different pH levels should be more informative.

In the experiments to be described, the range of pH has been extended to include solutions of acids and alkalies without the addition of salts. Experiments with horsehair have already shown that it supercontracts in hot dilute solutions of acids [20] or when treated with cold or hot solutions of alkalies [14]. However, similar experiments with fine wool fibers have not been recorded, possibly because of the difficulty of making length measurements on these fibers, which become very fragile. This difficulty has been overcome in the present experiments by using a simple method for measuring the fibers while they are still immersed in the test solutions. Kinetic studies of the contractions are also facilitated by this method.

It was of interest, also, to assess the relative effects of a series of anions and cations in acidic solutions and compare them with those previously found at pH 7 [4]. In this way it has been possible to obtain information concerning the importance of anion adsorption in relation to the state of ionization of the wool proteins. The theoretical aspects of this problem have been discussed in connection

with the thermal shrinkage of collagen in solutions of salts [5].

In addition, this study has provided useful information concerning the nature of the two-stage contractions first reported by Haly and Feughelman [12] and suggests a further explanation for this effect.

Materials and Methods

Corriedale 56's wool was detipped and cleaned by rinsing three times in cold light petroleum (b.p. 40–60° C.), once in cold ethanol, and several times in cold distilled water. The wool was dried in a stream of air at 40° C.

Acids and alkalies were A.R. quality, as were NaCl, NaI, KCl, and KI. The LiBr and LiI were B.D.H. Laboratory Reagents and the LiCl was supplied by Harrington Bros., London.

Measurements of supercontraction were made by two methods. In the first the fiber was attached at its ends to two hooks using softened polystyrene. The length of fiber (approximately 7 cm.) between the hooks was measured and the fiber, suspended by one hook from a stainless wire passing through a stopper, was lowered into a test tube. The wire was of such a length that the second hook rested on the bottom of the tube without straining the fiber during contraction. The hot salt solution was then added to cover the fiber and the tube incubated in a boiling water bath for the required time, the temperature of the salt solution being approximately 98.5° C. The salt solution was removed from the tube and the fiber recovered and measured. Measurements of the length of fiber were made with the fiber stretched just sufficiently to remove the crimp.

The second method of measurement permitted a study of the kinetics of contraction of the fibers. The fiber was attached with molten polystyrene to a short fine glass rod inserted in a rubber stopper closing the lower end of a 7 × 150 mm. pyrex tube. The upper end of the fiber was attached to a long fine glass rod passing through a stopper closing the upper end of the tube. A white-on-black scale was attached to the tube by rubber bands and both scale and tube were immersed in a test tube of water which was heated in a beaker of boiling water. The length of the fiber was measured on the scale after sliding the rod through the stopper until the crimp of the fiber was just removed. The rod was

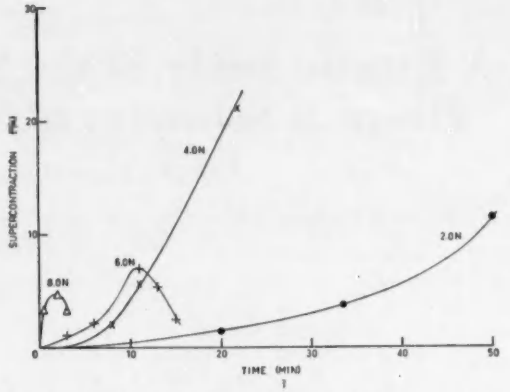

Fig. 1. The kinetics of contraction of wool fibers in solutions of HCl of different concentrations at 98.5° C.

then pushed down to slacken the fiber and, after bringing the fiber to temperature in the bath, the hot test solution was added and measurements of length made at appropriate intervals. The fiber was slackened after each measurement. The stoppers were boiled in concentrated HCl and washed before use. Before and after heating with the fibers, the pH values of the test solutions were measured at room temperature using a glass electrode and potentiometer (Jones, Melbourne). A soda glass electrode was used for the lithium salt solutions and a lithium glass electrode for the other salt solutions. Test solutions, excepting those containing relatively high concentrations of acid or alkali, were buffered with 0.1 *M* solutions of sodium salts as follows: <pH 4, formate; 4–6, acetate; 6–7.5, succinate; 7.5–10, tris hydroxymethyl amino methane or borate; > 10, piperidine. With the exception of solutions of salts in 1 or 4 *N* HCl, free halogen present in the salt solutions as a result of atmospheric oxidation was removed by the addition of a few crystals of sodium thiosulfate [10]. Rapid atmospheric oxidation prevented the complete elimination of free iodine from acid solutions of iodides. However, on testing solutions of 4 *M* LiBr or 6 *M* LiCl with starch iodide papers, no trace of free halogen could be demonstrated.

Several fibers were tested under each set of experimental conditions. Since the use of mean values for constructing the kinetic curves would introduce spurious two-stage effects and mask real two-stage effects, a single curve has been selected from about the center of the band of results for each set of conditions.

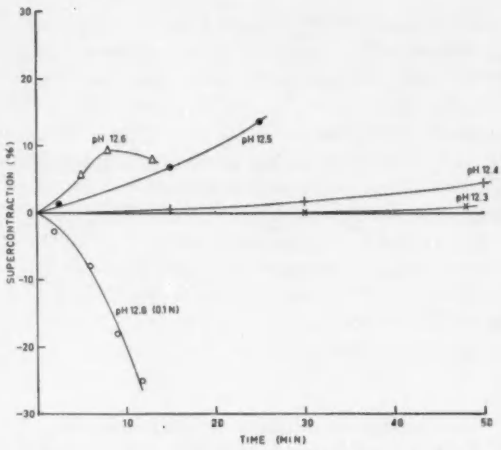

Fig. 2. Kinetics of contraction of wool fibers in solutions of NaOH of different concentrations at 98.5° C. Final pH values are indicated.

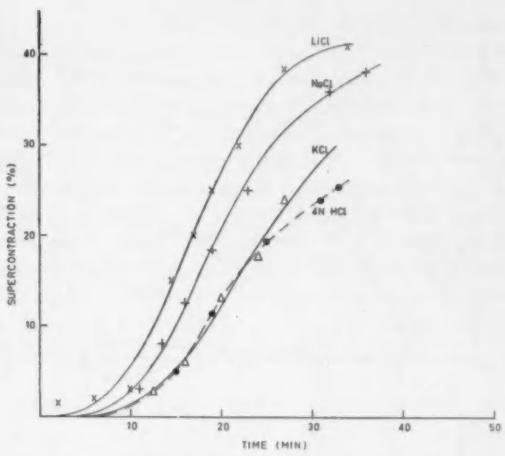

Fig. 3. Kinetics of contraction of wool fibers at 98.5° C. in solutions of 4 *N* HCl containing 1 *M* concentrations of salts.

Experimental and Results

Supercontraction in Solutions of Acids

The kinetic method was used to follow the contraction of wool fibers in solutions of 2, 4, 6, and 8 *N* HCl at 98.5° C. In dilute acid the contraction is slow (Figure 1), but with increasing concentration the initial rate is greatly increased. It is characteristic of the more concentrated solutions that, after a period of contraction, the fiber elongates and in some cases approaches the initial length before breaking. The maximum contraction attained is least with the more concentrated acid solutions and greatest with the least concentrated solutions tested. Soaking the fibers in the solutions for periods of up to 1 hr. before heating in the test solutions does not affect the rate of contraction.

Contraction in Solutions of Alkalies

The rates of contraction of wool fibers in solutions of alkalies are shown in Figure 2. In general, with increasing pH of the solutions the rate of contraction of the fibers also increases, but so too does the rate of the subsequent elongation. With increasing concentration the elongation is accelerated more than the contraction, so that with 0.1 *N* NaOH the fibers elongate almost immediately after contact with the alkaline solution; the increase in length may reach 30%. With highly alkaline solutions such as those used in this experiment the fibers become very fragile, and extreme care is required in handling them.

Contraction in Acid Solutions of Salts

The kinetic method was used to compare the contraction of fibers in solutions of 4 *N* HCl containing 1 *M* concentrations of the salts KCl, NaCl, or LiCl. Figure 3 shows that with solutions of KCl in 4 *N* HCl the rate of contraction is not appreciably different from that obtained with 4 *N* HCl, but the rate of contraction is increased by the presence of NaCl and even more so by LiCl. Similarly, the addition of 4 *M* LiCl, LiBr, or LiI to 1 *N* HCl increases the rate of contraction, the bromide giving faster contraction than the chloride and the iodide than the bromide (Figure 4).

The kinetic curves for contraction in 1 *N* HCl containing 4 *M* LiBr or NaI show a slight but definite shelf at contraction levels of 25–30% (Figure 4). This effect is more pronounced with LiI and takes the form of an initial contraction to about 25% followed by elongation of the fiber until a second period of contraction occurs (Figures 4 and 5). With 4 *M* solutions of each of these salts, the second period of contraction proceeds until the fiber is less than 30% of its original length. With 6 *M* LiCl most of the fibers broke after contracting about 50%, but Figure 4 shows that contraction was continuing steadily at this level.

Solutions of 4 *M* LiI in 1 *N* HCl cause the fibers to contract by 25–30% and then elongate by as

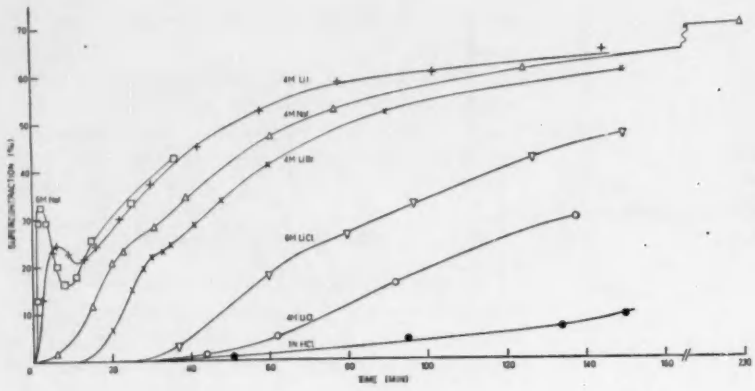

Fig. 4. Kinetics of contraction of wool fibers at 98.5° C. in 1 *N* HCl containing 4 *M* concentrations of salts.

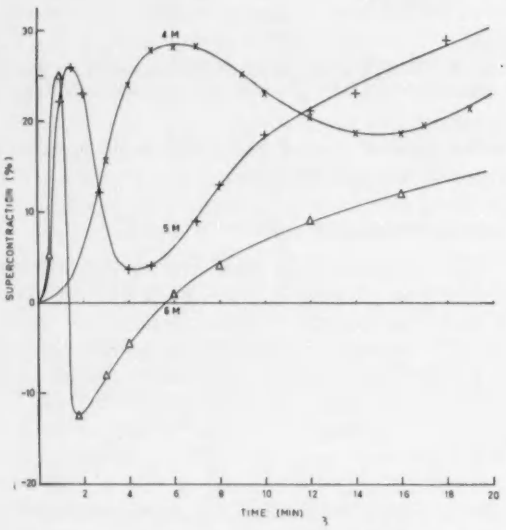

Fig. 5. Kinetics of contraction of wool fibers at 98.5° C. in 1 *N* HCl containing LiI.

much as 10% before the second stage of contraction develops. With 5 and 6 *M* LiI this effect is accentuated (Figure 5), and with 6 *M* LiI the elongation is greater than the initial contraction, so that for a short time the fiber length is increased by as much as 15% between the first and second stages of contraction.

The contractions in acid solutions of salts resemble those reported by Haly and Feughelman [12] in being reversible up to the first stage of contraction. For example, after 25% contraction of a wool fiber in 4 *M* LiBr/1 *N* HCl solution, washing in hot water restored the fiber length to within 1% of the original.

Microscopic examination of fibers contracted in 1 *N* HCl containing 4 *M* LiBr or NaI shows no apparent difference from fibers contracted in similar salt solutions at pH 8; corrugations appear in the cuticle [3, 13], and these become more marked as contraction proceeds. Longitudinal striations appear in the cortex, and the orthocortex and paracortex are readily distinguishable by differences in the degree of striation. After heating for prolonged periods with solutions causing 70% contraction, the cuticle appears puckered and rugous. With 6 *M* LiI the initial contraction causes the usual corrugations to appear; these disappear as the fiber returns to its original length. In the second stage of contraction, the cuticle becomes so loosely attached to the cortex that no obvious corrugations appear. During this process and the period of elongation, the longitudinal striation of the fiber becomes more pronounced until the cortex appears as a distorted mass of aligned cell residues.

From the microscopic study it was apparent that a portion of the fiber is extracted during the heating in 5 or 6 *M* LiI. A quantitative study of this was made by heating 100-mg. samples of wool in 25-ml. aliquots of 5 *M* LiI in 1 *N* HCl for different periods of time, washing three times in distilled water with a total period of soaking of 24 hr., and drying and weighing. In order to determine whether the kinetics of contraction of single fibers is affected by the reduction in liquor/wool ratio, a special vessel was constructed for observing the contraction of single fibers in liquor containing a bulk sample of wool. The apparatus consisted of a central vertical test tube connected by lateral tubes at the base with two narrower vertical tubes. These side tubes were fitted with stoppers, glass rods, and scales.

Single wool fibers were mounted in the usual manner in the side tubes, while the central tube contained 100 mg. of wool. The apparatus was placed in a boiling water bath, 25 ml. of the hot salt solution was added to the central tube, and the contraction of the two fibers followed in the usual manner. At frequent intervals liquid was sucked out of the side tubes by applying suction to the top of the central tube; in this way the liquor was kept well mixed.

The residues from the estimates of protein extracted from the wool were subjected to analysis for disulfide content using the method of Shinohara [17]. The changes in weight of the wool, supercontraction, and disulfide content with time of heating are shown in Figure 6. During the first stage of contraction there is little decrease in the weight of the fibers, but the disulfide content falls slightly. In the subsequent elongation of the fibers, the weight of the wool falls more rapidly and the disulfide content increases. These trends continue and become more evident in the second stage of contraction when, after 10 min., 70% of the wool has passed into solution and the disulfide content of the residue is 30–37% higher than that of the original wool. In solutions causing contractions of about 70%, such as 4 *M* LiBr in 1 *N* HCl, very little solution of protein occurs.

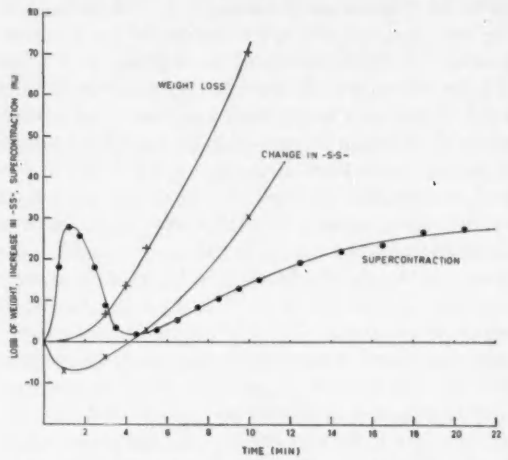

Fig. 6. Changes in weight, length, and disulfide content of wool fibers heated in a solution containing 5 *M* LiI and 1 *N* HCl.

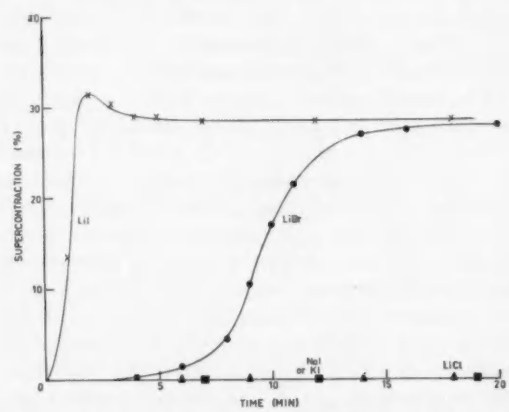

Fig. 7. Kinetics of contraction of wool fibers at 98.5° C. in 4 *M* salt solutions buffered at pH 8.0 with 0.1 *M* borate.

Contraction in Salt Solutions at Intermediate pH Values

Both methods were used in this study. Figures 7 and 8 show the kinetics of contraction of wool fibers in salt solutions of various compositions and pH; two stages of contraction can be observed only at the lower pH values (Figure 8). Contractions in alkaline solutions of LiI are characterized by rapid contraction to a maximum value followed by a rapid elongation to a more or less constant contraction (Figure 7). The decrease in the maximum contraction value which occurs as the pH increases (Figure 8) is also noteworthy. Figure 7 demonstrates the marked difference in rates of contraction in a series of salts having a common ion, the order of contraction rates being LiI > LiBr > LiCl and LiI > NaI. From data of the type shown in Figures 7 and 8 together with data from single

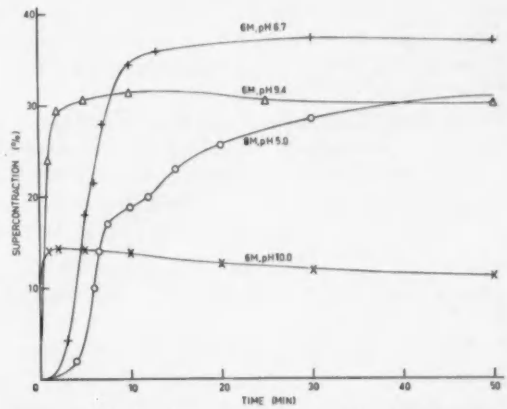

Fig. 8. Kinetics of contraction of wool fibers in solutions of LiBr at 98.5° C. under different conditions of concentration and pH.

measurements it has been possible to obtain a relationship between pH and the concentration required to give a predetermined contraction, say 20%, in 1 hr. Figure 9 shows that as the pH is raised the concentration of NaI required to give a certain initial rate of contraction is lowered; this increase in ease of contraction of fibers with increasing pH is particularly evident at pH values above 8.

Discussion

The curves representing the kinetics of contraction of wool fibers in 1 *N* HCl containing salts such as LiBr or NaI show some remarkable features. First, with 4 *M* LiBr or NaI the contractions occur in two stages (Figure 4) similar to those reported by Haly, Feughelman, and Griffith [12, 13]. The unusual feature of these curves lies in the contraction levels of the first stage and the final contractions compared with those obtained at higher pH values. Haly and Feughelman [12] quote values of about 15% for the first stage contraction of Corriedale wool and final contractions of about 41% in unbuffered 8 *M* LiBr, and similar values have been obtained at pH 5 with the wool used in these experiments. On the other hand, salt solutions in 1 *N* HCl give contractions of 25–35% in the first stage and final contractions of approximately 70%. This appears to be the greatest value yet recorded for supercontraction of wool fibers. It is of interest that the extensive contraction of 58% recorded by Speakman [18] was also obtained by heating fibers in dilute acid (0.1 *N* HCl), but in this case a pre-

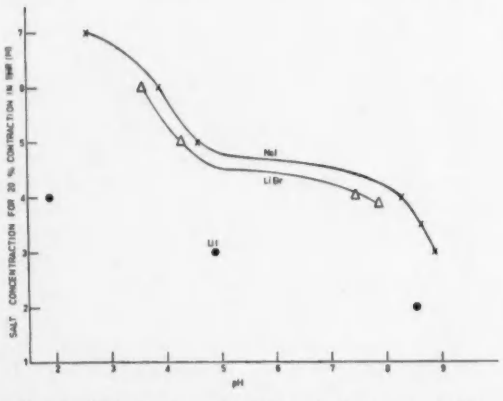

Fig. 9. Relation between pH and the concentration of NaI, LiBr, and LiI required to cause 20% supercontraction of wool fibers in 1 hr. at 98.5° C.

treatment with chlorine dioxide was necessary. With 4 *M* LiBr or LiI at pH 8.0, the maximum contraction is less than 35% (Figure 7), the contraction occurring apparently in a single stage.

Haly, Feughelman, and Griffith have sought to interpret the two-stage contraction of wool fibers in unbuffered LiBr solutions in terms of a model consisting of aligned peptide chains cross-linked at intervals by disulfide bonds and at intermediate points by strong and weak hydrogen bonds. They suggest that the first stage of contraction results from the breaking of the weak hydrogen bonds and the second stage from the breaking of the stronger hydrogen bonds which they tentatively associate with the tyrosine side chains [11]. The final contraction was thought to be limited by the disulfide bonds. By application of the formula of Eyring [7] for the mean distance between the ends of a random chain molecule, the mean distance between the various types of cross-linkage along the peptide chains was calculated and compared with the amino acid composition of wool. This model cannot be applied satisfactorily to the present data; such a quantitative approach is invalidated by the variability in levels of the first stage and final contractions in salt solutions (Figures 4 and 8) and in solutions of phenol [3]. If disulfide bonds were responsible for limiting the final level of contraction in 8 *M* LiBr near pH 5, as Haly, Feughelman, and Griffith suggest, a similar or lower level of contraction would be expected in acid solutions, since disulfide bonds have their maximum stability in 1 *N* acid [16]. The levels of contraction obtained in chlorine-free LiCl in 1 *N* HCl eliminates the possibility that free halogen formed by atmospheric oxidation is disrupting disulfide bonds and so permitting more extensive contractions.

The second unusual feature of the kinetics of contraction of wool fibers in 5 or 6 *M* LiI in 1 *N* HCl is the appearance of a period of elongation between the first and second stages of contraction (Figures 4 and 5). The phenomenon of contraction followed by elongation has been observed with wool fibers heated in various solutions of salts or phenol and in each case the phenomenon was associated with solution of a portion of the protein of the fiber [3, 6]. That a similar solution of protein takes place in acid solutions of 5 or 6 *M* LiI is shown by Figure 6. The partition of the contraction process into two stages by a period of elongation suggests, therefore, that we are dealing with the contraction of two

different structures at different rates. We can visualize the process of contraction as consisting of a swelling and loosening of the protein structure to such a degree that the polypeptide chains can change at a finite rate to a more or less random configuration; the fiber then shows the properties of an elastomer. Continuance of this loosening process would decrease the number of points of cohesion between the contractile units of the fiber until eventually solution of the unit protein structures occurred. As cohesion between the contracted units of the fiber decreased, slippage would tend to occur between individual units. This would lessen the stress responsible for deformation of uncontracted and noncontractile portions of the fiber, which would tend to return to its original length. In a fiber containing two contractile structures having different rates of contraction in acid solutions of salts, contraction and partial solution of the first structure followed by contraction of the second structure would give kinetics similar to those observed experimentally (Figures 4 and 5). Extensions to lengths greater than the original may be due to increased longitudinal swelling following configurational changes in the proteins of the fiber. That supercontracted wool fibers are swollen longitudinally is demonstrated by the fact that they contract further when removed from the salt solution, washed, and dried. The elongation itself cannot be attributed to this longitudinal swelling, since the phenomenon of increased contraction following washing and drying can be observed with supercontracted fibers whether or not they elongate following the contraction; swelling would not be expected to occur after the contraction process was complete. The fibers would be expected to approach an equilibrium value which would be influenced by both the extent of contraction and the amount of swelling in the particular solution being used.

If the elongation between the first and second stages of contraction is the result of slippage between contractile units of structure, the model of Feughelman, Haly, and Griffith, although providing an adequate explanation for the results on which it was based, cannot explain the kinetic curves of Figures 4 and 5. If slippage occurred between the contracted units of this model, it would be necessary to rupture disulfide bonds and the strong hydrogen bonds which, it is suggested, break during the second stage of contraction. Once sufficient bonds were broken to allow intermolecular slippage, no further contraction would be possible. The hypothesis that there are two contractile structures in wool fibers therefore appears preferable, since it applies over the whole range of experimental conditions. The sequence, contraction–elongation–contraction, can be observed qualitatively in fibers loosely suspended in the hot salt solution. Hence the elongation is not caused by the process of measurement.

Any attempt to identify the two contractile structures of the wool fiber with particular histological structures is difficult because there can be no certainty that the sequence of contraction of the two phases will be the same in solutions of different composition and under different conditions. The magnitude of the contractions obtained in each stage with acid solutions of salts (Figure 4) suggests, in fact, that under certain conditions only one phase or structure may contract. When the conditions are such that supercontraction takes place slowly, the fibers are observed to straighten and then curl tightly due to the more rapid contraction of the orthocortex as compared with that of the paracortex; the fibers again straighten when the orthocortex reaches maximum contraction and the extent of the contraction of the paracortex approaches that of the orthocortex. During measurement of the initial fiber length, sufficient stress must be applied to straighten the fiber; this involves straining the paracortex until its length equals that of the orthocortex. The first small decrease in measured length ($< 1\%$) is therefore due to contraction of the orthocortex. With further contraction of the orthocortex this segment is strained during measurement to equal the length of the paracortex; consequently the major changes in length measured are those of the paracortex. It follows that the two cortical segments do not constitute the two contractile structures. We may therefore postulate the following alternatives for consideration.

1. The microfibrils are of two types which have different thermal stabilities in salt solutions.
2. The microfibrils have regions of different thermal stability alternating along their length.
3. The microfibrils and matrix constitute the two structures involved in supercontraction.

The loss in weight of wool and the increase in disulfide content of the residue during treatment

with 5 *M* LiI in 1 *N* HCl (Figure 6) and the fact that this loss of weight becomes apparent during the process of extension following the first stage of contraction might suggest that sulfur-deficient components of the wool are being extracted from the proteins which contract during the first stage. However, much of this material appears to be derived from the orthocortex; consequently no close correlation can be made with the contraction behavior of the resistant paracortex or with the distribution of cystine between microfibrils and matrix in this segment of the fiber.

Few data are available concerning the x-ray diffraction patterns of fibers contracted to different levels by heating in salt solutions or by other methods of supercontraction. Astbury and Woods [1] state that fibers which had supercontracted to an unspecified level after treatment with 1% NaOH and steaming gave a disoriented α-pattern. Similarly, wool fibers which had contracted 20% in 10 *M* LiCl at 100° C. showed a disoriented α-pattern, but there was also loss of intensity of the pattern [9]. Thermal contraction to levels greater than 30% in solutions of phenol [21], salts [9], or cuprammonium hydroxide [19] resulted in loss of the α-pattern.

This rather slight evidence, although favoring the view that different contractile phases are involved, cannot differentiate among alternatives 1, 2, and 3. As regards alternative 2, the x-ray evidence would not be in accord with a model in which the regions of similar thermal stability were adjacent in adjacent microfibrils. Recent electronmicrographs [15] show two types of microfibrils in suitably treated cross sections of animal fibers, and this could support either alternative 1 or 2.

The third alternative can be considered in two ways. First, the salt solution may increase the plasticity of the matrix sufficiently to allow disorientation of the microfibrils, with a consequent increase in entropy and a shortening of the fiber. This first stage contraction would then be followed by a second stage, when the microfibrils themselves contracted as a result of the disordering of the aligned protein structures of the microfibrils. Second, both the matrix and microfibrils may contain aligned polypeptide chains cross-linked at intervals; differences in the thermal stability of these structures would lead to a two-stage contraction as these aligned units assumed a random arrangement.

The first of these alternatives cannot account adequately for the period of elongation between the two stages of contraction in acid solutions of salts. If disorientation and contraction are due to increased plasticity of the matrix permitting a more random arrangement of the microfibrils, the extension of this process to give solution of some protein constituents should facilitate the disorientation of the microfibrils still further. The chief difficulty with the second alternative is the observation by Fraser and MacRae [8] that dichroism of the N—H combination mode, *ca.* 4,860 $cm.^{-1}$, is restricted to those portions of the fiber which do not exchange readily with deuterium. If it is assumed that the crystalline regions of the fiber do not exchange readily, and bearing in mind the degree of orientation of the crystalline regions of the fiber indicated by the x-ray patterns, it might be suggested that all the oriented molecules reside in the crystalline regions. If the second theory is correct, therefore, the matrix must contain either aligned nonexchangeable material or exchangeable material in which the mean distance between cross-linkages along the fiber axis is greater than the distance between these cross-linkages when the protein assumes a random arrangement. The polypeptide chain between the cross-linkages could conceivably be sufficiently disoriented to reduce dichroism in the noncrystalline region to insignificant levels.

With solutions of HCl containing no added salt, the ionization of the carboxyl groups would be completely repressed whether the concentration of acid were 1 or 8 *N*. Consequently differences in behavior of the wool in solutions of different acid concentration must be due either to the hydrolysis of the wool proteins catalyzed by the hydrogen ions or to the effects of H_3O^+ and Cl^- in a manner comparable to the action of ions in salt solutions. The fact that the hydrogen ion is hydrated would suggest that, like the salts of Li^+, concentrated acid solutions could cause denaturation of proteins by an effect which does not involve the ionization of side chain groups or the hydrolysis of peptide bonds. Alternatively, hydrolysis of peptide linkages may increase the rate and extent of swelling and so accelerate contraction. It seems probable that solutions of salts in 1 *N* HCl bring about extensive contractions not as the result of peptide hydrolysis, which would tend to shorten the contractile units and so lessen the ultimate contraction, but rather

because certain cross-linkages, possibly salt linkages, are broken in acid solution. The reversibility of the first stage of contraction in acid solutions of LiBr would support this conclusion. In highly alkaline solutions, similar results would be expected were it not for the instability of disulfide bonds under these conditions. This would lead to solution of the proteins and consequently to the rapid initiation of the elongation following contraction.

The thermal instability of wool and collagen in solutions of salts such as those of Li^+ or I^- has been attributed to preferential adsorption of the anions by the protein [4, 5]. This theory predicts that if the resultant change in net charge were the major factor determining the stability of the protein fibers, the order of effectiveness of different ions in alkaline solutions would be reversed in experiments employing pH values below the isoelectric point of the protein. The experimental evidence for collagen showed that no such inversion occurred, although other evidence was obtained to show the important effect of the net charge on the stability of the collagen. It was suggested that another factor which is not influenced by the pH relative to the isoelectric point—the water of hydration of the cations carried into the collagen in association with the adsorbed anions—is sufficient to mask some of the effects due to changes in the net charge. Figures 3 and 4 show that the order of effectiveness of ions in causing thermal contraction of wool fibers in 1 *N* HCl is similar to that reported for salt solutions at pH 7 [4] although, as with collagen [5], the differences between ions are less at low pH values than in alkaline solutions (cf. Figures 4 and 7). It seems probable that the contractions of wool and collagen in solutions of salts have a common mechanism.

The curve relating pH and the concentration of NaI required to give 20% contraction in 1 hr. (Figure 9) is similar to that relating pH and thermal stability of wool proteins in buffer solutions as estimated by proteolysis [2]. In each case maximum stability was not observed in the isoelectric region of the wool protein but at lower pH values, and this may be related to the increasing instability of the disulfide cross-linkages with increasing pH. There is also a marked similarity between the curve of Figure 9 and titration curves for wool which suggests that the ionization of side chain groups has an important influence on the rate of contraction. This may be the reason for the differences in the effect of the pH of phenol solutions on the contraction of polyamide or silk fibers compared with that of horsehair [21].

Literature Cited

1. Astbury, W. T. and Woods, H. J., *Phil. Trans. Roy. Soc. London* **A232**, 333 (1933).
2. Crewther, W. G., *Proc. Int. Wool Text. Res. Conf. Aust. 1955* **C**, 227 (1956).
3. Crewther, W. G., *J. Soc. Dyers Colourists* **75**, 189 (1959).
4. Crewther, W. G. and Dowling, L. M., *Nature* **178**, 544 (1956).
5. Crewther, W. G. and Dowling, L. M., *J. Phys. Chem.* **62**, 678 (1958).
6. Crewther, W. G. and Dowling, L. M., unpublished results.
7. Eyring, H., *Phys. Rev.* **39**, 746 (1932).
8. Fraser, R. D. B. and MacRae, T. P., *J. Chem. Phys.* **28**, 1120 (1958).
9. Fraser, R. D. B. and MacRae, T. P., personal communication.
10. Griffith, J. and Alexander, A. E., TEXTILE RESEARCH JOURNAL **27**, 755 (1957).
11. Haly, A. R., Feughelman, M., and Griffith, J. C., *Nature* **180**, 1064 (1957).
12. Haly, A. R. and Feughelman, M., TEXTILE RESEARCH JOURNAL **27**, 919 (1957).
13. Haly, A. R. and Griffith, J., TEXTILE RESEARCH JOURNAL **28**, 32 (1958).
14. Lloyd, D. J. and Marriott, R. H., *Trans. Faraday Soc.* **30**, 944 (1934); Zahn, H., *Kolloid-Z.* **117**, 102 (1950).
15. Rogers, G. E., personal communication.
16. Sanger, F., Ryle, A. P., Smith, L. F., and Kitai, R., *Proc. Int. Wool Text. Res. Conf. Aust. 1955* **C**, 49 (1956).
17. Shinohara, K., *J. Biol. Chem.* **112**, 683 (1936).
18. Speakman, J. B., *J. Textile Inst.* **32**, T93 (1941).
19. Whewell, C. S. and Woods, H. J., "Fibrous Proteins," Soc. Dyers Colourists, Bradford, 50 (1947); Gupta, V. D., *Nature* **181**, 113 (1958).
20. Zahn, H., unpublished results; see [21].
21. Zahn, H., *Z. Naturforsch.* **2**, 286 (1947); Elöd, E. and Zahn, H., *Melliand Textilber.* **30**, 17 (1949).

Manuscript received November 17, 1958.

Photoelectric Twist Irregularity Tester

M. Uno, H. Saito, A. Shiomi, and T. Hiramatu

Kyoto Technical University, Japan

Abstract

The reflected light from a yarn squeezed flat shows its peak value when measured in a plane vertical to the twisted fibers. A twist irregularity tester based on this principle, which operates automatically and records the change of twist angle, was constructed. Several twist irregularity curves were obtained with both staple yarns and continuous filament yarns. Some factors affecting the accuracy of the test results were discussed, and the curve was compared with the twist angle measured by visual observation.

Introduction

To measure the number of turns of twist per inch of an unsized spun yarn, the specimens are generally set, one at a time, between two clamps, gauge length 10 in., and untwist-twisted until the specimen regains its original length [1]. The work is not only very tedious and inefficient, but does not give continuous recording of the result. Magni [5] improved this procedure, measuring the number of twists by untwist-twisting but without cutting the specimen each time. Henno [3] tried to stamp automatically the number of turns of twist on a paper when a continuous filament yarn was used. Gonsalves [2] contrived an automatic apparatus to count the number of photoelectric peaks due to twist of tire cord and got the frequency diagram of numbers of twist per unit length.

But it is in the case of staple yarns that the effect of twist is considered most important. Neither Henno's nor Gonsalves' method can be applied to staple yarns. Therefore, in a previous report [10], some trials were explained to get a twist irregularity curve of staple yarns automatically by the untwist-twist method. However, as Worner [11] pointed out, the untwist-twist method does not accurately measure the number of turns of twist, due to many ambiguous factors such as the initial yarn tension, elongation at no twist, and change of yarn character due to untwist-twist. So in the British Standards [6], only the removal of twist is used for measuring the twist of a yarn. Even when the yarn strength is treated theoretically, as Shorter mentioned [8], the twist angle is considered more suitable than the number of turns of twist.

The authors adopted the procedure of measuring the twist angle which has least defects and can be applied equally to either staple yarns or continuous filament yarns; they constructed a twist irregularity tester utilizing the change of peak position of reflected light quantity due to twist.

Principle of the Tester

It can be shown that, if a parallel light is cast obliquely on a smooth cylinder, the reflected light forms a cone of rays coaxial with the fiber; the semi-angle of the cone is equal to that between the fiber axis and the incident beam. Therefore, when light beam YY from lamp L is perpendicular to cylinder axis XX as shown in Figure 1, a photoelectric tube T placed on plane P, which contains beam YY and has the inclination angle θ to plane XY, measures the maximum quantity of reflected light when $\theta = 90°$ and the minimum when $\theta = 0°$.

Assuming that clusters of fibers are the aggregation of such cylinders, and utilizing the dependency of reflected light on the inclination θ, some studied the fiber orientation in webs and slivers; Orchard with card web [7], Uno for slivers [9], and Jeffries on cloth reflection [4]. But these are solely for such specimens the surfaces of which are wide and can be regarded as flat when compared with the spot size of the illuminating ray. In case of yarns, because the surface is round and too small in comparison to the spot size, the reflected light does not show the orientation of each fiber but rather indicates the direction of yarn axis due to the scattering from yarn sides, if due consideration is not taken to the light beam.

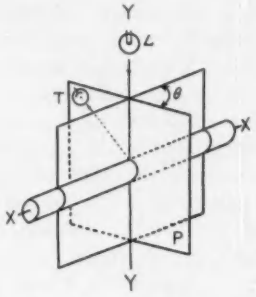

Fig. 1. Illustration of the optical arrangement.

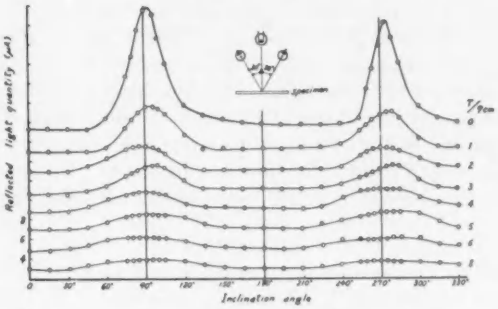

Fig. 2. Reflections from a yarn as it is (120-den. viscose filament yarn).

Figure 2 shows such an example not suitable for measuring the twist of yarn. A light beam from a 50-watt electric lamp was cast perpendicular to a specimen, rayon continuous filament yarn, 120 den. Two photomultipliers, inclined 30° respectively to the incident ray, measured the reflected light. The abscissa indicates the inclination angle θ explained in Figure 1. The ordinate is the reflected light quantity in μA, the origin of each curve being shifted stepwise to avoid the entanglement. The parameter in the figure is the number of turns of twist given to the 9-cm. specimen. Due to the increase of twist, the peak shifts slightly rightward until the number of twist reaches a certain value. But over that limit, the linear relationship between the peak shift and twist angle disappears and the peak returns roughly to the original zero-twist position. This suggests that, if the yarn becomes tight due to twist, the reflected light indicates the character of a cylinder as a whole, without showing the effect of the many oblique fibers composing a yarn.

To avoid this undesirable tendency, there are

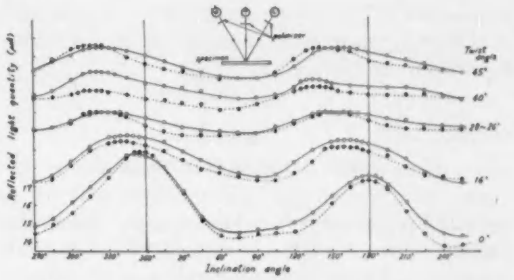

Fig. 3. Reflection when the effect of fibers lying perpendicular to the incident beam is exaggerated. Cotton intermediate roving.

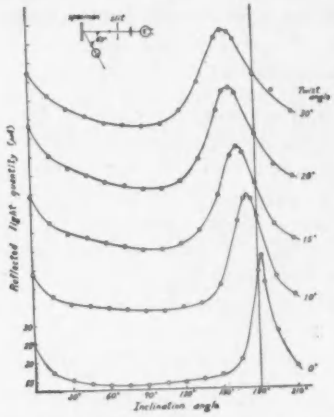

Fig. 4. Reflection when a slit is used (3000-den. viscose filaments).

three remedies, each of which will be explained below.

Exaggerating the Effect of Fibers Lying Perpendicular to the Incident Beam

With two electric lamps set on both sides of a yarn, and one photoelectric tube set vertically over the yarn, the reflection from fibers perpendicular to the incident beam can be exaggerated, because each side of the yarn is illuminated only once by one lamp. The result is shown in Figure 3, where the dotted line was obtained with the combination of polarized light and a filter lens. The peak of the curve shifts stepwise as the angle of twist increases, except in the result obtained for the twist angle of 45°. The latter is because of the crimps and distortion of the yarn at such high twist, and may not be found on ordinary yarns.

The combination of polarized light and filter

lens seems to give a better regularity of peak shift, probably because of the shut-out effect of scattered light from the yarn sides.

Using the Slit

By using a slit narrower than the diameter of a yarn, the specimen can be illuminated only on the central flat surface perpendicular to the beam; thus the side effect is perfectly eliminated. The result is shown in Figure 4, where good linearity between the angle of twist and the peak shift can be observed. The reason that the peak position for zero-twist yarn is not situated at $\theta = 0°$ or $180°$ is because of the misalignment of the specimen setting.

Making the Yarn Flat

If a round specimen is squeezed flat, the side effect may be almost neglected. Such a result is shown in Figure 5 with intermediate roving inserted between two glass plates and with beam cast normal to these plates. Again a good linearity between the angle of twist and the peak shift can be observed.

Of these three methods, the first is not suitable to get the balance position between two photo-tubes (explained later in detail); with the second it is very difficult to illuminate always the center part of the specimen when it is running. Therefore the third is used in designing the twist irregularity tester, the principle of which is explained as follows.

Assuming the linear relationship between the twist angle of a yarn and the peak shift, with the symmetry at the peak of the curve depicting the angle of rotation and the reflected light quantity, such a curve can be drawn as shown in Figure 6. There X_1 and X_2 indicate the light quantity received by photo-electric tubes P_1 and P_2 respectively, shown in Figure 7. These photoelectric tubes are set on two planes Z_1 and Z_2, each of which has the same angle of inclination to plane LTT normal to the surface fiber F_1 on the specimen XX made flat as explained above. L is the light source, the parallel beam from which is vertical to the flat surface of the specimen. Provided that two tubes are placed just at the same distance from the beam spot on the yarn, they will measure the same light quantity X_1 and X_2 as shown in Figure 6. If, then, another surface fiber F_2 comes under the spot, and

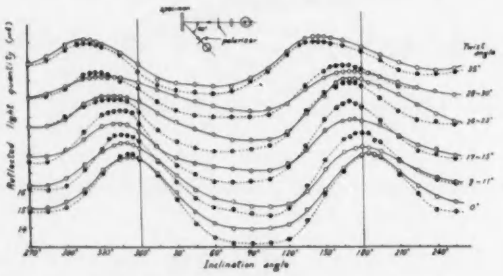

Fig. 5. Reflection from a flat yarn. Cotton intermediate roving.

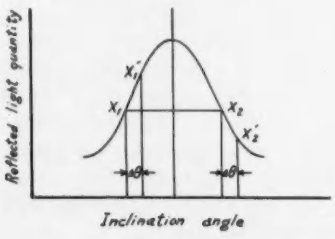

Fig. 6. Change of light quantity.

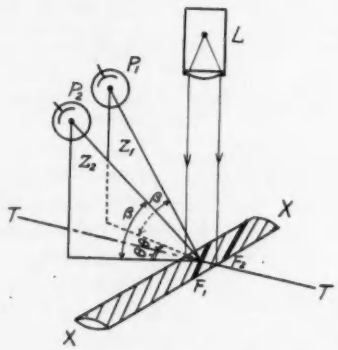

Fig. 7. Principle of the tester.

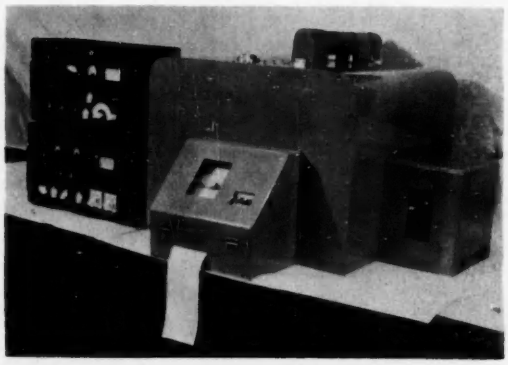

Fig. 8. The general view of the tester.

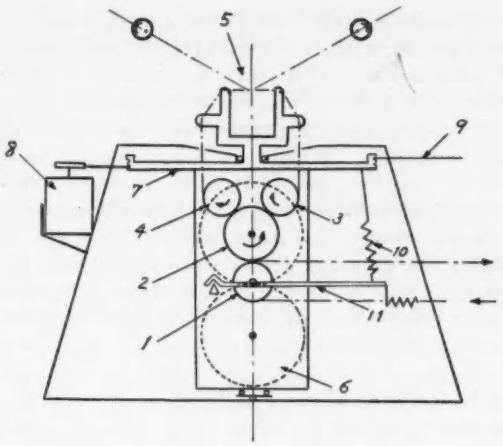

Fig. 9. Center part of the tester (10, spring; 11, tension device).

the angle of twist of F_2 is larger than that of F_1 by $\Delta\theta$, two photo tubes will indicate the light value X'_1 and X'_2 respectively. This unbalance of light value is electrically amplified and supplied to a balancing motor, which rotates two planes Z_1 and Z_2 as a whole around the incident light axis. When the unbalance is eliminated, the angle of rotation indicates the difference of twist angle between fibers F_1 and F_2. If the angle of rotation is drawn on a running paper, a record can be obtained which indicates the twist irregularity of the specimen.

Construction of the Tester

The general view of the twist irregularity tester utilizing the above-mentioned principle is shown in Figure 8. The yarn wound on a bobbin is put in the right small box, from which the specimen enters the center camera and returns again to the right. Light is cast vertically from the upper lamp house. The twist irregularity curve is recorded in the front center cabinet, on the surface of which are mounted three electric switches for starting and stopping the balancing motor, for running paper, and, for the specimen respectively. On the left side two cabinets are set, one being an electric source for photomultipliers, the other an amplifier for the balancing motor.

The center part of the tester is illustrated in Figure 9. The specimen enters the bottom of the pressure roller (1), which in turn pushes up the driving roller (2) and makes the latter contact with

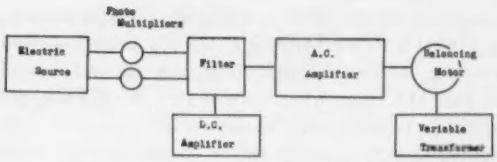

Fig. 10. Electric connection of the tester.

two driven rollers (3) and (4). Yarn is flattened by being rolled three times between these rollers; it proceeds upwards, entering the test region (5) and returning right after being caught again between rollers driven with a motor (6). This whole assembly is set on a disc (7) which is rotated by a balancing motor (8). The angle of rotation of the disc is the same as the change of twist angle, and is transmitted with rope (9) wound around the disc (7) to the recording part. The running speed of the specimen is 10 in./min., and that of the recording paper can be changed from 5 to 1 in./min. by the change gear mechanism. The length of the specimen is shortened on the paper to $\frac{1}{2}$ or $\frac{1}{10}$.

The electric connection is shown in Figure 10. By an electric source two photomultipliers are actuated not only with D.C. voltages alone, as is usual, but also with A.C. voltages on their first poles for the purpose of modulation. This is done with a transformer on which two coils are wound adversely in their winding direction; thus the modulation voltages differ in their phase angles just by 180°. The outputs of photomultipliers modulated by this method are put in a filter, from which the sum of A.C. components only is served to an A.C. amplifier to get an output sufficient to drive a balancing motor. A variable transformer is attached to drive the balancing motor when the output from the amplifier is cut out. The formulas for the electric curcuit and the way of balancing will be explained in the appendix.

Twist Irregularity Curves

The procedure to get the twist irregularity curves is as follows.

At first, the apparatus is switched on and left for 20–30 min. to get a stable condition. The first part of a yarn to be tested is cemented side by side with the end of the remaining specimen to avoid somewhat troublesome passing of the yarn, and then the motor is run to bring a new specimen to the test region. By controlling the voltage supplied to the

balancing motor with a variable transformer, the specimen is rotated slowly at the test region without running, and each photomultiplier output is read on the D.C. amplifier to get two peak positions, θ_1 and θ_2, respectively, as shown in Figure 11. The recording pen, initially set at 0° position when the yarn axis is on the plane containing two optical axes of photomultipliers, is now brought to the position $\theta_0 = (\theta_1 + \theta_2)/2$ by adjusting the modulation voltages after switching off the variable transformer. The yarn can now be run to get twist irregularity curves.

Figure 12 shows the results obtained with cotton yarns measured at the speed ratio (yarn speed/paper speed) of 1/2. Generally speaking, the curves are roughly similar in spite of the varieties of yarn count. On the other hand, the range of twist angle is considerably large, sometimes amounting to 20°. One reason is that the curve indicates the mean twist angle per centimeter, which is very small as compared with the usual gauge length of 10 in. But another is, of course, because the specimen is composed of staple fibers. In case of continuous filament yarns, the curves should be very flat, an example of which is shown in Figure 13. A is measured with 150-den. Terylene at the speed ratio of 1/10; B and C show the results with nylon and viscose yarns experimentally overtwisted in the laboratory. B shows as little variation as A, but in C, as the yarn is 120/2 den., the variation is increased due to the combined effect of single twist and ply twist. The same tendency can also be seen in D, obtained with viscose 1640/2-den. tire cord, 12 × 12 turns/in. Judging from the microscopic observation, the curve in this case does not indicate the cable twist, but rather shows the fiber arrangement due to single twist. The frequent peaks in the curve are mainly due to the variation of deep grooves by cable twist. This suggests that, if the spot diameter is reduced to a certain suitable dimension, the irregularity of ply or cable twist could be measured by counting the number of peaks per unit length, each of which appears at every groove made by ply or cable twist.

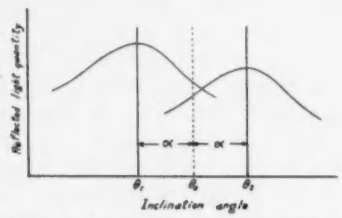

Fig. 11. Adjustment of the zero position.

Factors Affecting the Test Results

Flatness of the Specimen

As shown in Figure 2, if the yarn is round, the peak position of the photomultiplier output curve is liable to coincide with the yarn axis. Therefore the specimen should be squeezed as flat as possible to avoid this error. In other words, sized, plied, or highly twisted yarns should be tested under high squeezing pressure.

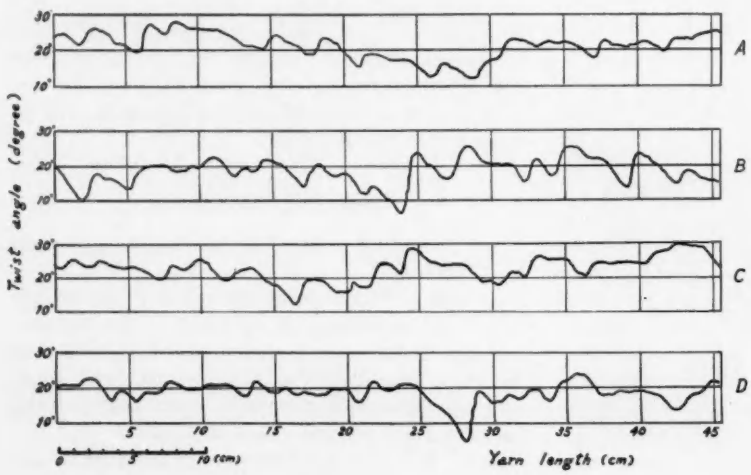

Fig. 12. Twist irregularity curves of cotton yarns (A, 30's; B, 20's; C, 16's; D, 12's).

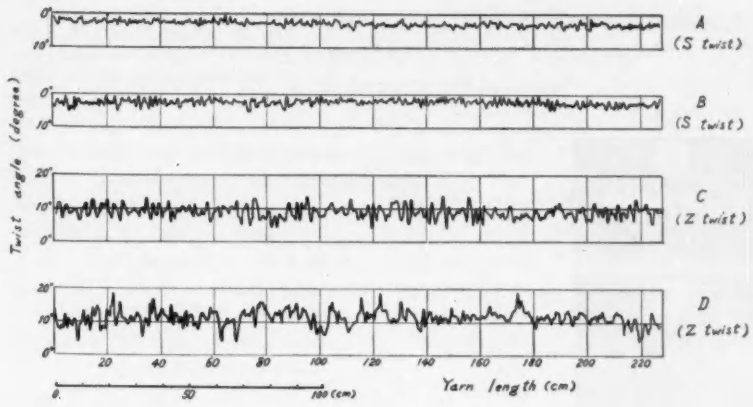

Fig. 13. Twist irregularity curves of continuous filament yarns (A, Terylene; B, nylon; C, viscose; D, viscose tire cord).

Turning of the Yarn

If the flattened yarn turns around its running axis at the test region, the measured twist angle differs from the true angle. To eliminate this error, the span of the yarn, that is, the distance of two yarn guides at the test region, should be shortened to a suitable value. The tester described here has the span of 13 mm. when the spot diameter is 10 mm.

Brightness of the Specimen

If the yarn at the test region is composed of two parts, A and B, and if A is brighter than B although they have the same dimensions, the observed twist angle is weighted much more by the twist angle of A. However, as the change of brightness along the yarn may be assumed not so rapid as the change of twist angles, this effect is negligible in most cases.

Sensitivity of the Tester

If the tester has low sensitivity, the curve obtained does not show the correct variation of the twist angle. The pen of this tester begins to move when the twist angle of a yarn changes about $\pm 0.5°$ under normal test condition, and this may be said accurate enough for usual testing.

Fluffiness of the Yarn

If the specimen is very fluffy, the steepness of the photomultiplier output is decreased, although the peak position may not be shifted. This decrease causes the sensibility reduction of the tester. When a large tuft is drawn in with the yarn, the measured twist angle is greatly influenced by it. One example of such cases is shown in Figure 14, observed with 120/2-den. viscose filament yarn. Three large peaks are due to the tufts of viscose staples purposely cemented on the yarn. In cases of very fluffy yarns, the specimen should be singed before testing.

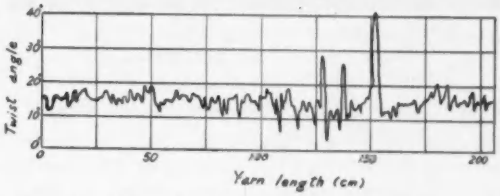

Fig. 14. Effect of tufts on a twist irregularity curve; viscose filament yarn.

Inertia of the Rotating Part

The inertia force of the rotating part set on the disc (7) in Figure 9 brings an error to the observed curve when the change of twist angle is rapid. Judging from this point, the motor used here was a little bit too heavy, and the yarn speed was too fast for changeful yarns.

Accuracy of the Result

In order to check the accuracy of the obtained curve, the twist angles of 20's cotton yarn after passing the irregularity tester were measured under an optical comparator with 20 × magnification. Twenty readings were made per centimeter at intervals of 0.5 mm., and the moving averages per centimeter are plotted in Figure 15, together with the irregularity curve (dotted) recorded with this

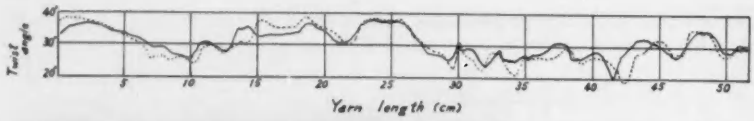

Fig. 15. Comparison of twist angles by visual observation and with the tester (dotted line); cotton 20's.

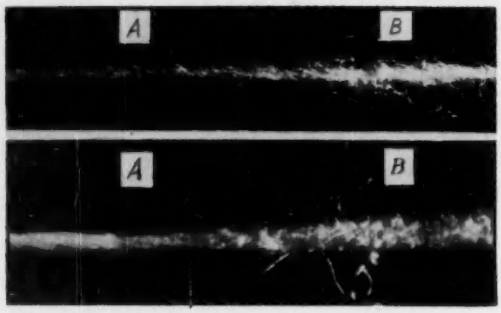

Fig. 16. Examples of yarn appearance. Upper, cotton 20's; lower, 120-den. viscose rayon.

tester. Although the coincidence is not so good as was expected at several places, both curves show the same tendency. The main reason of discrepancy may be the confused arrangement of surface fibers. When the yarn appearance is as neat as is shown at A in Figure 16, it is very easy and accurate to read the twist angle by visual observation. But at B, it is quite difficult to decide what angle should be read as the twist angle. In some cases, zero or negative twist angles were measured with fluffy yarn, in spite of the fact that the twist angle should be positive at any place in the case of staple yarns. One is also liable to measure the twist angle of the most distinct fibers, and the result may not be the average angle at the spot. Therefore the twist irregularity curve obtained with this tester may be much more representative of the average value than the result by visual observation in case of staple yarns. Continuous filament yarns have no such ambiguous factors except when tufts are purposely attached, and results obtained by visual observation and with this tester showed good coincidence.

Summary

It was shown that, when a yarn is observed flat, the reflected light from it shows its peak value when measured in a plane vertical to the twisted fibers. The squeezing method was used to construct a twist irregularity tester based on the above-mentioned principle. The tester contains two photomultipliers actuated with both D.C. and A.C. voltages, and operates automatically, recording the change of twist angle at the yarn speed of 10 in./min. Several examples of the observed twist irregularity curves are shown and, as expected, those of staple yarns are much more fluctuating than those of continuous filament yarns. Among several factors affecting the accuracy of the observed result, only the rapid brightness variation along a yarn may be an uncontrollable factor. But, as the error due to this could be assumed small, and the tester has the sensitivity of $\pm 0.5°$ for twist angle, the curve obtained with this tester is thought accurate enough for ordinary test. Although the curve does not show as good an agreement as was anticipated with the results of visual observation, this can be attributed to the random arrangement of surface fibers. In some cases, because the visual observation is misled by some clear surface fibers, this photoelectric tester may be most suitable to determine the twist angle.

The authors are now trying to attach to this tester a shadow-type yarn irregularity meter in order to record both irregularities of diameter and twist. The result will be reported in the next paper.

Acknowledgment

The authors wish to express their appreciation to the Japan Cotton Technical Institute, which sponsored this study, and to the Kurashiki Spinning Company for valuable suggestions. Special indebtedness is expressed to Sawa Shop and Yamashiro Shop for manufacturing the machine and electric parts respectively. Thanks are also due to Mr. Y. Kishida, who did the laboratory work.

Appendix

Generally a photomultiplier indicates a linear relationship between the output and the voltage supplied on its first pole, provided the voltage is higher than a certain value. Therefore, if an alternating voltage is superposed on the first pole, the output can be modulated in the following way.

In case of two multipliers modulated with alternating voltages, the phase angles of which are lag by 180° to each other, the output currents are written as follows:

$$i_1 = k_1 I_1 (V_1 + a \cos \omega t)$$
$$i_2 = k_2 I_2 (V_2 - b \cos \omega t)$$

where k_1, k_2 = constants, I_1, I_2 = light intensities cast to two photomultipliers, V_1, V_2 = voltages on the first poles, and a, b = modulation voltages. When the specimen is set at the state shown in Figure 7, I_1 can be assumed equal to I_2 $(= I)$. So the sum of two outputs is:

$$i_0 = i_1 + i_2$$
$$= (k_1 V_1 + k_2 V_2) I + (k_1 a - k_2 b) I \cos \omega t$$

If the D.C. component of this output is cut off by a filter, and a zero equilibrium of A.C. component is obtained by adjusting the modulation voltage,

$$k_1 a - k_2 b = 0$$

If there is a change of light intensity, ΔI, due to the offset of twist angle by $\Delta\theta$, after equilibrium is obtained, the output currents are:

$$i'_1 = k_1 (I + \Delta I)(V_1 + a \cos \omega t)$$
$$i'_2 = k_2 (I - \Delta I)(V_2 - b \cos \omega t)$$

Their sum is:

$$i' = i'_1 + i'_2 = k_1(I + \Delta I) V_1 + k_2 (I - \Delta I) V_2$$
$$+ (k_1 a - k_2 b) I \cos \omega t + (k_1 a + k_2 b) \Delta I \cos \omega t$$

As before, the D.C. component is cut off with a filter. On the other hand, the third term is zero by the equilibrium condition, so the remaining output is

$$i' = (k_1 a + k_2 b) \Delta I \cos \omega t$$

Because $(k_1 a + k_2 b)$ is constant in this case, the output is an alternating current and is proportional to ΔI, the amount of deviation from equilibrium. Thus the balancing motor is driven proportionally to $\Delta\theta$, and the rotating direction of it is determined by the sign of ΔI.

Literature Cited

1. ASTM Committee D-13 ASTM Standards on Textile Materials (D 76–53, D 180–54 T, and D 1380–56 T).
2. Gonsalves, V. E., *Enka Rayon Revue* **9**, 81 (July 1955).
3. Henno, H. and Jouhet, R., *Bull. L'Institut de France* (April 1957).
4. Jeffries, R., *J. Textile Inst.* **46**, A674 (1955).
5. Magni, A., *L'Industrie Textil* **790**, 479 (1952).
6. "Methods of Test for Textiles," *British Standards Handbook No. 11*, British Standards Institution, 87, 148 (1956).
7. Orchard, G. A. J., *J. Textile Inst.* **44**, A227 (1953).
8. Shorter, S. A., *J. Textile Inst.* **48**, A571 (1957).
9. Uno, M., Okuda, K., and Matsumura, T., *J. Text. Mach. Soc. (Japan)* **10**, 27 (1957).
10. Uno, M. and Shiomi, A., TEXTILE RESEARCH JOURNAL **27**, 818 (1957).
11. Worner, R. K., TEXTILE RESEARCH JOURNAL **26**, 455 (1956).

Manuscript received December 30, 1958.

Phenolic-Formaldehyde Resins as Finishing Agents for Cotton Fabrics

Leon H. Chance, Fred S. Perkerson, and Oscar J. McMillan, Jr.

Southern Regional Research Laboratory,[1] *New Orleans, Louisiana*

Abstract

Cotton fabric was treated with phenolic-formaldehyde resins and seven halogenated phenolic-formaldehyde resins and the properties of the fabric evaluated. The fabric was treated by padding it through a solution of phenol in alkaline aqueous formaldehyde, drying, and curing in an oven. All the fabrics had improved rot resistance and crease recovery. The halogenated phenols did not seem to have any advantage over plain phenol in imparting rot resistance to cotton fabric. Fabrics treated with *m*-chlorophenol and *m*-bromophenol had the highest crease recovery.

REFERENCES to the use of phenolic compounds as disinfectants [5, 8] and of phenolic-formaldehyde resins as finishing agents for textiles are numerous. The effectiveness of several phenolic-formaldehyde resins as rotproofing agents for viscose rayon was demonstrated in experiments by J. W. Bell et al. [3]. Phenolic resins have been recommended for use in wrinkle resistant finishes for textiles, and there are a number of patents claiming phenolic-formaldehyde resins as wrinkle resistant finishes for textiles [7, 9, 10]. There appears, however, to be a limited amount of data in the literature on the physical properties of cotton fabric treated with various phenolic-formaldehyde resins. Therefore, this work was carried out to provide more complete data on rot resistance, wrinkle resistance, etc. of cotton fabric treated with several phenolic-formaldehyde resins, including some halogenated phenols on which little or no data are available in the literature.

Materials and Test Methods

The fabric used throughout the experiments was cotton print cloth 80 × 80, 4 oz., peroxide bleached in a commercial continuous range.

The soil burial method was used in testing the rot resistance of the samples. The "soil" used in this study was a specially prepared mixture of equal parts of coarse river sand, well-rotted barnyard manure, and clay loam soil. The clay loam and manure were first partially air dried, pulverized, and sieved through a coarse screen prior to mixing with the river sand. The "soil" was placed in wooden drawers in a closed cabinet indoors. The "soil" was kept at a temperature of 90° C. ± 2° C., a moisture content of 28–30%, and a pH of 6.5–7. The shortcomings and variations of different methods of determining rot resistance of textiles are recognized, of course. Various techniques of testing fabrics by soil burial are described in detail by Batson et al. [2] and by Bertholet [4]. Each resin treated fabric was cut into strips ($1\frac{1}{4} \times 6$ in.) and placed at random in the soil beds. Five strips of each fabric were removed at two-week intervals for testing. The damage caused by microbiological attack was assessed by determining breaking strength by the strip method. The duration of the rot resistance tests was twelve weeks.

All of the textile tests reported herein were carried out essentially as specified by ASTM or Federal Specifications standard methods. Breaking strength was measured by the strip method [1a], except that a count of 80 threads was used instead of 1-in. width; flex abrasion using the Stoll Abrader [1b]; crease recovery by the Monsanto method [6a], but using a 500-g. weight; stiffness by the Tinius-Olsen method [6b]; and tear strength by the Elmendorf method [1c]. All of the test values reported are the average of five test samples.

[1] One of the laboratories of the Southern Utilization Research and Development Division, Agricultural Research Service, U. S. Department of Agriculture.

TABLE I. Test Results on Fabric Treated with Phenol-Formaldehyde Resins

Sample no.	Resin type	Resin add-on, %	Strip breaking strength (warp), lb.	Elmendorf tear (warp), lb.	Stiffness (warp) bending moment, 10^{-4} in. lb.	Flex abrasion (warp), cycles	Crease recovery angle (warp + fill), degrees	Halogen, %
1A	Phenol	6.9	45.6	1.3	4.40	187	226	—
1B	Phenol	9.3	45.0	1.3	6.15	120	243	—
2A	*o*-hydroxybenzyl alcohol	4.9	44.6	1.2	4.30	266	232	—
2B	*o*-hydroxybenzyl alcohol	6.9	40.6	1.1	4.50	145	253	—
3A	*o*-chlorophenol	5.7	46.1	1.3	7.35	157	233	0.86
3B	*o*-chlorophenol	7.0	45.0	1.3	5.80	167	245	0.96
4A	*p*-chlorophenol	3.7	45.7	1.5	5.60	218	217	0.39
4B	*p*-chlorophenol	3.9	47.6	1.4	5.10	181	222	0.86
5A	*m*-chlorophenol	5.0	40.5	1.3	4.40	144	260	1.22
5B	*m*-chlorophenol	5.8	38.0	1.2	4.10	120	280	1.48
6A	*o*-bromophenol	7.0	40.7	1.3	4.80	171	232	2.48
7A	*p*-bromophenol	5.0	47.9	1.4	4.45	226	231	1.41
7B	*p*-bromophenol	5.2	44.8	1.4	6.10	160	233	2.23
8A	*m*-bromophenol	4.0	43.0	1.4	3.80	214	—	2.04
8B	*m*-bromophenol	5.1	40.7	1.3	3.85	255	266	2.63
9A*	*m*-chlorophenol + *m*-bromophenol	4.2	40.5	1.3	3.25	143	267	—
9B*	*m*-chlorophenol + *m*-bromophenol	5.2	36.9	1.3	3.50	154	261	—
10A	*p*-fluorophenol	4.0	45.9	1.4	4.32	226	232	—
Control	untreated	—	43.1	2.5	6.50	603	159	—
Control	treated	0.5	45.5	1.9	3.50	368	210	—

* Equal parts by weight of *m*-chlorophenol and *m*-bromophenol.

Experimental

The preparation of each phenolic-formaldehyde solution will be given in detail below. The solutions were allowed to age at room temperature and were then applied to the fabric. The pH of the solutions was measured immediately prior to the padding operation, and in all cases was 8–9. In all solutions there was some unreacted formaldehyde at the time of application to the fabric, as observed by the strong odor of formaldehyde. The fabric was cut into strips about 8 in. wide and about 4 yd. long. Each sample was padded through the solution twice at the maximum squeeze roll pressure using a laboratory size Butterworth padder. The sample was dried for 15 min. by hanging in a forced draft oven at 110° C. It was then cured for 10 min. at 145° C. in the same manner. The sample was then washed thoroughly in hot water and pressed dry with a hot iron.

Phenol-Formaldehyde

Phenol (100.0 g.; 1.06 moles) was dissolved in 87.5 g. (1.08 moles) of 37% formaldehyde, and 17.5 g. of 20% sodium hydroxide was added. To this 5 g. of Tergitol 7 (a solution of sodium heptadecylsulfate)[2] was added and the solution diluted with 290 g. of distilled water to give a solution 20% by weight with respect to phenol. The solution was allowed to stand in a stoppered flask for 24 hr. at room temperature. A sample of fabric was then treated with this solution. A second sample of fabric was treated after the solution had aged for 105 hr. at room temperature.

o-Hydroxybenzyl Alcohol-Formaldehyde

A solution was prepared in the same manner described for phenol using 75.0 g. (0.60 mole) of *o*-hydroxybenzyl alcohol, 100.0 g. (1.2 moles) of 37% formaldehyde, 10.0 g. of 20% sodium hydroxide, 5.0 g. of Tergitol 7, and 310.0 g. of distilled water. The solution contained 15% by weight of *o*-hydroxybenzyl alcohol. A sample of fabric was treated immediately with the above solution, and a second sample was treated after the solution had aged for 24 hr.

[2] Throughout this paper, mention of trade names and firms does not imply their endorsement by the Department of Agriculture over similar products or firms not mentioned.

TABLE II. Properties of Fabric Treated with *m*-Chlorophenol-Formaldehyde Resin Before and After Softening and Laundering

Resin add-on, %	Softener	Strip breaking strength (warp), lb.	Elmendorf tear (warp), lb.	Stiffness (warp) bending moment, 10^{-4} in. lb.	Crease recovery (warp + fill), degrees	Flex abrasion (warp), cycles
		Before laundering				
7.2	None	39.3	1.2	4.2	275	136
7.2	Primenit VS	33.7	1.6	3.2	271	367
8.5	None	39.3	1.1	4.8	274	107
8.5	Primenit VS	34.4	1.6	2.8	282	254
		After 5 home launderings				
7.2	None	34.5	1.2	3.2	246	141
7.2	Primenit VS	34.8	1.5	2.9	258	368
8.5	None	36.3	1.2	3.3	257	108
8.5	Primenit VS	32.4	1.5	2.8	259	271

o-Chloro-, p-Chloro-, o-Bromo-, and p-Bromophenol-Formaldehyde

All of these solutions were prepared in the same way, using the same quantities of materials. The solutions were not diluted with water due to the insolubility of the *o*- and *p*-halophenols in water. *o*-Chlorophenol will be used as a typical example. The molar concentration of the chlorophenols was 0.78, and of the bromophenols, 0.58.

A solution was prepared using 100.0 g. of *o*-chlorophenol, 377.5 g. (4.6 moles) of 37% formaldehyde, 17.5 g. of 20% sodium hydroxide, and 5.0 g. of Tergitol 7. The solution contained 20% by weight of *o*-chlorophenol. A sample of fabric was treated with the solution after it had aged for 24 hr., and a second sample was treated after it had aged for 105 hr.

m-Chloro- and m-Bromophenol-Formaldehyde

m-Chloro- and *m*-bromophenol solutions were prepared using 32.5 g. (0.25 mole of *m*-chlorophenol, 0.19 mole of *m*-bromophenol) of the phenol, 225.0 g. (2.8 moles) of 37% formaldehyde, 17.5 g. of 20% sodium hydroxide, 5.0 g. of Tergitol 7, and 220.0 g. of distilled water. The solution contained 6.5% by weight of phenol. A sample of fabric was treated after the solution had aged for 1.5 hr., and a second sample treated after 24 hr.

m-Chloro- and m-Bromophenol-Formaldehyde Mixture

A mixture containing 100.0 g. of the above 6.5% solution of *m*-chlorophenol and 100.0 g. of the 6.5% solution of *m*-bromophenol was made; the solutions were approximately 3 hr. old at the time of mixing. A sample of fabric was treated with the 3-hr.-old solution, and a second sample treated after the solution was 24 hr. old.

p-Fluorophenol-Formaldehyde Resin

A solution was prepared using 10.0 g. (0.09 mole) of *p*-fluorophenol, 65.5 g. (0.80 mole) of 37% formaldehyde, 3.5 g. of 20% sodium hydroxide, 1.0 g. of Tergitol 7, and 20.0 g. of distilled water. The solution contained 10% by weight of *p*-fluorophenol. The solution was aged at room temperature for 24 hr. and then applied to a sample of fabric.

Control Fabrics

Two controls were used in all of the tests. One control was the original untreated 80 × 80 print cloth. The other was a treated control prepared by padding through a 24-hr.-old solution containing 100.0 g. of 37% formaldehyde, 7.0 g. of 20% sodium hydroxide, 2.0 g. of Tergitol 7, and 91.0 g. of water. The pH of the solution was 10.8. The fabric was dried and cured in the same manner as the other samples. The treated control fabric was extracted with 100 ml. of distilled water before washing. The pH of the water extract was 8, proving the fabric to be alkaline throughout the process.

Results and Discussion

The above treatments resulted in samples containing varying resin add-on and halogen content,

and are therefore not strictly comparable. However, the relative effects of the various resin treatments on the soil burial tests and physical properties can be seen from the data in the tables to follow. The *m*-chloro- and *m*-bromophenols were most reactive toward formaldehyde, and were most efficient in polymerizing on fabric. This was demonstrated, for example, in a resin add-on of 5.8% from a 24-hr.-old solution containing 6.5% *m*-chlorophenol. To obtain a comparable resin add-on from all of the other phenols a concentration of 15–20% of the phenol was required. *p*-Chloro- and *p*-bromophenols gave the lowest resin add-ons considering the concentration of phenol in the solution. For a given percent resin add-on there was a greater percentage of halogen when the meta halogenated phenols were used. In all cases the solutions which had been aged the longest gave fabrics with the highest resin add-on and halogen content. This was due presumably to a higher degree of methylolation of the phenols. The resin add-ons reported were not determined as accurately as the halogen content. For this reason the soil burial results of the halophenols are discussed on the basis of the halogen content.

Physical Test Results

Physical test results on 80 × 80 print cloth treated with phenol-formaldehyde type resins are given in Table I. In the majority of cases the breaking strength of the fabrics was not significantly affected by the resin treatment. In only two cases [*m*-chlorophenol (5B) and *m*-chlorophenol-*m*-bromophenol mixture (9B)] was there a loss in strength greater than 6%. Elmendorf tear strength losses varied from 40% [*p*-chlorophenol (4A)] to 56% [*o*-hydroxybenzyl alcohol (2B)]. All of the treated fabrics had a good hand, very little stiffness being observed. Stiffness tests showed all the resin treated fabrics except one [*o*-chlorophenol (3A)] to be less stiff than the untreated control. Losses in flex abrasion varied from about 56% [*o*-hydroxybenzyl alcohol (2A)] to 80% [*m*-chlorophenol (5B)].

The highest crease recovery angles (Monsanto method) were obtained from the *m*-chloro- and *m*-bromophenol resins. As shown in Table I, samples containing 5.8% of the *m*-chlorophenol resin had a crease recovery angle of 280° (warp and filling), and samples containing 5.1% of the *m*-bromophenol resin had a crease recovery angle of 266°. Samples containing 4.2% of *m*-bromophenol and *m*-chlorophenol mixed resin had a crease recovery angle of 267°. The untreated control had a crease recovery angle of 159° and the treated control, 210°. The large increase in crease recovery as well as the decrease in tear strength and flex abrasion of the treated control indicated cross-linking of the cellulose. A further indication of cross-linking was the insolubility of the treated control in cuprammonium solution, even after it had been boiled for 3 hr. in concentrated ammonium hydroxide, followed by boiling for three more hours in 10% aqueous sodium bisulfite. This was an interesting observation, since the cross-linking apparently took place with formaldehyde in an alkaline medium. Wood [11] has reported that reaction with formaldehyde in the presence of alkali causes temporary alterations in the physical characteristics of cellulose, but that apparently no stable condensation product is formed, since material treated in this way can be freed of formaldehyde by boiling with ammonia or sodium bisulfite solutions.

All of the samples had the yellow-brown color characteristic of phenolic resins. However, the samples can be vat dyed, and in this way the discoloration can be masked.

Effects of Softener

Samples of 80 × 80 cotton print cloth containing 7.2% and 8.5% *m*-chlorophenol-formaldehyde resin respectively were padded through a 1% aqueous emulsion of Primenit VS (a softener and water repellant containing octadecyl ethylene urea) and dried at 85° C. The effect on fabric properties is shown in Table II. There was an approximately 12% decrease in stiffness, a 33% increase in the tear strength, and an increase in flex abrasion. There was no significant change in the crease angles.

Effect of Home Laundering

Samples of 80 × 80 print cloth containing 7.2% and 8.5% *m*-chlorophenol-formaldehyde resin were given five successive home laundering cycles. The laundering tests consisted of five cycles in an agitator-type automatic machine using a standard detergent. Each cycle was followed by drying in an electric tumble dryer on a medium setting. The physical test results after the five cycles are shown

in Table II. In general there was no significant change in tear strength and abrasion resistance. However, there was a decrease in stiffness and a slight decrease in tensile strength. There was an average decrease in crease recovery angles of 20°.

Microscopical Observations

A fiber specimen from each of the resin treatments given in Table I was stained and a cross section prepared for microscopical examination. In each case the resin was largely on the surface. Penetration of the resin into the fiber was poor to very poor regardless of the age of the treating solution. Where penetration did occur it was spotty and largely in the immature fibers.

Soil Burial Results

Data on the strength retention of 80 × 80 cotton cloth treated with phenol-formaldehyde type resins and tested by the soil burial method are recorded in Table III. Sample 1A, with a phenol-formaldehyde resin deposit of 6.9%, retained 30% of its strength after 12 weeks. It is interesting to note that sample 2B, with an *o*-hydroxybenzyl-alcohol-formaldehyde resin deposit of 6.9%, retained 84% of its strength after 12 weeks. It appears that better results are obtained by beginning with the pure phenol-formaldehyde monomer, i.e., *o*-hydroxybenzyl alcohol. This might be attributed to a higher hydroxymethyl content than when starting with plain phenol. It is also interesting to note that the rot resistance of the samples of fabric treated with phenol-formaldehyde and *o*-hydroxybenzyl alcohol-formaldehyde showed rot resistance comparable to most of the halogenated phenols, and in some cases showed better rot resistance. Although not enough data are available to draw any definite conclusion as to the effect of the position of the halogen on rot resistance, certain trends can be seen. An attempt will be made in the following discussion to relate the soil burial results of the halogen containing fabrics to the percent halogen. It is realized, however, that other factors might be involved, such as the degree of cross-linking of the cellulose, uniformity of the resin treatment, etc. Sample 3B, with an *o*-chlorophenol-formaldehyde deposit of 7% and a chlorine content of 0.96%, retained 71% of its strength after 6 weeks; sample 4B, with a *p*-chlorophenol-formaldehyde deposit of 3.9% and a chlorine content of 0.86%, retained 70% of its strength after 6 weeks; and sample 5B, with an *m*-chlorophenol-formaldehyde resin deposit of 5.8% and a chlorine content of 1.48%, retained 85% of its strength after 6 weeks. If the chlorine content is considered, it can be concluded that *m*-chlorophenol is more effective than the others, or that for the chlorophenols, the probable order of effectiveness is meta > para > ortho. Through a comparison of samples 6A, 7A, 7B, 8A, and 8B in a similar manner after 6 weeks it appears that *m*- and *p*-bromophenols are more effective than *o*-bromophenol. Better rot resistance was obtained with 5.2% of the *p*-bromophenol resin samples than with 5.1% of the *m*-bromophenol resin samples, even though the percent bromine was slightly greater (2.23% versus 2.63%) with the meta. Thus, for the bromophenols, the probable order of effectiveness is para > meta > ortho. After six weeks soil burial, it appears that on the basis of mole percent of halogen add-on, chloro is more effective than bromo in the cases of ortho and meta phenols, but bromo is probably slightly more effective than chloro in the case of the para phenol resins. It appears from Table III that the most effective of the halophenol resins at the 5–7% resin level was *m*-chlorophenol (sample 5A), with a strength retention of 29% after 12 weeks. It was observed that a mixture of *m*-chlorophenol and *m*-bromophenol resins (9A and 9B) was less effective than *m*-chlorophenol and more effective than *m*-bromophenol. This again indicated that the *m*-chlorophenol was more effective than the *m*-bromophenol. *p*-Fluorophenol appeared to be the least effective of any of the treatments; samples with 4% resin had deteriorated at the end of two weeks. The activity of the soil beds was checked several times during the 12-week period by placing control samples in the beds. In all cases the controls deteriorated in about one week.

Bell et al. [3] treated viscose rayon yarns with several phenol-formaldehyde resins and reported results from samples tested by a horse-dung contact method. They reported that the presence of a halogenated resin led to a remarkable improvement in resistance to microorganisms. They reported *o*-chlorophenol-formaldehyde to be more effective than phenol-formaldehyde, and *p*-bromophenol-formaldehyde to be much more effective than either of these. These great differences were not observed in the treatments reported herein. No doubt the

kind of cellulosic material used, the method of application, and the method of testing rot resistance are important factors affecting the final results.

Summary

Cotton fabric was treated with phenol-formaldehyde resins and seven halogenated phenol-formaldehyde resins; the properties of the fabric were evaluated. The fabric was treated by padding it through a solution of the phenol in alkaline aqueous formaldehyde, drying, and curing at 145° C. All of the fabrics showed improved rot resistance when tested by the soil burial method. The best rot resistance was obtained from fabric treated with *o*-hydroxybenzyl alcohol-formaldehyde; samples containing 6.9% resin retained 84% of their strength after 12 weeks of soil burial. The most effective of the halophenols at the 5–7% resin level was *m*-chlorophenol, with a strength retention of 29% after 12 weeks soil burial. All of the treated fabrics had improved crease recovery. Fabrics treated with *m*-chlorophenol and *m*-bromophenol had the highest crease recovery angles. *m*-Chlorophenol, with a resin add-on of 5.8%, had a crease recovery angle of 280°, and *m*-bromophenol, with a resin add-on of 5.1%, had a crease recovery angle of 266°.

Acknowledgment

The authors wish to thank Dr. Ruby K. Worner, Julia M. Sloan, and Margarette Loughlin for the textile evaluation tests; Harold P. Pastor for the halogen analyses; and Ines V. deGruy for the microscopical observations.

Literature Cited

1. ASTM (a) D39-49, (b) D1175-55T, (c) D1424-56T. American Society for Testing Materials, Philadelphia.
2. Batson, D. M., Teunisson, D. J., and Porges, N., *Am. Dyestuff Reptr.* **33**, 423–27, 449–54 (1944).
3. Bell, J. W., Ramsey, M. M., and Whewell, C. S., *J. Soc Dyers Colourists* **71**, 660–67 (1955).
4. Bertolet, E. C., *Am. Dyestuff Reptr.* **33**, 21–24 (1944).
5. Fargher, R. G., Galloway, L. D., and Probert, M. E., *J. Textile Inst.* **21**, T245–60 (1930).
6. Federal Specifications CCC-T-191b (a) Method 5212, (b) Method 5202, U. S. Government Printing Office, Washington, D. C. (1951).

TABLE III. Strength Retention of Fabric Treated with Phenol-Formaldehyde Type Resins and Tested by the Soil Burial Method

Sample no.	Resin type	Age of treating solution, hr.	Resin add-on, %	Halogen, %	Moles of halogen	Breaking strength retention, %, vs. weeks in soil beds*					
						2	4	6	8	10	12
1A	phenol	24	6.9	—	—	102	97	93	67	37	30
1B	phenol	105	9.3	—	—	101	94	98	97	59	56
2A	*o*-hydroxybenzyl alcohol	0	4.9	—	—	85	74	52	28	13	4
2B	*o*-hydroxybenzyl alcohol	24	6.9	—	—	99	99	97	97	97	84
3A	*o*-chlorophenol	24	5.7	0.86	0.024	99	83	35	22	1	0
3B	*o*-chlorophenol	105	7.0	0.96	0.027	101	98	71	19	7	1
4A	*p*-chlorophenol	24	3.7	0.39	0.011	42	34	19	5	0	—
4B	*p*-chlorophenol	105	3.9	0.86	0.024	99	85	70	29	7	4
5A	*m*-chlorophenol	1.5	5.0	1.22	0.034	100	96	75	58	55	29
5B	*m*-chlorophenol	24	5.8	1.48	0.039	107	106	85	39	17	5
6A	*o*-bromophenol	24	7.0	2.48	0.031	23	4	6	0	—	—
7A	*p*-bromophenol	24	5.0	1.41	0.017	75	30	20	5	2	0
7B	*p*-bromophenol	105	5.2	2.23	0.028	105	92	97	42	10	0
8A	*m*-bromophenol	1.5	4.0	2.04	0.025	59	17	9	5	3	0
8B	*m*-bromophenol	24	5.1	2.63	0.033	23	4	6	0	—	—
9A†	*m*-chlorophenol + *m*-bromophenol	3	4.2	—	—	97	60	39	28	24	11
9B†	*m*-chlorophenol + *m*-bromophenol	24	5.2	—	—	59	26	20	5	0	—
10A	*p*-fluorophenol	24	4.0	—	—	0	—	—	—	—	—
Control	untreated	—	—	—	—	—	—	—	—	—	—
Control	treated	24	0.5	—	—	—	—	—	—	—	—

* All strengths are calculated as a percentage of the original resin treated fabric before soil burial.
† Equal parts by weight of *m*-chlorophenol and *m*-bromophenol.

7. Molinari, H., Brit. Patent 452,891 (September 1, 1936).
8. Morris, L. E., *J. Textile Inst.* **18**, T99–127 (1927).
9. Tootal Broadhurst Lee Co., Ltd., Foulds, R. P., Marsh, J. T., Wood, F. C., Boffey, H., and Tankard, J., Brit. Patent 291,473 (December 1, 1926).
10. Tootal Broadhurst Lee Co., Ltd., Foulds, R. P., Marsh, J. T., and Wood, F. C., Brit. Patent 291,474 (December 1, 1926).
11. Wood, F. C., *J. Soc. Chem. Ind.* **50**, 411T–418T (1931).

Manuscript received December 30, 1958.

Some Mechanical Properties of Single Wool Fibers in D_2O

M. Feughelman, A. R. Haly, and T. W. Mitchell

Wool Textile Research Laboratories, Commonwealth Scientific and Industrial Research Organization, Ryde, N.S.W., Australia

Abstract

Both the load–extension and the stress–relaxation curves were compared in the yield region for single wool fibers in water and in deuterium oxide. Also a comparison was made of the rate of penetration of water and deuterium oxide fronts into a dry fiber. In all cases the deuterium oxide acts in the wool fiber the same as water with the temperature of the fiber reduced by about 5–6° C.

Introduction

The physical properties of wool vary markedly with its regain. However, the part played in these phenomena by water molecules in the wool structure requires further investigation. As a possible means of obtaining more information on the behavior of water in wool, a number of simple experiments were carried out comparing the properties of wool in water and in deuterium oxide under the same physical conditions. Many properties of H_2O and D_2O are very similar. However, the intermolecular forces in D_2O and H_2O are significantly different. The difference of the intermolecular forces as measured by the heat of sublimation [5] at 0° K is 0.30 ± 0.15 kcal./g. mol. Further, Kirschenbaum [4] quotes at 25° C. the ratio of the viscosities of the two liquids as

$$\frac{D_2O}{H_2O} = 1.232$$

Both these results indicate that one might expect a significant difference in the properties of wool in H_2O as against D_2O where the phenomenon being studied involves the rupture of intermolecular bonds. The simple experiments that were chosen were (a) the load–extension relationship in the yield region of a single fiber at a constant rate of extension at saturation regain (in the liquid); (b) the stress relaxation in the yield region at saturation regain; and (c) the rate of penetration of liquid H_2O and D_2O fronts into a dry fiber.

Experimental

The apparatus for measuring load–extension and stress–relaxation is illustrated schematically in Figure 1. The fiber is in the form of a loop with both ends held by a tapered plug P. The loop passes over a small hook on a stiff calibrated cantilever C to the end of which a mirror M is attached. The whole of the fiber extending unit is sealed with a clear perspex front A. The wool fiber is pulled from the outside by means of a rod E which slides through an O-ring seal as it passes into the apparatus. The D_2O or H_2O is forced in through a trap U by means of a hypodermic syringe. Light from a small pinpoint source S is reflected from M and focused by means of a lens system (L) onto a rotating drum D. The wool fiber is extended at a con-

stant rate by the rod E and the drum D rotates with constant velocity. The image S′ of S on the drum is photographed on film wrapped around the drum. The extension of the fiber is measured by the movement of S′ on the film due to the drum's rotation, and the movement of the cantilever vertically which causes S′ to move vertically measures the force on the fiber. By stopping E at a fixed extension of the fiber, the point S′ traces out the stress–relaxation curve for the fiber on the film, the rotation of the drum supplying the time coordinate. The rate of extension of the fibers was kept constant at 7.2%/min.

The deflection at the hook on the cantilever C due to a total load of 20 g. was 0.5_2 mm. For the yield region between 2% and 28% extension the load on the double fibers increased by about 4 g. That is, a deflection change in the cantilever at the hook was about 0.1 mm. during the extension from 2% to 28%. The length of the fiber loops used was 40 mm., so that this deflection introduced a reduction in the rate of extension of the fiber in the yield region of 0.07%/min. compared with the movement of the rod E. This correction was considered negligible compared with the figure of 7.2%/min. for the rate of movement of E. Similarly, during stress relaxation the maximum movement of the cantilever due to a drop of force of about 2 g. in the double fiber during the experiment caused a change in fiber length of 0.6%. This was negligible compared with the strain of 28% at which the fiber was originally held.

The rate of penetration of a liquid H_2O and D_2O front into a dry fiber was measured using the technique described by Haly [3] elsewhere.

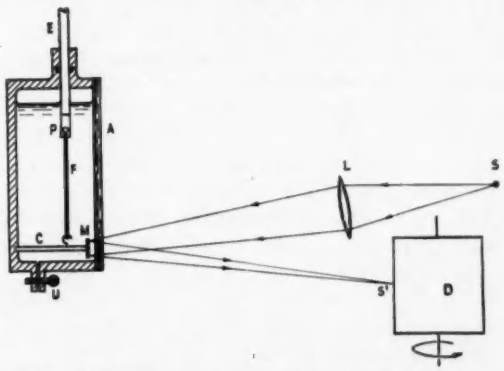

Fig. 1. Diagram of the apparatus used to measure the mechanical properties of single fibers in D_2O.

TABLE I. Change of Force at 15% Extension and Variation of Stress Change During Relaxation at Extension of 28% After 5 min. in D_2O Against H_2O, Both at 20° C.

Rate of extension constant at 7.2%/min.

		Increase; D_2O against H_2O
Fiber	F_{15}, %	Stress change, %
1	5.0	11.7
2	4.5	8.5
3	4.8	12.6

In all cases wool fibers were from penned Corriedale sheep hand fed for uniformity of growth. These fibers were supplied by the Sheep Biology Laboratory of CSIRO. The coefficient of variation [2] of the cross-sectional areas along individual fibers has been shown to be about 5%.

Results

Load–extension curves were determined for single fibers up to extensions of 28%. The experiments were carried out alternately in water and D_2O following a relaxation in H_2O at 52–54° C. for 1 hr. At the end of each 28% extension the fiber was allowed to stress-relax for about five minutes. The experiments were carried out at room temperature (20° C). No difference was detectable in the slopes of the Hookean or yield regions for the wool fibers in H_2O and D_2O. However, the force at 15% extension (F_{15}) was found to be higher in D_2O than in H_2O (see Table I) by approximately 4.8%.

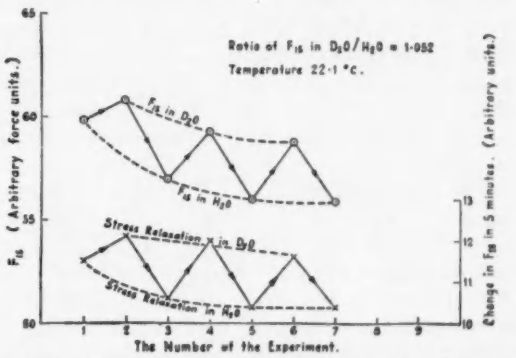
Ratio of F15 in D2O/H2O = 1·052
Temperature 22·1 °C.
F15 in D2O
F15 in H2O
Stress Relaxation in D2O
Stress Relaxation in H2O
F15 (Arbitrary force units.)
Change in F28 in 5 minutes. (Arbitrary units.)
The Number of the Experiment.

Fig. 2. Comparison of mechanical properties of wool fibers in D_2O and H_2O. The experimental points in the upper diagram give the results of a number of successive experiments to find the force at 15% extension in these media. The fiber was immersed alternately in H_2O and in D_2O, and was relaxed in H_2O at 50° C. between immersions. The lower diagram gives the results of a similar series of experiments, but here the property plotted is stress-relaxation as measured by the decrease, during 5 min., of the force at 28% extension.

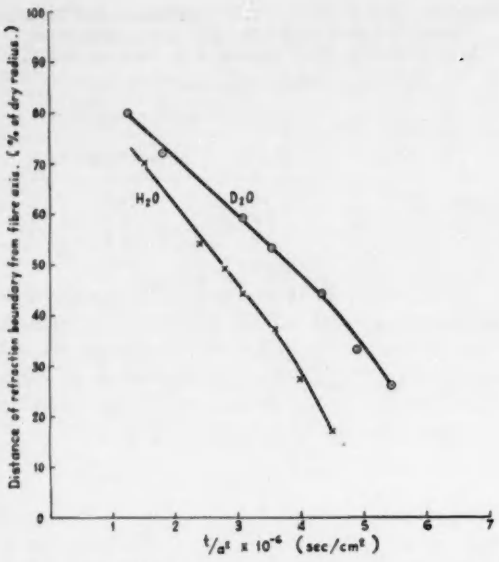

Fig. 3. The distance of the optical refraction boundary from the fiber axis (expressed as a percentage of the dry radius of the fiber) plotted against time/radius² when deuterium oxide or water enters a dry wool fiber. The time scale has been reduced by dividing by the square of the radius to correct for different diameters of the fibers from which these readings were obtained.

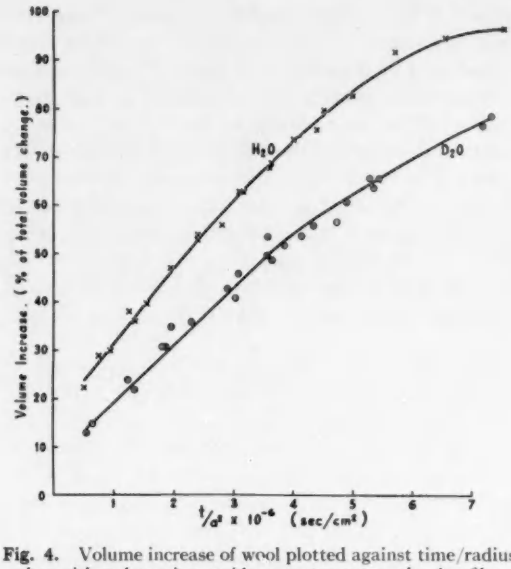

Fig. 4. Volume increase of wool plotted against time/radius² when either deuterium oxide or water enters the dry fiber.

This value is the mean of the results for three fibers, every one of which was subjected to a successive immersion alternately in H_2O and D_2O (see Figure 2). Also, the value of the change in stress in 5 min. after the fiber had been extended to 28% was found to be about 11% higher in D_2O than in H_2O (Table I). Again this value was estimated from the oscillations in the value of the relaxed stress in 5 min. for one fiber for each alternate experiment (Figure 2).

The velocity of the front of H_2O and D_2O entering into a dry wool fiber at 25° C. was measured. The results of this, normalized for radius, were plotted (Figure 3) and showed a higher velocity of H_2O front entry into the initially dry wool by a factor of 1.4_0. However, the equilibrium regain (volumetric) indicated by the final equilibrium swelling of the fiber showed no significant difference between H_2O and D_2O.

Calculations and Discussion

In all three cases considered the wool fibers in D_2O act as if in H_2O at a lower temperature. For single fibers at an extension rate of 7.2%/min. the value F_{15} increases by 0.855%/° C. decrease in temperature. The stress relaxation increases by 1.87%/° C. decrease in temperature. Both these results were obtained by repeating experiments of load extension and stress relaxation on single fibers in water at 20° C. and 10° C. in the same way as in the comparative H_2O–D_2O experiments. From these figures it was found that the greater value of F_{15} at 20° C. in D_2O is equivalent to a temperature drop in H_2O of 4.8/0.855 = 5.6° C. and in the case of the stress relaxation of 11/1.87 = 5.9° C.

In the case of water absorption into a dry fiber, one of us (A. R. H.) has from previous work at this laboratory obtained a value for the temperature coefficient of the slope of the approximately linear portion of the volume–time curve (see Figure 4). This value was equivalent to an energy of activation of 10 ± 1.5 kcal./g.mol. In the case of D_2O going into wool, the slope of this linear portion of the volume versus time curve decreases by a factor of 1.3_3. This change on the basis of an activation energy of 10 kcal./g.mol. is equivalent to a temperature drop of 4.9° C.

In all three cases dealt with the D_2O acts in the wool in the same manner as H_2O at a temperature reduced by about 5–6° C.

In the case of water absorption into the wool structure, the water is diffusing through a hydrogen

bonding medium, involving the making and breaking of hydrogen bonds. Both stress–relaxation (i.e., stress change at a fixed strain) and extension in the yield region involve the movement of main chains and side chains in the keratin structure. This movement would also, in the presence of water, involve the making and breaking of bonds similar to those involved in the diffusion of the water through the wool. The fact that the D_2O behaves in all three cases as H_2O with the temperature depressed by roughly 5–6° C. appears in agreement with this concept.

It is of interest to note that the dielectric properties of solid D_2O which are related to the rate of making and breaking of bonds in the structure have been shown [1] to be equivalent to ice with the temperature lowered by 4° C. On the other hand, in the liquid state the viscosity of D_2O at 20° C. can be shown from the values quoted by Kirshenbaum [4] to be equivalent to the viscosity of water 8° C. lower in temperature.

Literature Cited

1. Auty, R. P. and Cole, R. H., *J. Chem. Phys.* **20**, 1309–1314 (1952).
2. Feughelman, M., *J. Textile Inst.* **45**, T630 (1954).
3. Haly, A. R., *Proc. Int. Wool Text. Res. Conf. Austr.* **D**, 195–201 (1955).
4. Kirshenbaum, I., "The Physical Properties and Analysis of Heavy Water," New York, McGraw-Hill, 33 (1951).
5. Whalley, E., *Trans. Faraday Soc.* **53**, 1578 (1957).

Manuscript received January 5, 1959.

Properties of Fabrics Produced from Three Extra Long Staple Cottons

George F. Ruppenicker, Jr. and John J. Brown

Southern Regional Research Laboratory,[1] *New Orleans, Louisiana*

Abstract

Results are reported of a comparative evaluation of the properties of fabrics produced from the American-Egyptian Pima S-1, Egyptian Karnak, and a high strength Upland cotton, Hybrid Strain 330. Relationships of some fiber and yarn properties to fabric properties are shown. The reactions of fabrics woven from these cottons to chemical finishing treatments (mercerization, scouring, bleaching, and dyeing) are also discussed.

In general, it was found that the Pima S-1 cotton produced fabrics which were approximately equal in breaking and tearing strength to those made from Hybrid Strain 330 cotton and which were stronger than those made from Karnak. Grey fabrics made from Pima S-1 had higher elongation, greater resistance to flex abrasion, and better draping qualities than those made from the other two cottons. The finishing treatments had varied effects on the fabrics, but in most cases those made from Pima S-1 remained equal to or better than those made from the other cottons in the properties measured. Fiber and yarn properties were closely related to fabric properties.

Introduction

As new and improved cotton varieties are developed, it is necessary that they be thoroughly evaluated in terms of their processing performance and fiber, yarn, and fabric properties in order to determine their commercial potentials. The results of these evaluations help guide cotton breeders in developing new cottons for specific end uses, speed commercial utilization, and assist textile mills in obtaining optimum use value from these new cottons.

A report on the processing characteristics and

[1] One of the laboratories of the Southern Utilization Research and Development Division, Agricultural Research Service, U. S. Department of Agriculture.

yarn properties of extra long staple American-Egyptian Pima S-1 cotton has been published [3]. It was found that the Pima S-1 cotton processed equally as well as the Egyptian variety Karnak, and that the yarns made from Pima S-1 were stronger and more uniform than the Karnak yarns.

The purpose of this report is to present the results of a comparative evaluation of the properties of fabrics produced from Pima S-1, Karnak, and a high strength experimental strain, Hybrid Strain 330, and to show the degree to which certain fiber and yarn properties, such as strength and elongation, carry over into fabric constructions. The effects of chemical finishing treatments on the properties of the fabrics woven from these cottons are also discussed.

Materials and Methods

Samples

The Pima S-1 cotton was from the 1953 commercial crop, and the Egyptian Karnak was purchased on the open market. The Hybrid Strain 330 was an experimental cotton obtained by the Cotton and Cordage Research Branch, Crops Research Division, ARS, having been developed at the Pee Dee Agricultural Experiment Station, Florence, S. C., by W. H. Jenkins and D. C. Harrell. Hybrid Strain 330 is a long staple Upland cotton possessing a high fiber strength and a low fiber elongation, and was derived from Hopi Acala and Triple Hybrid crosses with Earlistaple (a long staple Upland cotton). This was an experimental cotton and, due to its low yield characteristics, was not released for commercial production. The similarity of the fiber properties of Hybrid Strain 330, other than its unusually low fiber elongation, with those of the Pima S-1 make it an excellent comparison cotton for this evaluation. One bale of each cotton was used in this evaluation.

A summary of the fiber properties of the three cottons is shown in Table I. Generally, these fiber properties are as follows.

Grade. The Pima S-1 was slightly higher in grade than the Karnak and was one grade lower than the Hybrid Strain 330. (Since the Karnak was graded according to Egyptian standards, an exact comparison cannot be made.)

Length. The staple length of all three cottons was $1\frac{7}{16}$ in. The Pima S-1 and Hybrid Strain 330 varieties had longer mean lengths and more uniform fiber length distributions than the Karnak, as measured by the Suter-Webb and Fibrograph methods of length determination.

Fineness. The Pima S-1 was finer than the Hybrid Strain 330 and coarser than the Karnak according to each of the three methods used for measuring this property.

Strength. Hybrid Strain 330 had greater tenacity than the other two cottons, as shown by the Pressley indices and Stelometer values at zero gauge. There were no appreciable differences in the tenacities of the cottons as determined by the Stelometer at $\frac{1}{8}$-in. gauge. It was noted, however, that the strength differential between the zero gauge and the $\frac{1}{8}$-in. gauge was greatest for the Hybrid Strain 330, indicating poor uniformity of strength along the fiber length [10].

Elongation. The fiber elongation of the Pima S-1 was 19% higher than that of the Karnak and 63% higher than that of the Hybrid Strain 330.

Wax content. The wax content of the Hybrid Strain 330 was less than that of either the Pima S-1 or Karnak.

Processing and Testing Procedures

The cottons were processed alike on conventional cotton processing equipment with the comber being set to remove 15% noils from the Karnak cotton. With this same setting 10% noils were removed from the Pima S-1 and 11% from the Hybrid Strain 330.

All yarns (46/1 and 58/2) were spun with a twist multiplier of 3.75 for both singles and plied constructions. A semi-broadcloth fabric, 112 × 64 construction, weighing approximately 3.80 oz./sq. yd., was selected to evaluate the three cottons. 58/2 yarns were used in the warp so that the grey fabrics would be tested in the raw cotton form without sizing.

The fabrics were woven at a width of 37 in. and finished to a width of 35 in. The finishing processes included mercerization, scouring, hydrogen peroxide bleaching, and vat dyeing. The mercerization was done on a padder, and subsequent operations were completed on a jig. In order to eliminate any variation in chemical processing from one fabric to another, the grey fabrics were sewn together and finished as one lot. Samples of the fabrics for testing were removed after each stage of the finishing procedure.

TABLE I. Fiber Properties of Pima S-1, Karnak, and Hybrid Strain 330 Cottons

Fiber property	Pima S-1	Karnak	Hybrid Strain 330
Grade	Grade 3	Fully good $\frac{1}{8}$ to good fully good	Grade 2
Length			
Classer, in.	$1\frac{7}{16}$	$1\frac{7}{16}$	$1\frac{7}{16}$
Array, Suter-Webb method			
U.Q., in.	1.42	1.35	1.45
Mean, in.	1.22	1.07	1.22
C.V., %	24	34	28
Fibrograph method			
U.H.M., in.	1.37	1.25	1.41
Mean, in.	1.16	0.96	1.20
U.R., %	85	77	85
Fineness			
Linear density, Suter-Webb method, μg./in. (millitex)*	3.2 (126)	2.8 (110)	3.7 (146)
Micronaire reading	3.9	3.2	4.2
Specific area, Arealometer method, mm.²/mm.³	486	550	480
Maturity			
Sodium hydroxide method, %	94	86	92
Strength			
Pressley			
Zero gauge, lb./mg. (g./tex)	8.92 (47.8)	9.18 (49.2)	10.03 (53.8)
Stelometer			
Zero gauge, g./tex	42.0	43.7	46.7
$\frac{1}{8}$ in. gauge, g./tex	30.5	29.1	29.1
Elongation			
Stelometer			
$\frac{1}{8}$ in. gauge, %	11.25	9.45	6.88
Wax content, %	0.73	0.73	0.61

* Wherever applicable, the fiber or yarn number in tex is given in parenthesis for information [2] (tex = g./km.).

The fabrics were tested in accordance with Federal Specifications, Textile Test Methods, CCC-T-191b, for warp and filling breaking strength using strips raveled to 112 ends and 64 picks, respectively [12b]; tearing strength by the tongue method [12c]; abrasion resistance by the flexing (Stoll) method, using a flex bar load of 4 lb. and a pressure plate load of 1 lb. [12d]; and crimp in yarn from fabrics by the load–elongation method [12a]. Draping properties of the fabrics were measured on a drapemeter developed by Fabric Research Laboratories, Inc. [4].

Single strand yarn strength and elongation at break tests were made on the Uster[2] automatic single strand tester. Twenty breaks were made from each of seven bobbins (i.e., 140 breaks for each test), using a 50-cm. gauge length, a constant rate of loading, and an average 10 sec. to break. All fiber properties were determined by ASTM methods [1a–g], except for the wax content determinations [5].

Differences in yarn and fabric property values were tested for statistical significance. In all cases where significance is mentioned the differences were significant at the 95% probability level.

Results and Discussion

Strength

The breaking and tearing strengths of the grey, mercerized, bleached, and dyed fabrics made from Pima S-1, Karnak, and Hybrid Strain 330 cottons are shown in Table II. In order to show the

[2] The use of trade names does not imply their endorsement by the Department of Agriculture over similar products not mentioned.

TABLE II. Single Strand Break Factor of Warp and Filling Yarns and Breaking and Tearing Strengths of Fabrics Made from Pima S-1, Karnak, and Hybrid Strain 330 Cottons.

	Pima S-1	Karnak	Hybrid Strain 330
Yarns (single strand break factor)			
58/2 Warp (10.2 tex × 2)	517	432	518
46/1 Filling (12.8 tex)	464	395	469
Fabrics, lb.			
Breaking strength*			
Grey			
Warp	144.2	132.4	147.0
Filling	42.1	32.6	43.8
Mercerized			
Warp	150.4	141.8	151.8
Filling	42.8	40.6	44.5
Scoured and bleached			
Warp	148.4	139.6	158.2
Filling	42.8	37.7	47.5
Dyed			
Warp	149.0	141.4	156.6
Filling	41.5	37.7	47.8
Tearing strength (tongue method)			
Grey			
Warp	8.6	6.7	8.5
Filling	4.8	4.1	4.8
Mercerized			
Warp	8.0	7.4	7.9
Filling	5.2	4.4	4.9
Scoured and bleached			
Warp	7.8	6.7	7.8
Filling	5.5	4.5	5.3
Dyed			
Warp	6.4	6.3	6.9
Filling	5.1	4.5	5.4

* Raveled strip method using a thread count of 112 × 64.

relationship between yarn and fabric strengths, the breaking strengths of the warp and filling yarns used to weave the three fabrics are also included in this table.

There was a poor relationship between yarn strength and fiber bundle strength at either zero or $\frac{1}{8}$-in. gauge. The Pima S-1 made yarns that were considerably stronger than those spun from the Karnak, and approximately equal in strength to those spun from the high strength Hybrid Strain 330. Although fiber strength is a main determinant of yarn strength, other fiber properties such as length, length variability, fineness, elongation, and uniformity of strength along fiber length are contributing factors [6, 7, 8, 9, 10, 13]. The lower strength of the Karnak yarns can probably be attributed primarily to the shorter fiber mean length and less uniform fiber length distribution of the Karnak cotton. The greater nonuniformity of strength along the fiber length of the Hybrid Strain 330 may explain, in part, why this high strength cotton did not produce yarns that were significantly stronger than those spun from the Pima S-1.

Fabric breaking strengths were closely related to yarn strengths. An analysis of the warp and filling breaking strengths of the grey fabrics showed that the Pima S-1 was approximately equal to the Hybrid Strain 330 and considerably stronger than the Karnak fabric. The finishing operations had no significant effect on the breaking strength of the Pima S-1 fabric. However, the Karnak fabric increased significantly in breaking strength due to mercerization, and the Hybrid Strain 330 fabric showed a significant increase after scouring and bleaching. The completely finished and dyed Pima S-1 fabric was still significantly stronger than the Karnak fabric but not as strong as the Hybrid Strain 330 fabric. These variations in breaking strength during finishing may be partly due to differences in the amount of natural waxes present on the raw cottons. As shown in Table I, the wax content of the Hybrid Strain 330 cotton was less than that of either the Pima S-1 or Karnak.

A comparison of the warp and filling tearing strengths of the fabrics showed that, generally, the Pima S-1 was equal to the Hybrid Strain 330 and stronger than the Karnak in the grey and after mercerization, scouring, bleaching, and dyeing. One exception was in the warpwise tearing strength of the dyed fabrics. The Pima S-1 was approximately equal to the Karnak, but its tearing strength was significantly less than that of the Hybrid Strain 330 fabric. Over-all, the fabrics increased in tearing strength fillingwise and decreased warpwise as a result of chemical finishing.

Elongation

Table III shows the elongation at break of fabrics made from the three cottons in the grey and after each finishing process and the single strand elongation at break of the warp and filling yarns used to weave the fabrics. The warp and filling crimp was determined on yarns taken from the fabrics and is also given in this table.

There was a good relationship between fiber and

TABLE III. Single Strand Elongation at Break of Warp and Filling Yarns, Crimp in Yarns from Fabrics, and Elongation at Break of Fabrics Made from Pima S-1, Karnak, and Hybrid Strain 330 Cottons

	Pima S-1	Karnak	Hybrid Strain 330
Yarn elongation at break, %			
58/2 Warp (10.2 tex × 2)	7.7	7.0	6.3
46/1 Filling (12.8 tex)	8.0	7.0	6.1
Crimp in yarns from fabrics, %			
Grey			
Warp	8.2	8.5	8.2
Filling	3.1	2.9	2.1
Mercerized			
Warp	5.0	4.7	7.6
Filling	7.6	4.4	3.3
Scoured and bleached			
Warp	4.1	3.9	3.5
Filling	7.0	4.4	2.9
Dyed			
Warp	4.2	4.1	4.4
Filling	5.4	4.3	3.9
Elongation at break of fabrics, %			
Grey			
Warp	16.5	15.8	14.4
Filling	12.5	9.9	10.7
Mercerized			
Warp	15.3	12.4	13.9
Filling	15.7	12.2	12.0
Scoured and bleached			
Warp	14.1	13.0	12.6
Filling	16.2	13.2	11.8
Dyed			
Warp	13.8	11.3	12.1
Filling	15.2	14.4	12.8

yarn elongation. The high elongation Pima S-1 cotton made the yarns with the highest elongation and the low elongation Hybrid Strain 330 cotton spun into yarns with the lowest elongation.

Variations in fiber and yarn elongation at break had no determinable effect on the crimp of the warp yarns in the fabrics. However, differences in fiber and yarn elongation at break were found to have some effect on the crimp of the filling yarns, with the yarns from the Pima S-1 fabric having the highest crimp and those from the Hybrid Strain 330 the lowest. The grey fabric samples had much more crimp in the warp than in the filling yarns, which is not unusual for a fabric of this type construction. The finished fabrics were processed under warp tension and framed out to a width 2 in.

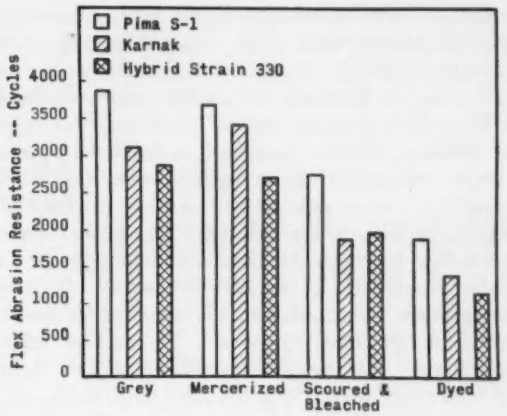

Fig. 1. Flex abrasion resistance (warp) of fabrics made from Pima S-1, Karnak, and Hybrid Strain 330 cottons.

narrower than the grey width, resulting in much of the crimp being transferred from the warp to the filling.

Fiber and yarn elongation at break carried over to some extent into fabric form. Before finishing and after each finishing process, the Pima S-1 fabric had a significantly higher elongation at break in both the warp and filling than the other two fabrics. In most cases the Karnak fabric had a higher elongation at break than the Hybrid Strain 330 fabric. In general, warp elongation decreased and filling elongation increased as a result of the successive finishing operations. This was probably due to the redistribution of crimp resulting from the method of finishing.

Abrasion Resistance

As shown in Figure 1, the fabric woven from Pima S-1 cotton was much better than the other two fabrics in flex abrasion resistance in the grey and after each stage of the finishing operations. The abrasion resistance of the Karnak fabric was, in most cases, better than that of the Hybrid Strain 330 fabric. Mercerization did not significantly change the abrasion resistance of any of the fabrics. The abrasion resistance of the fabrics was reduced considerably after scouring, bleaching, and dyeing. The dyed samples could withstand only 40–50% of the flex abrasion cycles withstood by the original grey samples. This is believed to be partly due to the removal of natural oils and waxes from the cottons during the finishing opera-

tions. Structural changes in the fabrics resulting from finishing would also have some effect on abrasion resistance.

The results indicate that a fabric produced from a high elongation cotton can withstand this type of abrasion better than one made from a low elongation cotton. Since the fiber strengths of the three cottons are essentially the same (Stelometer values at ⅛-in. gauge), the high elongation Pima S-1 cotton has a greater toughness index [11] than either the Hybrid Strain 330 or Karnak. Toughness, or the ability of a textile material to absorb work, is indicative of its flex life and abrasion resistance. The toughness indices of the three cottons were Pima S-1: 1.72, Karnak: 1.38, and Hybrid Strain 330: 1.00.

Drapeability

The draping properties of the fabrics were measured by Fabric Research Laboratories, Inc. Table IV shows the results of this test. Since the draping characteristics of a fabric are believed to be affected, to some extent, by fiber stiffness [11], the elastic properties of the cottons expressed in terms of average stiffness (secant modulus) are also shown in this table.

The fabrics made from the cottons with a low modulus or stiffness had better draping characteristics than those made from cottons with higher modulus. The average fiber stiffness of the Pima S-1 was slightly lower than that of the Karnak and considerably lower than that of the Hybrid Strain 330. Fabric made from the Pima S-1 had better draping properties than that made from the Hybrid Strain 330 cotton in the grey and after each of the finishing processes. The Pima S-1 fabric also had better draping properties than the Karnak in the grey and after dyeing, but there were no appreciable differences between these two fabrics after either mercerization or bleaching. Mercerization improved the drapeability of all three fabrics, but the subsequent finishing operations had a stiffening effect, resulting in larger drape coefficients. The apparent relationship between the elastic properties of a cotton and fabric drapeability should be of significance to cotton breeders, since drapeability is considered an important property in many fabric end uses.

TABLE IV. Average Fiber Stiffness and Drape Coefficients of Fabrics Made from Pima S-1, Karnak, and Hybrid Strain 330 Cottons

	Pima S-1	Karnak	Hybrid Strain 330
Average fiber stiffness*	271	308	423
Fabric drape coefficient, % F†			
Grey	68.5	73.0	76.9
Mercerized	60.5	59.0	66.9
Scoured and bleached	66.6	68.0	73.9
Dyed	63.6	69.7	76.2

* Based on Stelometer ratios of tenacity and break elongation at ⅛-in. gauge length. Average stiffness = tenacity (g./tex) × 100/elongation at break (%).

† Results obtained from a drapemeter developed by Fabric Research Laboratories, Inc. Fabrics having the lower drape coefficients have better draping properties.

Hand and Appearance

The hand or "feel" of a fabric is closely related to its draping properties. A subjective hand evaluation of the finished fabrics disclosed that the Pima S-1 and Karnak fabrics had a soft, smooth hand while the Hybrid Strain 330 fabric was notably harder and harsher than were the other two fabrics.

The Pima S-1 grey fabric was approximately the same color as the Karnak fabric and considerably darker than the Hybrid Strain 330 fabric. The raw cottons also showed these same differences in color. The Hybrid Strain 330 fabric was whiter than the other two fabrics after bleaching. However, there were no differences in the shades of the dyed fabrics when examined under either daylight or artificial light. This indicates that, for this finishing procedure, all three cottons had approximately the same affinity for the vat dye used.

Conclusions

Generally, the results of this evaluation showed that the Pima S-1 cotton produced fabrics that were either equal to or better than those made from Karnak or Hybrid Strain 330 cottons. Fiber and yarn properties were closely related to fabric properties. The finishing treatments had varied effects on the properties of the fabrics.

Strength. In the grey, the Pima S-1 and Hybrid Strain 330 fabrics were approximately equal in breaking strength and both were significantly stronger than the Karnak fabric. After finishing, the Hybrid Strain 330 fabric had a higher breaking strength than the Pima S-1 fabric. The tearing

strength data of the grey and finished fabrics showed that, generally, the Pima S-1 and Hybrid Strain 330 fabrics were about equal in this property with both being stronger than the Karnak fabric. Fabric breaking and tearing strengths were closely related to yarn strengths, but there was a poor relationship between fiber and yarn strengths.

Elongation. Fabric woven from the high elongation Pima S-1 cotton had a significantly higher elongation at break than that woven from either the Karnak or low elongation Hybrid Strain 330 cotton, indicating that fiber and yarn elongation carried over, to some extent, into fabric form. In most cases the Karnak fabric had a higher elongation than the Hybrid Strain 330 fabric.

Abrasion resistance. Fabric made from Pima S-1 cotton was much better than fabrics made from Karnak and Hybrid Strain 330 cottons in flex abrasion resistance, both before and after chemical finishing. The Hybrid Strain 330 fabric had the lowest resistance to flex abrasion. The data indicate that fabric abrasion resistance is closely related to the fiber toughness index.

Drapability. The Pima S-1 fabric exhibited better draping qualities than either the Karnak or Hybrid Strain 330 fabrics. The Hybrid Strain 330 fabric had the poorest draping properties. It was shown that fabrics made from cottons with a low modulus or average stiffness have better draping characteristics than those made from cottons with a high modulus.

Hand and appearance. All three cottons produced fabrics of excellent quality and appearance. Although the Hybrid Strain 330 fabric was whiter than the other fabrics after bleaching, there were no differences in the shades of the dyed fabrics. The dyed Pima S-1 and Karnak fabrics had a softer and smoother hand than the dyed Hybrid Strain 330 fabric.

Acknowledgments

The authors wish to express their appreciation to the Cotton and Cordage Research Branch, Crops Research Division for its assistance in the selection of the Pima S-1 and Hybrid Strain 330 cottons; to fellow members of the Cotton Mechanical Laboratory for processing the cottons into yarns and fabrics; to members of the Cotton Chemical Laboratory for finishing the fabrics; to members of the Product Evaluation group, Instrumentation and Analysis, for conducting the various tests on the fibers, yarns and fabrics; to Herschel W. Little for his help and guidance in making the statistical analysis of the data; and to Fabric Research Laboratories, Inc. for performing the drapeability tests.

Literature Cited

1. ASTM, (a) D1440-55, (b) D1442-54, (c) D1445-57, (d) D1447-54T, (e) D1448-56, (f) D1449-55T, (g) "ASTM Standards on Textile Materials," Appendix XIII, November, 1957. Am. Soc. Testing Materials, Philadelphia, Pa.
2. Bayes, A. W., *J. Textile Inst.* **48**, P225–267 (1957).
3. Brown, J. J., Howell, N. A., Fiori, L. A., and Sands, J. E., TEXTILE RESEARCH JOURNAL **25**, 404–414 (1955).
4. Chu, C. C., Cummings, C. L., and Teixeira, N. A., TEXTILE RESEARCH JOURNAL **20**, 539–548 (1950).
5. Conrad, C. M., *Ind. Eng. Chem., Anal. Ed.* **16**, 745–748 (1944).
6. Fiori, L. A. and Brown, J. J., TEXTILE RESEARCH JOURNAL **21**, 750–757 (1951).
7. Fiori, L. A., Brown, J. J., and Sands, J. E., TEXTILE RESEARCH JOURNAL **24**, 503–507 (1954).
8. Fiori, L. A., Brown, J. J., and Sands, J. E., TEXTILE RESEARCH JOURNAL **26**, 296–302 (1956).
9. Fiori, L. A., Sands, J. E., Little, H. W., and Grant, J. N., TEXTILE RESEARCH JOURNAL **26**, 553–564 (1956).
10. Orr, R. S., DeLuca, L. B., Burgis, A. W., and Grant, J. N., TEXTILE RESEARCH JOURNAL **29**, 144–150 (1959).
11. Smith, H. DeW., *Am. Soc. Testing Materials Proc.* **44**, 543–592 (1944).
12. U. S. Federal Supply Service, "Textile Test Methods," Fed. Specifications CCC-T-191b. Methods (a) 4112, (b) 5104, (c) 5134, (d) 5300 (1951).
13. Webb, R. W., U. S. Dept. Agr., *Market Res. Rept.* **197** (1957).

Manuscript received January 19, 1959.

Isolation and Identification of Urocanic Acid Found in Extracts of Raw Wool

Charles H. Binkley and Francis T. Jones

Western Regional Research Laboratory,[1] *Albany, California*

In A study of the natural causes of nonscourable discoloration of wool, the question of the presence of urocanic acid in suint was raised. Neither the action of alkali as discussed by Serra and de Matos [12] nor of bacterial pigments studied by Seddon [11] and by Fraser and Mulcock [5] will account for the experimentally induced discoloration when wool is held in the presence of suint at 55° C. and at high humidities; the color is due to neither alkali nor bacterial pigments. As it is nonscourable, it is not caused by lanaurin, the deeply colored suint component discussed by Rimington and Stewart [10]. It was thought possible that urocanic acid, which has been shown by Zenisek and Kral [18] to be present in human perspiration, might also be present in suint and might, either directly or through interaction with other suint components, cause or contribute significantly to this experimental wool discoloration and be involved in natural wool discoloration. Urocanic acid alone on wool when held at 55° C. at high humidities causes discoloration, though less than that caused by suint under the same conditions. However, the concentration of urocanic acid in suint is low and its wool discoloring effect per mole is low as compared with other components of suint. Insofar as suint components may cause wool discoloration, the effect of urocanic acid must be relatively small.

We have found urocanic acid, in two isomeric forms, to be present in the water extract of a raw wool. One of these isomers we have isolated as its flavianate and have identified it by comparing its crystallographic properties with those of the flavianate of synthetic urocanic acid (Figure 1).

[1] A laboratory of the Western Utilization Research and Development Division, Agricultural Research Service, U. S. Department of Agriculture.

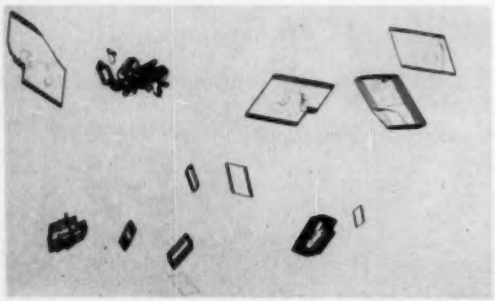

Fig. 1. Characteristic crystals of trans urocanic acid flavianate.

Experimental

Aqueous Extracts of Raw Wool

Water extracts were made from the root ends of wool locks taken from a fleece well skirted to eliminate possible contamination by urine or fecal matter. The root ends were separated by cutting below the area of contamination and discarding the tips. After we removed the wool waxes in a Soxhlet extractor, using petroleum ether, 1 lb. of the root-end wool was extracted with 3 successive 2-l. portions of water at 60° C. The combined washings were filtered and concentrated to 250 ml. by boiling. This concentrate was then cooled and centrifuged to remove flocculating suint components. The clarified solution was shaken with n-butanol saturated with aqueous ammonia and the n-butanol solution, containing the urocanic acid, was decanted. The extraction was repeated until the residue showed no urocanic acid by chromatographic test. The n-butanol solution was then evaporated to a convenient small volume. Urocanic acid was separated from this extract by the techniques of paper chromatography.

Chromatographic Methods

The methods of paper chromatography were used to guide the initial fractionation of the water extract and for the subsequent purification of the

urocanic acid. The stainless-steel tank and rack equipment described by Hunter, Houston, and Owens [6] was used with multiple 9 × 9-in. papers. Whatman No. 1 paper was used throughout the work. Ultraviolet absorption, ninhydrin, and diazosulfanilic acid, as suggested by Ames and Mitchell [2], were used as indicators for the urocanic acid and the amino acids from which it was separated on the papers. The principal solvents used to develop the chromatograms were 70% tertiary butanol with 30% 0.2 *N* ammonia and 70% tertiary butanol with 30% of 3% formic acid. Other solvents mentioned by Block[2] were found suitable and were used to show differences in chromatographic behavior of the two urocanic acid isomers (Table I).

TABLE I. Approximate R_f Values of Two Urocanic Acid Isomers With Various Irrigating Solvents

Irrigating solvent	Solvent pH	Approximate R_f values of isomers: From suint and synthetic (trans)	Approximate R_f values of isomers: From suint and irradiated synthetic (cis)
70/30 t-butanol/0.2 *N* ammonia	10	43	67
70/30 t-butanol/3% formic acid	2.9	67	67
40/40/20/4 t-butanol/methyl ethyl ketone/water/diethyl amine	11.4	33	62
3/1 l-propyl alcohol/1 *N* acetic acid	2.5	68	68
80/20/4 methanol/water/pyridine	8.3	61	61

Separation of Urocanic Acid

To separate urocanic acid from amino acids, the n-butanol concentrate was streaked on papers. These were developed overnight with t-butanol–formic acid solvent. Each developed paper was inspected and marked with only the edges exposed under an ultraviolet lamp. The highly absorbing zone containing both urocanic acid isomers was cut out and eluted with slowly dropping water after packing the strips in a tube. The eluate was next chromatographed with the t-butanol ammonia solvent to separate the cis and trans isomers. From these papers the lower R_f (slower moving)[3] and highly ultraviolet-absorbing band containing the more abundant trans isomer was marked and cut out. After we discarded the irradiated ends of these strips, the urocanic acid was recovered by elution.

Crystals for Identification

The eluate containing the principal isomer of urocanic acid was treated with an excess of flavianic acid. After crystals had formed, the solution was removed and the crystals were dissolved in a hot dilute flavianic acid solution. As this solution cooled and stood, the urocanic acid flavianate formed crystals suitable for characterization.

The crystals become opaque and lose their form when heated to 153–155° C. in air or in 2 mm. vacuum as water of crystallization is lost. The compound melts with decomposition at about 250° C. Analysis shows the salt to be urocanic acid flavianate, with 1 mole of water of crystallization.

Formula: $C_2H_6O_2N_2 \cdot C_{10}H_6O_8N_2S \cdot H_2O$

	Analysis: Theory %	Analysis: Found %
Carbon	40.85	40.9
Hydrogen	2.98	3.01
Nitrogen	11.9	11.7
Sulfur	6.8	7.03
Water (loss, 154°, 2 mm.)	3.83	4.12

Results

Chromatography of the Mixed Isomers

Two-dimensional chromatograms showed multiple identification spots for the suint urocanic acid, while one spot only was obtained for the synthetic compound. When the synthetic urocanic acid spot was irradiated under an ultraviolet lamp, even for the brief period of inspection after acid irrigation, subsequent chromatography with a basic irrigant gave two identification spots. This is consistent with Stoermer's rule [13] for the formation of a less stable ethylenic isomer by the ultraviolet irradiation of the more stable form. Paper chromatography shows the same two isomers to be present in suint. When a synthetic urocanic acid solution was held under an ultraviolet lamp or left standing in the diffuse light of the laboratory, it

[2] Block's Manual [3] was used as a guide throughout this work.

[3] $R_f = \frac{\text{movement of band}}{\text{movement of advancing front of liquid}}$

gave the same two-dimensional chromatogram patterns as did the suint urocanic acid. The R_f values for the two isomers were independent of the urocanic acid source. Their identity in chromatography is further demonstrated by enhancement of both isomer spots by addition of the irradiated synthetic compound to the suint urocanic acid.

The R_f values for the two isomers depend on the irrigating solvent. They were consistent, whether pure trans isomer, mixed isomers giving two spots, or two-dimensional separation of the mixture was used. The approximate values are shown in Table I.

Isomerization

Edlbacher and Hertz [4] and others [8, 9] have found that synthetic urocanic acid and its salts have higher melting points than do the corresponding compounds obtained after ultraviolet or sunlight irradiation of the synthetic urocanic acid. By analogy with fumaric and maleic acids and with *o*-hydroxy cinnamic acids, they show synthetic urocanic acid to be trans and the compound obtained by its irradiation to be cis. The difference in chromatographic behavior is consistent with this view. In the cis isomer, basic dissociation would be suppressed by the proximity of the carboxyl to the 1-amino group. There should be no change in solubility or in solvent partition for the cis isomer with change in pH of the irrigating solvent in the alkaline range in which the 1-amino group of the trans isomer is dissociating. Thus the synthetic urocanic acid used in this study[4] and the more abundant fraction of the suint urocanic acid must be trans, while the isomer produced by irradiation and the lesser fraction in suint must be cis.

Origin

The origin of the urocanic acid was not explored. It may be significant, in view of the appearance of urocanic acid as a bacterial metabolite of histidine [7, 17], that the suint sample studied contained appreciable histidine and was neutral. (pH 6.4–7.6 was found for the suint of random locks of wool from the fleece used.) Other evidence may have bearing on this question. Urocanic acid was found in the water extract of a clean wool that had been strongly irradiated with ultraviolet light. Hydrolysis of the extract resulted in an increase of the urocanic acid detected by chromatography. Furthermore, urocanic acid has been found among photolytic products of histidine [14]. Thus the urocanic acid may originate from histidine in wool and appear in suint by any of a variety of paths where the initial step is action of sunlight and weather on the fleece. The original assumption of an analogy between presence of urocanic acid in human perspiration and in suint may not be valid.

Quantity

The amount of urocanic acid found was estimated on the basis of the extinction coefficient of the eluate containing both isomers, compared with the synthetic urocanic acid. This method showed approximately 100 mg. per pound of the raw wool used.

Crystallization

A gum in the eluates interfered with crystallization of urocanic acid from suint. Although crystals suitable for identification could not be obtained, those that were obtained in the presence of the gum showed high birefringence and were of the same crystal form as synthetic urocanic acid. The gum was shown to originate with the chromatographic paper and presumably consisted of hemicelluloses. Ultraviolet spectroscopy demonstrated an unidentified component of a blank eluate to be also in the urocanic acid eluate. The absorption spectra of eluted urocanic acid and of the synthetic compound were the same after corrections were made for this impurity. Nitric, picric, and picrolonic acids have been used by others [4] in identifying urocanic acid, but these were unsatisfactory with the eluate. The use of flavianic acid by Vickery [15, 16] in an analytic system for basic amino acids suggested its use for the small amount of urocanic acid in the eluates in the presence of paper impurities. When flavianic acid was added to the eluate, crystals of trans urocanic acid monoflavianate monohydrate were readily obtained. These were recrystallized from dilute flavianic acid for identification. The optical and crystallographic properties were the same for this and for the compound prepared from synthetic urocanic acid.

[4] Urocanic acid for this study was prepared in this laboratory by W. Gordon Rose, using the Akabori method [1].

Optical and Crystallographic Properties

Form and habit. Crystals of synthetic trans urocanic acid monoflavianate monohydrate were obtained by adding an aqueous solution of repurified flavianic acid to a warm aqueous solution of synthetic trans urocanic acid. Yellow bladed or prismatic crystals grew on the container walls almost at once. After digestion overnight, these crystals were separated and given a quick rinse with cold water on a vacuum filter. Crystals prepared in this way were used for measurement of refractive indices. Figure 1 shows crystals grown on a microscope slide by cooling a warm saturated solution of the salt. It was necessary to seed the drop with a few crystal fragments in order to make sure that the stable phase was formed.

When drops of aqueous solutions of urocanic acid and of flavianic acid are mixed on a microscope slide, crystals of a metastable compound are often formed. These crystals usually transform slowly to the stable phase described below.

The crystals of the stable phase usually grow as thick blades or prismatic tablets two or three times as long as their width. Twins are occasionally seen. End views are rare. The ends of the crystals are characteristically rough and slightly convex. The sides frequently show imperfect development.

Optic orientation. All views show oblique extinction. One common view that shows an extinction angle of about 15° gives an interference figure approximately centered between the acute and obtuse bisectrices. The refractive indices α' and β are measurable on this view. Another common view (Figure 1) that shows an extinction angle of 25° gives an interference figure nearly centered between the obtuse bisectrix and the optic normal. The refractive indices α and γ' can be measured on this view, which is also shown by the twinned crystals. The α vibration directions in the two portions of the twins make an angle of 51° which is bisected by the twin boundary. The acute end angle on the silhouette of this view is 65°.

End views show an eight-sided silhouette and give an interference figure that shows the acute bisectrix and one melatope. Both the axial plane and the acute bisectrix are inclined a few degrees from the microscope axis. This view gives refractive indices close to β and γ.

Refractive indices (sodium light, 27° C.). $\alpha = 1.450$, $\beta = 1.765$, $\gamma = 1.93$, $\alpha' = 1.494$, $\gamma' = 1.86$.

Optical axial angle. (−) 2V = 60°, calculated from α, β, and γ.

Crystal system. Triclinic.

Fusion behavior. Crystals become opaque at about 175° C., indicating loss of water of crystallization. Further heating results in melting with decomposition, bubbling, and darkening. No crystals form from the melt.

Acknowledgments

The authors are indebted to Glen F. Bailey for the extensive spectrographic work involved in this study and its interpretation, to Lawrence M. White for the microanalyses, to W. Gordon Rose for preparation of an ample supply of urocanic acid, and to Harold P. Lundgren for suggesting the project and for his helpful discussions during its progress.

Literature Cited

1. Akabori, S., Ose, S., and Kaneko, T., *Proc. Imp. Acad. Japan* **16**, 191 (1940).
2. Ames, B. H. and Mitchell, H. K., *J. Am. Chem. Soc.* **74**, 252 (1952).
3. Block, R. J., Durrum, E. L., and Zweig, G., "A Manual of Paper Chromatography and Paper Electrophoresis," Academic Press, New York (1955).
4. Edlbacher, S. and Hertz, Fr., *Annalen Physiol. Chem.* **279**, 63 (1943).
5. Fraser, I. E. B. and Mulcock, A. P., *Nature* **177**, 628 (1956).
6. Hunter, I. R., Houston, D. F., and Owens, H. S., *Anal. Chem.* **28**, 283 (1956).
7. Magasanik, B. and Bowser, H. R., *J. Biol. Chem.* **213**, 571 (1955).
8. Masuda, K., *J. Pharm. Soc. Japan* **76**, 325 (1956).
9. Pasini, C. and Vercellone, A., *Gazz. chim. ital.* **85**, 349 (1955).
10. Rimington, C. and Stewart, A. M., *Proc. Roy. Soc.* **B110**, 75 (1932).
11. Seddon, H. R., *Sci. Bul.* (Dept. Agr. N.S. Wales) **54**, 96 (1937).
12. Serra, J. A. and de Matos, R. M. A., *J. Textile Inst.* **42**, T329 (1951).
13. Stoermer, R., *Annalen* **342**, 1 (1905).
14. Tomohiro, Y., *Nagasaki Igakkai Zassi* **28**, 1117 (1953).
15. Vickery, H. B., *J. Biol. Chem.* **71**, 303 (1927).
16. Vickery, H. B., *J. Biol. Chem.* **132**, 325 (1940).
17. Wickremasinghe, R. L. and Fry, B. A., *Biochem. J.* **58**, 268 (1955).
18. Ženíšek, A. and Král, J. A., *Biochem. et Biophys. Acta* **12**, 479 (1953).

Manuscript received December 17, 1958.

The Mechanism of Pilling[1]

Daniel Gintis and Edward J. Mead

"Dacron"[2] Research Laboratory, E. I. du Pont de Nemours and Co., Inc., Kinston, North Carolina

Abstract

Studies of the mechanism of pilling have demonstrated that pilling propensity is determined by the rates of fuzz formation, entanglement, and pill wearoff. Motion pictures of fabrics subjected to an abrading action showed that the abradant acted on exposed fiber sections to pull loops which then opened to form fuzz. A pill formed quickly when the fuzz density reached a critical level. The fibers were then twisted and entangled, gradually involving nearby fibers. As the abrading action continued, pills wore away.

Techniques were developed which permitted independent quantitative study of each of these three phenomena. The physical properties of several textile fibers were correlated with their behavior in these tests. Interfiber friction and bending stiffness were important factors in fuzz formation. Entanglement tendency was correlated with denier, cross-sectional shape, and bending stiffness. Pill wearoff was determined by abrasion resistance and tenacity.

The general applicability of this mechanism has been demonstrated with modified polyester fibers. The reduced pilling tendency of ribbon staple fibers was attributed to a directional bending which reduced their entanglement tendency. Heat-setting increased bending stiffness, which reduced pilling by lowering fuzzing tendency. The most pronounced effect on pilling tendency of polyester fibers was obtained by changes in abrasion resistance, which affected the rate of pill wearoff.

Introduction

Pilling has long been recognized as a problem in staple fabrics. With the advent of the new synthetic fibers, the problems became more acute. A considerable degree of success in controlling pilling has been obtained through studies on the effects of yarn and fabric variables (yarn twist, fabric tightness, heat-setting, etc.) on pilling [2]. However, relatively little attention has been devoted to the mechanism of pilling.

Pilling studies have shown that there are three distinct stages in the life span of a pill. First, fibers are surfaced as a result of some mechanical action on the fabric. Second, surfaced fibers entangle or mat into the familiar configuration of a pill. Finally, the pill may be worn or pulled away from the fabric. In a given fabric construction, the rate or extent to which these stages occur is determined by the physical properties of the fibers which comprise the fabric. By determining those properties which operate in the fuzz formation, entanglement, and pill breakoff steps, an understanding of the over-all mechanism of pilling can be achieved.

To evaluate a variety of fibers in each of the three stages independently, it was necessary to develop tests designed specifically to isolate each stage. This information was then correlated with various physical properties of the fiber in an effort to determine those properties which contributed most significantly to the pilling performance.

Results and Discussion

Time Lapse Motion Picture Study

To study this problem, it was desirable to follow the motions of fibers subjected to an abrading action. An apparatus was constructed which permitted microscopic examination of this action during the formation of a pill. The elements of this apparatus are shown in Figure 1. The system consisted of a single position pill tester mounted in the field of a stereoscopic microscope. A small segment was cut out of the abradant, permitting a view of the fabric once during each revolution. When the apparatus is operated at sufficient speed,

[1] Presented at the Fall Meeting of The Fiber Society, Montreal, Canada, September 10, 1958.

[2] Registered trademark for Du Pont's polyester fiber.

motion appears to be continuous. Since it was impossible to predict which fibers would be involved in the action, a camera was synchronized to the tester so that one frame was exposed during each revolution.

From a series of pictures taken of a variety of fabrics, it has been possible to draw several conclusions. The existence of the first two stages (fuzz formation and entanglement) was readily observable. In addition, fuzz formation was found to occur in an entirely unexpected way. Loose fiber ends which were present on the fabric surface did not grow longer when the fabric was brushed or abraded. Rather, new fuzz was formed as contact was made at some point along the fiber length, leading to a loop which finally pulled free at its looser end.

This loop concept of fuzz formation appeared to be logical after considering the fact that a loose fiber end could quickly align itself in the direction of the abrading action, thereby minimizing the force which could be applied to it. A fiber held at both ends presented a loop which could be snagged by the abradant. This loop mechanism of fuzz formation has been confirmed by R. W. Dennison [3] using an independent approach. The method involved dyeing a fabric with a dye having poor lightfastness, exposing the dyed sample to ultraviolet radiation, and pilling the fabric. The fiber ends involved in the pills were deeply dyed, proving that they came from the interior of the fabric where the ultraviolet light had not faded the dye.

Fuzz Tendency

A method was developed for determining quantitatively and reproducibly the amount of fuzz which is surfaced on a fabric under the influence of a brushing action. This involved uniform brushing, shaving, and weighing the fuzz from a known area of fabric.

Fabric was mounted on a foam rubber covered disk attached to a frame, which in turn fitted over the vertical posts of the brush and sponge pill tester [1]. This arrangement was tested against brushes of varying stiffness from the heavy denier nylon pill test brush to a very uniform low pile nylon rug. The samples were brushed for a measured length of time and sheared.[3] The fuzz was weighed and the cycle repeated. In this way

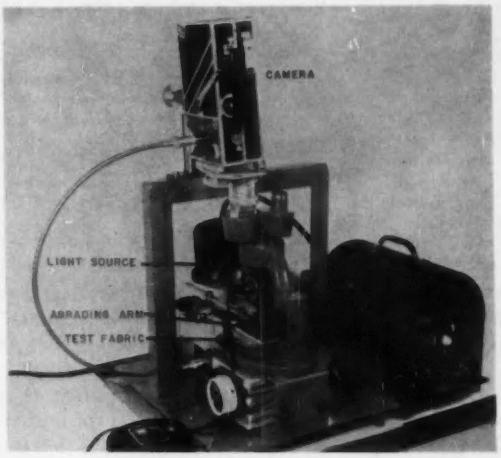

Fig. 1. Equipment for time lapse motion picture studies.

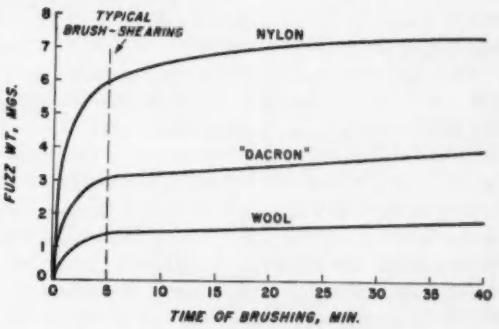

Fig. 2. Typical curves for fuzz formation.

it was observed that the amount of fuzz raised initially tended to rise sharply as a function of brushing time, leveling off as it approached a nearly horizontal asymptote. Typical curves in which the amount of fuzz produced is plotted as a function of time are shown in Figure 2. The fact that the curves tend to flatten out is in good agreement with the beneficial effect of brush shearing as a measure to control pilling. A commercial brush shearing operation removes the fuzz represented by the first section of the curve. The tendency of the fabric to fuzz is then determined by the fuzz tendency curve past this point.

[3] A system of rotation in which the test is periodically interrupted and the holders systematically shifted from position to position has greatly increased test-to-test reproducibility and eliminated entirely position-to-position variation which is often encountered using the brush and sponge pill tester.

TABLE I. Fuzz Tendency of Various Textile Fibers

(3-den./fil. Boiled-Off Staple)

Fiber	Flex life, cycles*	Tenacity		Modulus		Friction, mg.**	Fuzz, mg.
		g./den.	g./tex	g./den.	g./tex		
Nylon	26,000	4.5	0.50	6	0.67	0.29	6.0
Rayon	70	2.6	0.29	69	7.66	0.22	4.4
"Dacron"	13,000	3.9	0.43	29	3.22	0.35	3.1
"Orlon"	1,870	2.2	0.24	52	5.77	0.35	3.1
Wool	3,620	1.4	0.16	24	2.66	0.15	0.4
Acetate	20	1.4	0.16	13	1.44	0.30	0.4

* Half-life to break through 90° flexing over a 1 mil wire with a 0.3 g./den. (0.033 g./tex) load.
** The method of Röder was used [6].

Comparison of various textile fibers. It was of particular interest to use this technique to compare several common textile fibers in their relative fuzzing tendencies. This was done on a series of matched 2 × 2 twill fabrics. These data are summarized in Table I below along with several important single fiber properties.

For a fiber end to pull out of the yarn bundle, not only is it necessary for interfiber frictional forces to be overcome, but the fiber must also bend as it works its way under and over the cross-yarns of the fabric network. Thus, fibers which resist this bending (stiff fibers) will have increased frictional restraining forces. When the restraining force exceeds the fiber breaking strength, the fiber will break rather than pull out. Therefore, the fiber breaking strength determines the limit of the abrading force which can be applied—hence, the maximum length of fibers which can be raised. On the other hand, the breaking of weak fibers during abrasion will provide more ends leading to a shorter but more dense fuzz.

By use of these concepts, the fuzzing tendency listed in Table I can be explained. Nylon is most prone toward fuzzing, due to high strength, a moderate interfiber friction, and low stiffness. Wool and acetate are low tenacity fibers, so the fibers break instead of pulling out, resulting in short fuzz. Rayon, "Dacron," and "Orlon"[4] are intermediate in behavior. "Dacron" has a high strength but also has a high interfiber friction and stiffness. Rayon has a moderate strength, a high stiffness, and a low interfiber friction. "Orlon" has an intermediate strength, a high interfiber friction, and a high stiffness. Flex life and abrasion resistance appear to exert a relatively unimportant contribution until later stages of the abrading action.

[4] Registered trademark for DuPont's acrylic fiber.

TABLE II. Fuzz Tendency of Heat-Set Fabrics

Heat-setting temperature, ° C.	Fuzz, mg.	
	Heat set only	Boiled off and heat set
Control	6.5	10.2
120	—	9.9
140	11.9	8.6
160	11.6	7.8
180	7.8	7.1
200	8.5	5.2
220	5.0	6.4

The effect of heat-setting on fuzz tendency. In addition to a study of fibers which vary widely in chemical composition, it is also of interest to investigate the effects of fuzzing which result from modifications of a given fiber.

The effect of heat-setting on fuzz tendency was determined by examining fabrics of "Dacron" which had been subjected under tension to a hot air oven at several temperatures. Results are listed in Table II. As can be seen from the data, peak fuzzing occurred at the 140–160° C. level. This coincided with a minimum in bending stiffness as measured by the sonic technique discussed later. The same series of fabrics was examined after scouring at the boil. The results (also in Table II) indicated that a water boiloff procedure was equivalent to air heat-setting at about 140° C. Thus, the maximum had been reached, and subsequent heat-setting reduced the fuzz tendency.

Effect of cross section on fuzz tendency. It has been proposed that fibers with a ribbon cross section are effective in reducing the tendency of a

TABLE III. Pilling and Fuzzing in Ribbon Fibers

Filament ratio	Fuzz, mg. 1st min.	2nd min.	3rd min.	Total	Pills/in.[2]
1.0 (Round)	4.2	7.8	3.0	15.0	15
1.8 Filament ratio ribbon	7.4	7.1	2.5	17.0	10.9
2.6 Filament ratio ribbon	8.1	6.3	2.2	16.6	8.7
3.4 Filament ratio ribbon	8.7	5.7	1.7	16.1	9.0

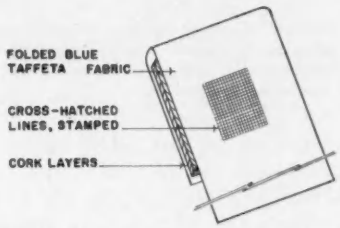

Fig. 3. Diagram of controlled fuzz sample (sewing machine technique).

fabric to pill. In order to examine this possibility, fabrics were prepared from 3-den./fil. ribbon fibers having various filament ratios.[5] The control item had the standard round cross section which could, of course, be regarded as a ribbon having a filament ratio of one. Matched fabrics of 100% "Dacron" in a 2 × 2 twill construction were woven from these filaments, and resulting fabrics were examined for fuzz and pill tendencies. A summary of the results of these tests is given in Table III.

These results show an unusual effect. After a mild brushing action (first minute), the fuzz level on the ribbon fabrics was higher than on the round item. After more severe brushing cycles, however, the weight of the fuzz on the ribbon items was less than that found on the round item. Thus, the ribbon fabrics had a high initial rate of fuzz formation, but the rate subsequently decreased to a level below that of the round fibers. This indicated that the brush shearing operation was more effective on fabrics of ribbon fibers, a fact which is in agreement with the observation that ribbon fibers form fuzzier yarns and fuzzier greige fabrics than round fibers. Since the total fuzz level is the same for the round and ribbon items while the pill level (after 3-min. brush) decreases, some stage other than fuzz tendency must be affected by this modification.

The difference in fuzz tendency between round and ribbon fibers depends on bending and frictional effects. If the ribbon is bent across its minor axis, as it usually is, its bending stiffness would be less than for round fibers. The friction between ribbon fibers is dependent on the transverse loading. For high loadings, ribbons will line up with their flat sides in contact resulting in high frictional values. Thus, the measured fuzz tendency represents a combination of these bending and frictional forces.

[5] Filament ratio is the ratio of the length to the width of a ribbon cross section.

Entanglement Tendency

In order to compare various fibers in their tendency to become entangled, it was necessary to find methods of preparing samples in which the amount and distribution of fuzz were accurately controlled. A technique utilizing a fabric sample was investigated. In this case, data from the fuzz tendency test were used to determine the brushing time necessary to produce a given weight of fuzz. The sample was then pilled in the usual manner against the sponge. Although methods of this type did offer some promise of separating fibers according to their relative entanglement tendencies, more success was attained using two techniques described below, which are essentially single-fiber in nature.

Sewing machine technique. In the first method, samples were prepared by means of a portable sewing machine. A single filament of the yarn to be tested was wound on the lower bobbin of the machine. A nylon sewing thread was used as the upper spool supply yarn. A continuous filament taffeta fabric was folded around layers of fine grain cork in a booklike manner. Tension on the nylon sewing thread was adjusted to pull the tension-free test filament through the cork layers to the upper fabric surface. The sample was sewn by accurately placing the stitches at the intersections of a stamped, cross-hatched pattern. A diagram of the sample mock-up is shown in Figure 3. The upper surface containing the rows of sewing thread was covered with a pressure sensitive tape which

secured the lower ends of the fibers on the final sample. The under surface, containing the network of single filaments, was then sanded with a fine sandpaper until the lower fabric peeled off easily. An electric shaver was then used to remove any filament still protruding from the cork surface. The layers of cork were peeled off, leaving a network of protruding fibers whose height was equal to the thickness of the cork layers and whose spacing was determined by the dimensions of the cross-hatched pattern. This covered an area of about $1\frac{1}{2} \times 1\frac{1}{2}$ in. The routine sponge cycle of the brush and sponge pill tester was used to pill the sample.

Investigation of these samples disclosed the fact that for a given filament and a given spacing, there exists a critical height below which the sample will not pill under the conditions of the standard pill test, even when the test is extended for periods of 1 hr. or more. Variations of $\frac{1}{32}$ in. in fuzz height were sufficient to show differences between no pilling and complete pilling. The minimum height at which pilling occurred (in inches $\times$ 32) was taken as the critical height. Staple fibers and very weak continuous filament fibers were not adaptable to this method; hence, another method was developed which was not subject to these limitations.

Metal spacer technique. The second technique consisted of a method for arranging a row of individual fibers parallel to one another and accurately spaced in such a way that they could be cut to a predetermined uniform height. The rows were then spaced to form a lattice work which could be pill tested. In this method, a staple fiber or single filament removed from the tow was placed in position on a notched paddle to achieve accurate spacing of the fibers. Transparent pressure sensitive tape was then carefully placed a measured distance from a central slot. This distance determined the fuzz height in the final sample. A razor blade was then run through the slot to cut the filaments. The strips of tape with attached filaments were then separated from the paddle and placed along the upper edge of a metal spacer to which a layer of $\frac{1}{32}$-in. cork was cemented. The rows were accurately spaced by the thickness of the spacers. Diagrams showing stages of a sample in preparation appear in Figure 4. The assembled sample locked together in a miniature printer's chase frame was pilled on the brush and sponge pill tester.

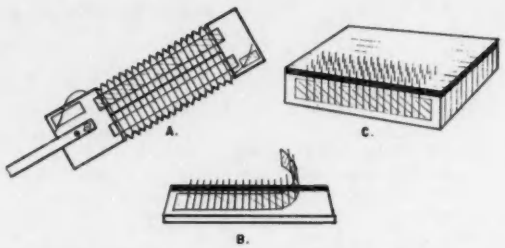

Fig. 4. Diagram of controlled fuzz sample (metal spacer technique) showing A: filament wrapped around notched paddle, B: placement of row of filaments on metal spacer, C: partially assembled sample.

Pills which formed from weak fibers showed a tendency to break off. It is significant that even with the weakest fibers tested there was no evidence of fibers breaking or wearing away unless these fibers were engaged in pills. As explained previously, a fiber held only at one end can align itself with any abrading action and thus escape damage. However, once a pill is formed, motion is restricted and forces can be directed normal to the fiber axis.

Comparison of various textile fibers in entanglement tendency. A series of fibers and their critical heights are shown in Table IV. When 3 den./fil. fibers having approximately the same cross-sectional shape were compared ("Vicara,"[6] acetate, nylon, rayon, and "Dacron"), the effect of polymer differences on entanglement tendency was obtained.

As a first attempt at correlating the physical properties of fibers with their entanglement tendencies, the stress–strain curves of several fibers were superimposed and compared. This has been done in Figure 5. When the general shapes of these curves were compared with the fiber critical

TABLE IV. Entanglement Tendency for Various Textile Fibers

Fiber	Critical height* (1/32 in.)
"Vicara"	11–
Acetate	10
Wool, 64–70's	10
"Orlon"	10–
Rayon	9
Nylon	9
"Dacron" (Ribbon)	9
"Dacron" (Round)	7
Cotton, St. Vincent (1.1 den./fil.)	6

* The signs after the critical heights indicate intermediate values.

[6] Registered trademark for Virginia-Carolina Chemical Corporation's vegetable-protein fiber.

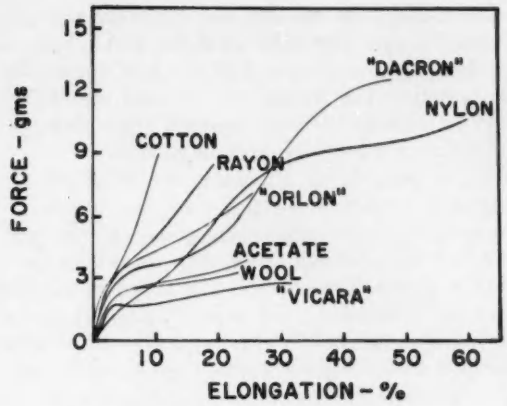

Fig. 5. Stress–strain curves for several common textile fibers (after boiloff).

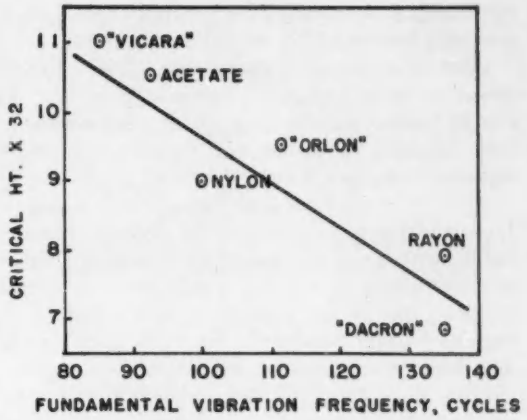

Fig. 6. Relationship between sonic stiffness and critical height (3 den./fil. fibers).

heights the surprising observation was made that the fibers with the greatest tendency to entangle (cotton, "Dacron") have the more vertical stress-strain curves while those with the highest critical heights (Vicara, wool, acetate) have the more horizontal stress–strain curves. This implies that stiffness is important to entanglement tendency, since the slope of the curve is a measure of longitudinal stiffness. These data would also suggest that deformations greater than the yield point are involved, since the best fit is obtained when considering that portion of the curve in this region.

In view of the relationship between stiffness and critical height, another, more direct, measure of bending stiffness was investigated. One of the simplest methods of measuring bending stiffness at low stress depends on the determination of the frequency of sympathetic vibration induced by a signal generator [4, 5]. When denier and length are held constant, the fundamental frequency of vibration is directly related to bending stiffness. Measurements on nonround cross sections normally must be corrected for dissymmetry, since the fundamental frequency obtained will be a measure of the bending in the direction of least resistance, i.e., across the minor axis for a ribbon. However, the minimum forces to bend the fiber can be compared in the method described without correction.

Sonic bending frequencies were measured and plotted against critical heights as they appear in Table IV; Figure 6 shows the result. Unfortunately it has not been possible to determine from these data whether a better fit with entanglement tendency is obtained at high deformation (stress–strain curve above the yield point) or at low stress (sonic bending stiffness). From time lapse movie observations, it is quite clear that severe distortions of the fibers do take place; however, the forces which determine the action at the instant of entanglement were not measured.

There are two other important differences between these methods of determining stiffness. Whereas the stress–strain behavior was determined at low speeds in a longitudinal direction, sonic bending frequency takes place at high speeds and involves compressional forces as well as longitudinal stress. In either case the fibers with the highest stiffness at a given denier show the greatest tendency to become entangled. Stiffness itself cannot be the controlling factor. This is apparent from the data in Table V, where very large changes in denier were required before fibers could resist the applied forces and exhibit reduced entanglement tendencies. This behavior is apparently the result of some fiber property which is indirectly related to stiffness. Two possibilities which suggest themselves are recovery and yield point. Unfortunately neither of these offers a complete answer under the

TABLE V. The Effect of Denier on Critical Height

Nylon			"Dacron"		
Denier	Tex	Critical height	Denier	Tex	Critical height
2	0.22	9	1½	0.17	7–
3	0.33	9	3	0.33	7
10	1.11	11	5	0.56	8
75	8.33	17			

conditions at which they are generally determined, and additional study is needed in this area.

Effect of denier on critical height. The effect of denier on critical height is shown in Table V. As can be seen from the data given, comparatively large changes in denier were required to effect significant changes in critical height.

Effect of cross section on entanglement tendency. It is of interest to consider the difference in entanglement tendency caused by changes in cross-sectional shape of a given textile fiber. For this purpose, the same fibers were used which were examined under fuzzing tendency discussed above. The data are summarized in Table VI.

From these data, the striking conclusion can be reached that most of the advantage of ribbon fibers is obtained at low filament ratios. This difference in critical height suggests that on fabrics having an equal amount of fuzz there should be less pills on the ribbon sample. The data in Table III support this conclusion.

In addition, the fact that the ribbon filaments show almost equal critical heights and pilling tendencies regardless of their filament ratios suggests that the mere possession of a nonround cross section is sufficient to interfere with entanglement. This effect is most probably due to the restricted bending directions for the ribbons, which reduce the probability of assuming a pilling configuration.

Pill Wearoff

In order to evaluate the last step of pilling independently of the others, it was possible to use the sponge cycle of the brush and sponge tester. The pill count was determined after various periods of sponging. The items tested were the same twill fabrics used to measure fuzz tendencies. Typical curves are shown in Figure 7. After a short induction period during which fuzz is forming, pills build up at a rate dependent on their fuzz and entanglement tendencies. As the abrasion continues, the resulting pilling represents an equilibrium between the rates of formation and wearoff. Since the fuzz rate diminishes on continued abrasion, the pill wearoff becomes the dominant feature. This in turn depends on the physical properties of the fibers involved. "Dacron" and nylon did not show any tendency to lose pills due to their exceptional strength and abrasion resistance. Rayon built up to a high level and then fell off quite rapidly due to its extremely low flex life and moderate strength. "Orlon" acrylic fiber behaved similarly, but because its flex life is far greater than rayon, it did not fall so rapidly. The pilling on wool and acetate decreased rapidly, as was expected from their low tenacities and low resistance to abrasion.

It is possible to eliminate the effect of the chemical nature of the fibers on the rate of pill wearoff by using samples of a given polymer with different physical properties. This was done using fabrics prepared from a series of polyester samples varying in abrasion resistance. The results appear in Figure 8, where the physical properties of these samples were compared to their pill wearoff rates.

In general, pills are removed during wear by the breaking of the anchoring fibers. There is some value for the average breaking strength at breakoff under given wearing conditions. Most synthetics are stronger than this required minimum, so the most important factor controlling this step becomes the amount of flexing necessary to reduce the fiber strength to the level of the abrading forces. Above this minimum strength, flex life is the controlling factor in pill wearoff.

Discussion

The concepts described in this paper have been summarized in Table VII. The three distinct stages of pilling are listed on the left side of the chart. The fiber properties which have significant effects on these stages are shown on the right.

In order to bring a loose fiber end to the fabric surface, it is necessary to slide, bend, and twist the fiber around its neighbors against the force of friction which tends to hold the fiber in place. The breaking strength of the fiber determines the limit of the force which may be applied. The process of entangling fibers to form the pill again involves some of these same forces. Here, stiffness, bending recovery, cross section, and denier are important. Surface characteristics (friction) and

TABLE VI. Entanglement Tendencies of Filament Ratio Series

Filament ratio	Critical height
1 (Round)	7
1.8	9+
2.6	10−
3.4	10−
4.1	10

TABLE VII. Fiber Properties Affecting the Stages of Pilling

Stage	Fiber property
Fuzz formation	Friction
	Stiffness
	Breaking strength
	Abrasion resistance
Entanglement	Shape
	Denier
	Stiffness
	Recovery
	Friction
	Elongation
Pill wearoff	Breaking strength
	Flex life

elongation also contribute. Finally, breaking strength and abrasion resistance control the pill breakoff stage.

In any pilling problem, it is first necessary to assess the relative importance of the various stages. Those fiber properties can then be examined which contribute to the stage under consideration. There are cases in which a given property affects more than one stage of pilling. In these cases, it is necessary to first determine the relative importance of that property to the stages concerned.

Since pilling occurs in a stepwise fashion, a major change in the rate of fuzz formation (the first step) has the greatest effect on pilling. Therefore, any property which alters the amount of fuzz produced will have a pronounced effect on pilling. However, in many fabrics, surface nap is desirable for aesthetic reasons. In these cases, the surface nap produced must be kept below the critical level or pilling must be controlled through modifications to the fiber properties which are effective in the other stages. Unfortunately, entanglement tendency is less important to pilling than fuzz formation. Modification in fiber properties which change entanglement tendency will, therefore, not appreciably affect the problem. On the other hand, pill wearoff does play an important role. This is the mechanism by which pilling is controlled in many present-day fabrics. Therefore, the fiber properties which affect this step become significant.

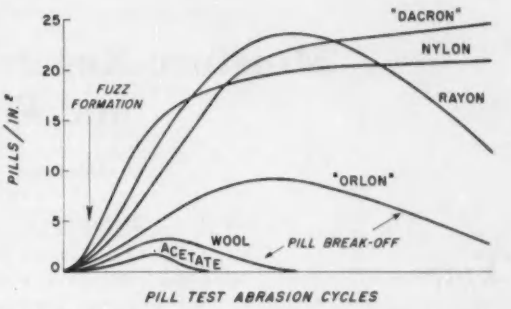

Fig. 7. Typical pill curves for several common textile fibers.

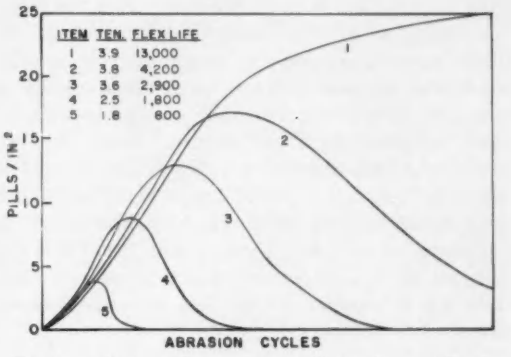

Fig. 8. Pill curves for several modified polyester fibers.

Literature Cited

1. A.S.T.M. Manual D-13 (Brush and Sponge Pill Tester), American Society for Testing Materials, Philadelphia, Penna.
2. Baird, E. M., Hatfield, P., and Morris, G. J., *J. Textile Inst.* **47**, T181 (1956).
3. Dennison, R. W., Du Pont Company, Textile Research Laboratory, Wilmington, Delaware (private communication).
4. Guthrie, J. C., Morton, D. H., and Oliver, P. H., Jr., *J. Textile Inst.* **45**, T912 (1954).
5. Kärrholm, E. M. and Schröder, B., TEXTILE RESEARCH JOURNAL **23**, 207 (1953).
6. Röder, H. L., *J. Textile Inst.* **44**, T247 (1953).

Manuscript received October 6, 1958.

Moisture Regain of Specialty Hair and Fur Fibers

Werner von Bergen

J. P. Stevens & Co., Inc., Garfield, New Jersey

THE moisture regain of wool as a function of relative humidity, under both adsorption and desorption conditions, has been well established, but very little information is available concerning the moisture regain of keratin fibers other than wool. In manufacturing circles the assumption is usually made that the less common keratin fibers (such as specialty hair and fur) closely resemble wool in their moisture regain properties. Since the importance of the hygroscopic properties of wool is well established, one would expect equal or greater importance to hold for the costlier fibers such as cashmere, vicuna, and angora rabbit fur. It is the purpose of this paper to report moisture regain data for a number of the less common keratin fibers.

Materials Studied

The following table lists the fibers studied; the method of scouring is given in parentheses. Wool and top were included in both sets of samples as governing controls.

Specialty Hair Fibers	pH
Texas Mohair:	
1. Scoured kid 36s (neutral)	8.6
2. Scoured adult 28/30s (soap, soda)	9.9
Cashmere:	
1. Scoured Chinese (neutral)	8.3
2. White Mongolian dehaired (neutral)	7.7
Alpaca-Peru: Scoured white	7.6
Vicuna-Peru: Scoured tan (neutral)	8.2
Camel Hair-China: Scoured natural (soap, soda)	8.9
Wool: Scoured Austral 70s (soap, soda)	8.9
Fur Fibers	
Angora Rabbit: French, first grade, white	5.8
Common Rabbit:	
1. French, pulled, white	6.4
2. California, boiled, white	3.5
3. Grey boiled	2.6
Beaver:	
1. Natural cut	3.3*
2. Natural boiled	2.7
Muskrat: Guard hair, bleached, natural grey	6.5
Wool: Austral top 70s	8.9

* The low pH indicates that the sample may be a mixture of boiled and cut fur.

In previous studies of this nature of wool, the samples were carefully purified by long washing and extraction to free them from all impurities. These elaborate purification procedures were not used in this research, since it was felt that the mill man would be more interested to know how the samples behave in their normal condition.

Procedure

Wherever possible, moisture regain was determined on 200-g. samples composed of portions from various bales or bags. Each gross sample was separated into two subsamples for test. The first subsample was thoroughly wet out in distilled water for ½ hr. and then centrifuged for 1 min. The second subsample was dried for 5 min. in a Baird conditioning oven at 120° C.

Both samples were then conditioned for 72 hr. to equilibrium at 65% RH and 70° F. The moisture regain for both wet and dry fibers was established by running duplicate tests on 10-g. samples in a Brabender oven to determine their regain. Following this, new samples of 25 g. each were brought into a special conditioning room at 65% RH. The humidity in the room was then raised within 1 hr. to 90% and kept there for a minimum of 4 hr., or until the samples reached constant weight. The humidity in the room was then restored to 65% and new samples of 25 g. each were brought in. Finally, the humidity in the room was reduced to 20% and kept there for 4 hr. or until the samples reached constant weight.

In summary, the samples which were exposed to 90% RH reached their equilibrium through adsorption, whereas those kept at 20% RH reached their equilibrium through desorption. As in each instance two samples were involved, one originally

TABLE I. Moisture Pickup of Samples Wet Out and Centrifuged

Sample	Moisture pickup, %	Sample	Moisture pickup, %
Kid mohair	40.0	Angora rabbit	54
Adult mohair	36.0	Common French rabbit	97
Chinese cashmere	54.4	Common California rabbit	92
Mongolian cashmere	44.0	Common grey rabbit	75
Alpaca	41.0	Beaver, cut	49
Vicuna	52.0	Beaver, boiled	70
Camel hair	43.0	Muskrat	71
Wool	44.0	Wool top	55

wet and the other originally dry, these samples will be designated as "wet" and "dry" respectively in this report. These test conditions were chosen because this type of adsorption and desorption will occur in mill practice [3].

Results

Table I shows the variation in the moisture pickup of the samples after they had been wet out and centrifuged. The fur fibers hold so much more water probably because of their lumping together. Any chemical treatment such as boiling with acid, pulling, and bleaching will worsen this condition.

Tables II and III record the regain of the samples at three humidity levels, 20%, 65%, and 90%, all at a constant temperature of 70° F, under both adsorption and desorption conditions.

Discussion

The reduction in the relative humidity from 65% to 20% caused the regain differences between the wet and dry samples at 65% almost to disappear; in fact, the regain of the wet sample is occasionally below that of the dry. Comparing the data at 65% with those at 90% reveals that the hysteresis in the moisture regain at the upper level is about the same magnitude at the lower level as far as the specialty hair fibers are concerned. However, the scoured wool samples showed a reversal in the hysteresis, with the moisture regain of the wet samples being lower than that of the dry samples by 1.2%. The fur fibers show similar behavior; at 20% RH the moisture differences between wet and dry samples disappears, while at 90% RH three samples (California rabbit, cut beaver, and muskrat) show a reversal in hysteresis behavior; i.e., the moisture regain of the dry sample is higher than that of the wet.

It is evident that the adsorptive and desorptive

TABLE II. Moisture Regain of Specialty Hair Fibers at 70° F.

	20% RH		65% RH		90% RH	
	Dry	Wet	Dry	Wet	Dry	Wet
Mohair						
Kid	8.7	8.9	14.7	16.7	21.9	23.6
Adult	8.4	9.2	14.9	17.6	22.1	23.2
Cashmere						
Chinese	8.1	7.4	12.6	16.6	19.0	23.2
Mongolian	—	8.4	—	16.8	—	22.2
Alpaca	8.3	8.4	14.4	17.2	21.4	24.5
Vicuna	8.4	7.8	13.3	16.4	20.6	24.4
Camel hair	8.0	8.4	14.3	17.4	21.9	—
Wool	7.5	8.3	14.0	17.8	21.9	20.7

TABLE III. Moisture Regain of Fur Fibers at 70° F.

	20% RH		65% RH		90% RH	
	Dry	Wet	Dry	Wet	Dry	Wet
Rabbit						
Angora French	6.7	7.3	12.6	13.3	21.2	22.1
Common pulled French	—	6.7	—	14.9	—	20.2
Common California	7.0	7.1	13.3	15.2	20.2	17.9
Common grey	5.2	6.4	10.0	12.9	18.6	20.3
Beaver						
Cut	5.4	6.6	11.2	12.4	22.4	21.5
Boiled	6.4	6.4	12.4	13.5	17.0	17.8
Muskrat	7.1	7.5	15.1	15.9	20.3	17.5
Wool top	7.4	7.4	14.7	17.0	19.5	22.9

powers of the specialty hair fibers tests are remarkably similar to wool. The values given for mohair are very close to those published for wool [1, 2], and the same marked hysteresis exists in the moisture content of the specialty hair fibers between adsorptive and desorptive conditions. Table IV gives a comparison between published data on

TABLE IV. Comparison of Moisture Regain Data on Mohair

Speakman			This study				
				Kid		Adult	
Relative humidity, %	Adsorption	Desorption	Relative humidity, %	Dry	Wet	Dry	Wet
7	3.41	4.87					
25	6.93	8.6	20	8.7	8.9	8.4	9.2
63.3	14.41	16.26	65	14.7	16.7	14.9	17.6
92.5	24.24	25.82	90	21.9	23.4	22.1	23.2

TABLE V. Comparison of Average Moisture Regain Data at 70° F. for Hair and Fur Fibers

	Specialty hair fibers	Fur fibers
Relative humidity, %	Moisture regain, %	Moisture regain, %
20	8.4	6.6
65	15.5	13.1
90	22.3	19.7

mohair and the results obtained on kid and adult mohair in this study.

The moisture regain of the fur fibers is approximately 2% lower than that of wool and the specialty hair fibers. Since the fur fibers are finer (14 μ or less in diameter), the affinity for water is decreased. This finding coincides with Speakman's statement that the affinity of wool for water appears to increase slightly as the wool becomes coarser. The moisture regain of the fur fibers does not seem to be much affected by the various chemical treatments some of these fibers have undergone, such as pulling, boiling in acid, and bleaching.

Table V gives a comparison of the average difference in the moisture regain between the specialty hair fibers and the fur fibers at the three humidity levels tested.

Conclusion

The moisture adsorptive and desorptive powers of the specialty hair fibers are remarkably similar to wool. The same hysteresis exists in the moisture content of mohair, cashmere, alpaca, vicuna, and camel hair fibers between adsorptive and desorptive conditions.

The moisture regain of fur fibers such as rabbit, beaver, and muskrat is approximately 2% lower than for wool and the specialty hair fibers.

At 65% RH and 70° F. the average moisture regain of the specialty hair fibers is about 15%; that for the fur fibers is 13%.

Literature Cited

1. Nicholls, C. H. and Speakman, J. B., *J. Textile Inst.* **46T**, 424 (1955).
2. Speakman, J. B., *J. Soc. Chem. Ind.* (May 2, 1930).
3. Speakman, J. B. and Cooper, C. A., *J. Textile Inst.* **27T**, 183 (1936).

Manuscript received February 13, 1959.

Letters to the Editor

Short communications in the form of Letters to the Editor are intended to provide prompt publication of significant new research results and to permit an exchange of views on papers previously published in the JOURNAL. These communications are not submitted to formal review as are research papers, and the editors do not assume any share of the author's responsibility for the information given or the opinions expressed. When work previously published in the JOURNAL is the subject of critical comment, the authors of the original paper are given an opportunity to submit a reply, which will be published concurrently when possible.

The Relationship Between Breaking Time and Breaking Load for a Worsted Fabric Tested on CRE and CRT Machines

Textile Research Section
National Research Council
Ottawa, Canada
February 24, 1959

To the Editor

TEXTILE RESEARCH JOURNAL

Dear Sir:

Since submission of the paper "A Study of the Relationship Between Breaking Time and Breaking Load for Fabrics Tested on CRE and CRT Machines," (March 1959), two of the authors have completed a similar study on a worsted serge fabric. In view of the importance of wool as a textile fiber in many countries, the present data should add to the usefulness of the paper. It does not alter the conclusions drawn from the data for the fabrics previously tested.

The worsted serge had the following characteristics: 9.9 oz./sq.yd.; 65 warp yarns and 55 weft yarns/in.; 2-ply yarns. The same randomization of specimens, specimen size, and testing conditions were used as in the previous work, except that the CRE machine was an Instron (Model TT-C). This machine provided essentially constant rates of extension without appreciable periods of initial acceleration. The CRT pendulum machine was the Scott machine, having capacities of 150 and 300 lb.

With specimens which show a gradual break, as with this worsted fabric, it is difficult to judge the breaking time visually, so the time required to reach the maximum load was taken as the criterion. Although some similar difficulty had been experienced at the longer breaking times with the fabrics previously studied, the magnitude of the effect had not been great enough to require a changeover from using the time of visible-break as the criterion of breaking time. Some consideration of this matter may be necessary in test methods based on the constant breaking time principle.

With the Instron machine, the breaking load has to be read from the load–elongation chart, and it is difficult to determine during a test just when the maximum has been reached, as loads close to the maximum may be sustained over an appreciable interval of time as individual yarns break in succession before the load drops sharply as the specimen obviously breaks apart. This is especially noticeable at the longer breaking times; e.g., for visible-break times of 9.3, 25.2, and 76 sec. the respective time intervals between the attainment of maximum load and the visible break were 1.9, 4.9, and 11.0 sec. The times required to reach maximum load were therefore determined from the breaking load vs. elongation curves after completion of the tests. This can be readily done since the chart movement is of known constant speed in each case and directly proportional to the clamp separation since there is negligible movement of the clamp attached to the weighing mechanism.

In order to obtain strictly comparable breaking

TABLE I. Worsted Serge—Warp

Machine type and capacity	Speed of pulling clamp (constant), in./min.	Breaking time,* sec.	Breaking load: Av. for 15 specimens, lb.	Breaking load: Std. deviation, lb.	Breaking load: Error of mean at 95% probability, lb.	Elongation at max. load, %
CRE—100 lb. cap.	1	65.1	62.4	1.1	±0.6	36.2
	1	63.3	62.6	1.5	0.9	35.2
	1.67	36.9	63.6	0.9	0.5	34.2
	3	20.7	65.8	1.2	0.7	34.5
	3	20.3	65.3	1.3	0.7	33.8
	5	11.8	67.6	1.2	0.7	32.8
	6	10.0	67.2	1.1	0.6	33.3
	8.33	7.4	69.1	1.1	0.6	34.2
	8.33	7.3	69.4	1.2	0.7	33.8
	12	5.0	69.9	1.5	0.9	33.1
	20	3.1	71.7	1.7	1.0	34.1
—200 lb. cap.	20	3.1	72.0	0.8	0.5	34.4
CRT (Pendulum)— 150 lb. cap.	12	6.8	70.0	1.2	0.7	32.3
	12	6.9	68.5	1.2	0.7	31.7
	12	6.7	68.5	0.9	0.5	—
	4.4	20.7	65.0	0.9	0.5	34.7
	4.4	20.5	65.0	1.0	0.6	34.3

* Time to reach maximum load.

TABLE II

Breaking time interval, sec.	Rate of decrease in br. load with increase in br. time: lb./sec.	%/sec.*
3 – 5	0.90	1.3
5 – 7.5	0.54	0.78
7.5–10	0.40	0.59
10 –15	0.28	0.42
15 –20	0.19	0.30
20 –25	0.15	0.23
25 –30	0.12	0.19
50 –60	0.03	0.05

* Calculated as percentage of the breaking load for the mid-point of time interval.

TABLE III. Variation of Average Breaking Loads (lb.) with CRE (Instron) Machine over Suggested Breaking-Time Limits of 20 ± 3 sec. and 60 ± 10 sec.

(Values taken from br. load vs br. time curves)

At 17 sec.	66.0
At 23 sec.	65.0
Decrease (17 sec.–23 sec.)	1.0 = 1.5%
At 50 sec.	62.8
At 70 sec.	62.4
Decrease (50 sec.–70 sec.)	0.4 = 0.6%

TABLE IV. Variation of Breaking Times Within Sets of Specimens Tested at Constant Speed per Set on CRE & CRT Machines

	Av. for 15 specimens, sec.	Range, sec.
CRT machine	20.7	19.2–22.1
CRT machine	20.5	18.6–21.5
CRE machine	20.7	18.7–24.1
CRE machine	20.3	17.8–22.3
CRE machine	65	58 –72
CRE machine	63	55 –71

TABLE V. Speed of Pulling Clamp Required to Produce Breaking Times of Approximately 20 sec. and 60 sec. with 1-in. Raveled Strips and 3-in. Initial Clamp Separation

Approx. breaking time	Approx. speed required, in./min.: CRE	CRT (pendulum)*
20 sec.—to max. load	3.0	4.4
20 sec.—to visible break	3.7	5.2
60 sec.—to max. load	1.1	1.5
60 sec.—to visible break	1.3	1.7

* The speeds shown for the CRT pendulum machine apply to the particular machine and capacity used.

times on the CRT pendulum machine, the breaking time here was also taken as the time required to reach maximum load, but a record was also made of the time required for visible breaking of the specimen. The latter was measured with a stopwatch, and the position of the pen on the chart at the moment the stopwatch clicked was marked by a second operator. Since the pen ceases to move

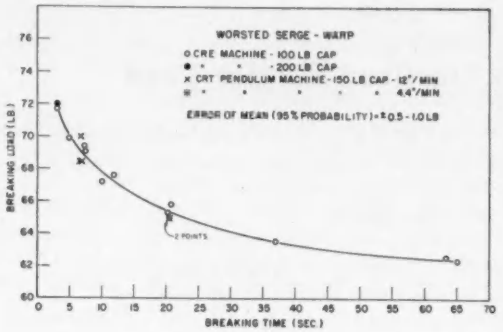
WORSTED SERGE - WARP
○ CRE MACHINE - 100 LB CAP
● " " - 200 LB CAP
× CRT PENDULUM MACHINE - 150 LB CAP - 12"/MIN
⊠ " " " " " 4.4"/MIN
ERROR OF MEAN (95% PROBABILITY) = ± 0.5 - 1.0 LB
BREAKING LOAD (LB.)
BREAKING TIME (SEC.)
2 POINTS

Fig. 1

when the pendulum stops, whereas the chart continues in motion, the time interval between the point of maximum load and the marked point corresponding to the stopwatch timing of the visible break could be readily calculated. The time to reach maximum load was then obtained by subtracting this calculated time interval from the time recorded by stopwatch. The average time intervals between the attainment of maximum load and the visible break were 1.4 sec. and 3.0 sec. when the respective times for visible break were 8.3 sec. and 23.7 sec. The measurement of time in relation to load and elongation on the charts of the pendulum machine is, however, less precise than with the highly sensitive recording system of the Instron machine.

The data obtained for the worsted serge are given in Table I and Figure 1. Analyses of the data are given in Tables II–V for comparison with the analyses published for the fabrics previously studied.

Conclusions

The breaking load for the warp direction of the worsted serge decreased with increase in breaking time, the rate of change decreasing as the breaking time increased. The breaking load at 60-sec. breaking time was 13% less than that obtained at the minimum breaking time of 3.1 sec. achieved on the CRE machine at 20 in./min. rate of extension.

Good agreement was found between the breaking loads obtained on the CRE and the CRT pendulum machines when compared at equal breaking times.

The data obtained for this worsted serge indicate that the suggested breaking time of 20 ± 3 sec., previously investigated and found satisfactory for several other types of fabric [TEXTILE RESEARCH JOURNAL **29**, 235–251 (1959)], should also be suitable for measuring the breaking load of wool fabrics on different types of machines.

AUDREY S. TWEEDIE
MARGARET T. MITTON

Space Density of Fibers in Idealized Singles Yarn

Fabric Research Laboratories, Inc.
1000 Providence Highway
Dedham, Massachusetts
March 11, 1959

To the Editor

TEXTILE RESEARCH JOURNAL

Dear Sir:

In the January 1958 issue of TEXTILE RESEARCH JOURNAL, the undersigned presented a theoretical analysis of the influence of geometry on torque developed in singles yarn twisting. The effects of fiber torsion and fiber bending were considered, and the total yarn torque was determined by summation (integration) over the yarn area of the contribution to the yarn torque of fiber torque and fiber bending moment.

As part of the analysis, the number of fibers, dN_f, present in a differential element of yarn cross-sectional area, dA, was given in Equation 8 for the idealized geometry of close packed fibers as

$$dN_f = \frac{N_f}{\pi R_y^2} 2\pi r\, dr \cos\theta \tag{1}$$

where N_f is the total number of fibers in the yarn, R_y is the twisted yarn radius, $2\pi r\, dr = dA$ = yarn differential element of area, and θ, the variable helix angle, is defined by $\tan\theta = 2\pi Tr$.

Actual integration of Equation 1 yields

$$\int dN_f = N_f \frac{2\,(1 - \cos\theta_s)}{\tan^2\theta_s \cos\theta_s} \tag{2}$$

where θ_s is the surface helix angle of the yarn.

Actually, the left and right hand sides of Equation 2 should be identical. The factor $\frac{2\,(1 - \cos\theta_s)}{\tan^2\theta_s \cos\theta_s}$ is unity at $\theta_s = 0$ and decreases as θ_s increases. Thus, generally, the use of Equation 1 for number of fibers gives results below what they should be and, as will be seen, is in error since it does not properly consider the radial growth resulting from twisting the idealized close packed yarn. While this error does not alter either the basic analysis or the principal conclusions presented in the original article, the numerical values of the theoretical results will be modified.

For the idealized yarn

$$dN_f = \frac{2\pi r\, dr \cos\theta}{A_f} p \tag{3}$$

where all terms are as already defined and, in addition, A_f is the fiber cross-sectional area and p is the packing factor of the fibers in the zero-twist close-packed yarn state, assumed constant with twist. Thus

$$N_f A_f = \pi R_0^2 p \tag{4}$$

where R_0 is the radius of the zero-twist yarn.

Integration of Equation 3 yields

$$N_f = \frac{p}{A_f} \pi R_y^2 \left[\frac{2\,(1 - \cos\theta_s)}{\tan^2\theta_s \cos\theta_s} \right] \tag{5}$$

which, after substitution of p/A_f from Equation 4, becomes

$$N_f = \frac{N_f}{\pi R_0^2} \pi R_y^2 \frac{2\,(1 - \cos\theta_s)}{\tan^2\theta_s \cos\theta_s} \tag{6}$$

from which

$$R_y^2 = R_0^2 \left[\frac{\tan^2\theta_s \cos\theta_s}{2\,(1 - \cos\theta_s)} \right] \tag{7}$$

From Equation 7, it can be seen that $R_y^2 \geq R_0^2$, indicating the anticipated increase in idealized close-packed yarn radius with increased yarn twist.

It is now possible to rewrite Equation 3 in terms of yarn parameters. From Equations 5 and 3, there results

$$dN_f = \frac{N_f}{\pi R_y^2} \frac{\tan^2\theta_s\,(\cos\theta_s)}{2\,(1 - \cos\theta_s)} 2\pi r\, dr \cos\theta \tag{8}$$

Alternatively, from Equations 3 and 4

$$dN_f = \frac{N_f}{\pi R_0^2} 2\pi r\, dr \cos\theta \tag{9}$$

Generally Equation 8 is the more convenient expression to use. When integrated the necessary identity $\int dN_f = N_f$ results.

The use of Equation 8 rather than 1 changes the numerical results of torque reported in the previously referenced article by the factor $\frac{\tan^2 \theta_s \cos \theta_s}{2 (1 - \cos \theta_s)}$. For small angles θ_s, the effect is small. Ratios of torques are not changed. This factor should be present in the final expressions for torque, Equations 10, 32, 35, and 36, and those results shown as ordinates on Figures 3, 8, and 9 should be multiplied by it. For convenience, a table of numerical values of the factor is given below for various helix angles.

θ_s, °	Factor $\frac{\tan^2 \theta_s \cos \theta_s}{2 (1 - \cos \theta_s)}$
0	1.00
10	1.00
20	1.03
25	1.04
30	1.07
35	1.11
45	1.20

The turning point at $\theta_s = 45°$ is thereby eliminated from Figure 8 and the curves of Figure 9 rise more steeply, at higher helix angles, than shown.

MILTON M. PLATT
WILLIAM G. KLEIN
WALTER J. HAMBURGER

Acrylonitrile-Stabilized Wool Keratin Derivatives

Western Regional Research Laboratory[1]
Albany 10, California
March 2, 1959

To the Editor

TEXTILE RESEARCH JOURNAL

Dear Sir:

Many wool protein properties are best studied in solution, so that it is important to have stable, soluble derivatives simply related to the native fiber. Recent reports by Harrap and Woods [1, 2] characterizing stabilized wool protein derivatives suggest that a short account of our own continuing and parallel work would be timely.

Continuing the molecular characterization of cortical cells made by acid treatment [6], we have found that the cortical cell protein, made water-soluble by reduction with mercaptoethanol, is conveniently stabilized by acrylonitrile. Use of acrylonitrile for this purpose at this laboratory was initiated by J. E. Moore. As applied in near-neutral aqueous media at room temperature, this reagent appears to react relatively quickly and specifically with available thiol groups. The small, inert cyanoethyl group introduced may be presumed to have less effect on wool protein properties than larger or ionized groups. It is also of interest to compare properties of wool derivatives exposed to warm alkaline conditions with those of acid-treated preparations.

A representative cortical cell preparation from fine Merino wool treated 48 hr. in 6 *N* HCl at 30° C. was reduced and treated with acrylonitrile. The main product was recovered as a precipitate near pH 5.5, near its presumed isoelectric point. At pH 7 in 0.1 *N* NaCl the material showed a single ultracentrifuge boundary. At a concentration of 1.5%, the sedimentation constant was 2.0 S referred to water at 20° C. It therefore sediments a little more slowly than the reduced cortical cell protein previously studied [6], stabilized by excess reducing agent. Determination of molecular weights by a method due to Archibald [3] gave values between 33,000 and 42,000 for a 0.7% solution at pH 8.0 in 0.1 *M* sodium phosphate buffer. Measurements at lower protein concentrations indicate a limiting value at about 55,000. Higher values to as much as 400,000 were found in 0.1 *N* NaCl at pH 5.5.

These results were supplemented and made more intelligible by light-scattering studies. Solutions clarified by low-speed centrifugation and ultrafine filtration were visibly turbid, and showed large dissymmetry of scattering. Plots of reciprocal scattered intensity (Hc/τ) versus protein concentration showed upward curvature at low concentra-

[1] A laboratory of the Western Utilization Research and Development Division, Agricultural Research Service, U. S. Department of Agriculture.

tions, extrapolating to a molecular weight of 300,000. However, high-speed centrifugation at 150,000 G for ½ hr. removed 6–12% of the sample as a well-defined gelatinous pellet. Further study of this high-molecular fraction is appropriate. The resulting clear solution showed negligible dissymmetry. The turbidity remained approximately constant from pH 7.5 to 9.0 and from 1.4 to 2.3, but increased rapidly below 7.5 and above 2.5, indicating aggregation as the zone of precipitation is approached. The turbidity also increased as pH was lowered below 1.4.

On the basis of this survey, molecular-weight determinations were made on solutions clarified by high-speed centrifugation and ultrafine filtration at pH 8.0, using sodium phosphate buffers. At ionic strengths of 0.24, 0.12, and 0.06, the observed weight-average molecular weights were 58,800, 57,100, and 52,600, respectively. The slope of the reciprocal intensity (Hc/τ) versus concentration plot changed from negative to positive at about ionic strength 0.1 as the ionic strength was decreased. In 0.1 *N* NaCl, pH 8.2 (adjusted with NaOH), a value of 53,800 was observed. A single determination, at pH 1.9 (adjusted with HCl), $\mu = 0.03$, gave a molecular weight of 59,900. These molecular weights were calculated from intercept values, neglecting multicomponent corrections [5]. Such a correction may remove the apparent trend of the values with ionic strength.

Solutions of this protein became turbid reversibly on cooling. The protein can be easily recovered by dialysis. Carrying a sample through a cycle, such as solution at pH 2, recovery by dialysis, and re-solution at pH 8, does not change the molecular weight.

These results apply to a fraction representing at least 20% and possibly a majority of the original wool. This material has a molecular weight considerably lower than those observed by Harrap and Woods [1, 2], although more in agreement with earlier studies of O'Donnell and Woods [4].

Literature Cited

1. Harrap, B. S., and Woods, E. F., *Australian J. Chem.* **11**, 581 (1958).
2. Harrap, B. S. and Woods, E. F., *Australian J. Chem.* **11**, 592 (1958).
3. Kegeles, G., Klainer, S. M., and Salem, W. J., *J. Phys. Chem.* **61**, 1286 (1957).
4. O'Donnell, I. J. and Woods, E. F., *J. Polymer Sci.* **21**, 397 (1956).
5. Timasheff, S. N., Dintzis, H. M., Kirkwood, J. G., and Coleman, B. D., *J. Am. Chem. Soc.* **79**, 782 (1957).
6. Ward, W. H. and Bartulovich, J. J., *J. Phys. Chem.* **60**, 1208 (1956).

YOSHIO TOMIMATSU
JOHN J. BARTULOVICH
WILFRED H. WARD